



Design, synthesis and *in vitro* biological evaluation of a novel class of anti-adenovirus agents based on 3-amino-1,2-propanediol

Sarah Mazzotta^{a,b,c,1}, Judith Berastegui-Cabrera^{d,1}, Margarita Vega-Holm^{a,*},
María del Rosario García-Lozano^{a,e}, Marta Carretero-Ledesma^d, Francesca Aiello^b,
José Manuel Vega-Pérez^a, Jerónimo Pachón^{d,f}, Fernando Iglesias-Guerra^{a,*},
Javier Sánchez-Céspedes^{d,*}

^a Department of Organic and Medicinal Chemistry, Faculty of Pharmacy, University of Seville, E-41071 Seville, Spain

^b Department of Pharmacy, Health and Nutritional Sciences, University of Calabria, 87036 Arcavacata di Rende (CS), Italy

^c Department of Pharmaceutical Sciences, University of Milan, 20133 Milan, Italy

^d Unit of Infectious Diseases, Microbiology and Preventive Medicine, Institute of Biomedicine of Seville (IBiS), University Hospital Virgen del Rocío/CSIC/University of Seville, E41013 Seville, Spain

^e Institute of Biomedicine of Seville (IBiS), SeLiver Group, University Hospital Virgen del Rocío/CSIC/University of Seville, E41013 Seville, Spain

^f Department of Medicine, University of Seville, E-41009 Seville, Spain

ARTICLE INFO

Keywords:

Adenovirus
Antiviral drugs
Aminoalcohol
Ester
Carbamate
Triazole
Urea

ABSTRACT

Nowadays there is not an effective drug for the treatment of infections caused by human adenovirus (HAdV) which supposes a clinical challenge, especially for paediatric and immunosuppressed patients. Here, we describe the design, synthesis and biological evaluation as anti-adenovirus agents of a new library (57 compounds) of diester, monoester and triazole derivatives based on 3-amino-1,2-propanediol skeleton.

Seven compounds (**17**, **20**, **26**, **34**, **44**, **60** and **66**) were selected based on their high anti-HAdV activity at low micromolar concentration (IC₅₀ from 2.47 to 5.75 μM) and low cytotoxicity (CC₅₀ from 28.70 to >200 μM). In addition, our mechanistic assays revealed that compounds **20** and **44** might be targeting specifically the HAdV DNA replication process, and compound **66** would be targeting HAdV E1A mRNA transcription. For compounds **17**, **20**, **34** and **60**, the mechanism of action seems to be associated with later steps after HAdV DNA replication.

1. Introduction

Adenovirus (HAdV) represents a significant viral pathogen, responsible for a wide range of global clinical diseases, mostly in immunocompromised patients [1,2]. It's a non-enveloped virus consisting of an icosahedral capsid containing a linear double-stranded DNA (dsDNA) genome of 34–36 kb. HAdVs belong to the family *Adenoviridae* that includes more than 100 serotypes classified into 7 species (HAdV A-G) [3–5]. HAdV serotypes are traditionally associated with self-limited

respiratory (1–3, 5 and 7) [6,7], conjunctival (8, 19 and 37) [8] and gastrointestinal infections (40 and 41) [9], presenting significant morbidity and mortality in immunosuppressed patients and also in healthy individuals, being a well-known causative agent of community-acquired pneumonia [1,10].

At present, there are no drugs specifically approved to treat HAdV infections. Usually, drugs approved for the treatment of other viral infections are used off-label to manage serious HAdV-induced diseases, such as ribavirin (**1**), ganciclovir (GCV, **2**), cidofovir (CDV, **3**) and

Abbreviations: BCV, brincidofovir; CC₅₀, cytotoxic concentration 50%; CDV, cidofovir; COSY, correlation spectroscopy; CuAAC, copper(I)-catalysed alkyne-azide 1,3-dipolar cycloaddition; DCM, dichloromethane; DEPT, distortionless enhancement by polarization transfer; DMAP, 4-(dimethylamino)-pyridine; DMF, dimethylformamide; EMEM, minimum essential medium Eagle; FBS, fetal bovine serum; GCV, ganciclovir; HAdV, human adenovirus; HMBC, heteronuclear multiple bond correlation; HEPES, 4-(2-hydroxyethyl)-1-piperazineethanesulfonic acid; HSQC, heteronuclear single quantum correlation; IC₅₀, half maximal inhibitory concentration; *mcpba*, meta-chloroperbenzoic acid; NOESY, nuclear overhauser effect spectroscopy; SAR, structure-activity relationship; SI, selectivity index; THF, tetrahydrofuran; TLC, thin layer chromatography; TMS, tetramethylsilane.

* Corresponding authors.

E-mail addresses: mvegaholm@us.es (M. Vega-Holm), iglesias@us.es (F. Iglesias-Guerra), jsanchez-ibis@us.es (J. Sánchez-Céspedes).

¹ S.M., J.B.C joint as co-first authors.

<https://doi.org/10.1016/j.bioorg.2021.105095>

Received 7 March 2021; Received in revised form 9 May 2021; Accepted 10 June 2021

Available online 13 June 2021

0045-2068/© 2021 The Author(s).

Published by Elsevier Inc.

This is an open access article under the CC BY-NC-ND license

(<http://creativecommons.org/licenses/by-nc-nd/4.0/>).

brincidofovir (BCV, **4**) (Fig. 1), which display no suitable clinical results in terms of efficacy or safety [11–13]. CDV, an acyclic nucleoside analogue of cytosine, is a broad spectrum antiviral drug approved for the treatment of cytomegalovirus (CMV) retinitis and represents, in most cases, the drug of choice in the clinical setting [14,15]. Unfortunately, its low oral bioavailability, and its nephrotoxicity and myelosuppression effects, are undesirable factors that limit the use of CDV [16].

The unsatisfactory results of current antiviral drugs highlight the need to find new effective anti-HAdV agents. Drug repurposing of existing drugs approved for other pharmacological indication is gaining interest as strategy for the development of new antiviral drugs. In this sense, the salicylanilide anthelmintic drug niclosamide (**5**, Fig. 1) was reported to display significant anti-HAdV activity, targeting the microtubular transport of the viral particles to the nucleus [17]. Among natural products, polyphenolic compounds have been found to have antiviral activity, such as epigallocatechin gallate (**6**, Fig. 1), that showed inhibitory activity against several viruses including HAdV [18].

During the years, interesting novel structural diversified molecular entities have been described as new potential antiviral candidates against HAdV infections. Many of these compounds include common structural features such as amide, urea, esters functions and aromatic portions [19–25].

A series of new 5-aminouracil derivatives were synthesized by Nikitenko *et al.* with antiviral activity against HAdV5 (**7**, Fig. 1) [19]. A set of optimized salicylamide derivatives with potent anti-HAdV activity at low micromolar concentrations was recently described (**8**, Fig. 1) [20], as well as a library of benzoic acid esters (**9**, Fig. 1) [21].

Our group synthesized a new set of ureas/thioureas derivatives based on piperazine scaffold (**10**, Fig. 1) as well as a collection of serinol

derived benzoic acid esters (**11a** and **11b**, Fig. 1) searching for new effective HAdV agents [22–25].

As part of our continuous efforts to develop new anti-HAdV compounds with suitable active/safety profiles and different mode of action [22–25], in this work we describe the design, synthesis and biological evaluation of a library (57 compounds) of 3-amino-1,2-propanediol derivatives.

2. Results and discussion

2.1. Chemistry

2.1.1. Design

We aimed to develop a set of new anti-HAdV molecules keeping in mind the structure of CDV (that represents one of the current therapeutic options for severe HAdV infections). Our approach involves the analysis of cidofovir molecule in which three regions can be identified as points for structural modifications to generate chemical diversity (Fig. 2).

1) The central skeleton that can be considered a three carbon aminoglycerol chain. Related to this, the first step was the election of the central core as starting point for the following chemical construction process: 3-amino-1,2-propanediol.

2) The nitrogen pyrimidine base. In our model we replaced it with an acyclic aryl urea moiety introduced at the nitrogen of the skeleton. Aryl urea derivatives are an important class of compounds possessing a wide spectrum of biological activities, such as anticancer, antibacterial, antiviral, etc [22–26].

3) The phosphonate group at secondary position. Carbon 1 and 2 positions become important points of structural variability of our

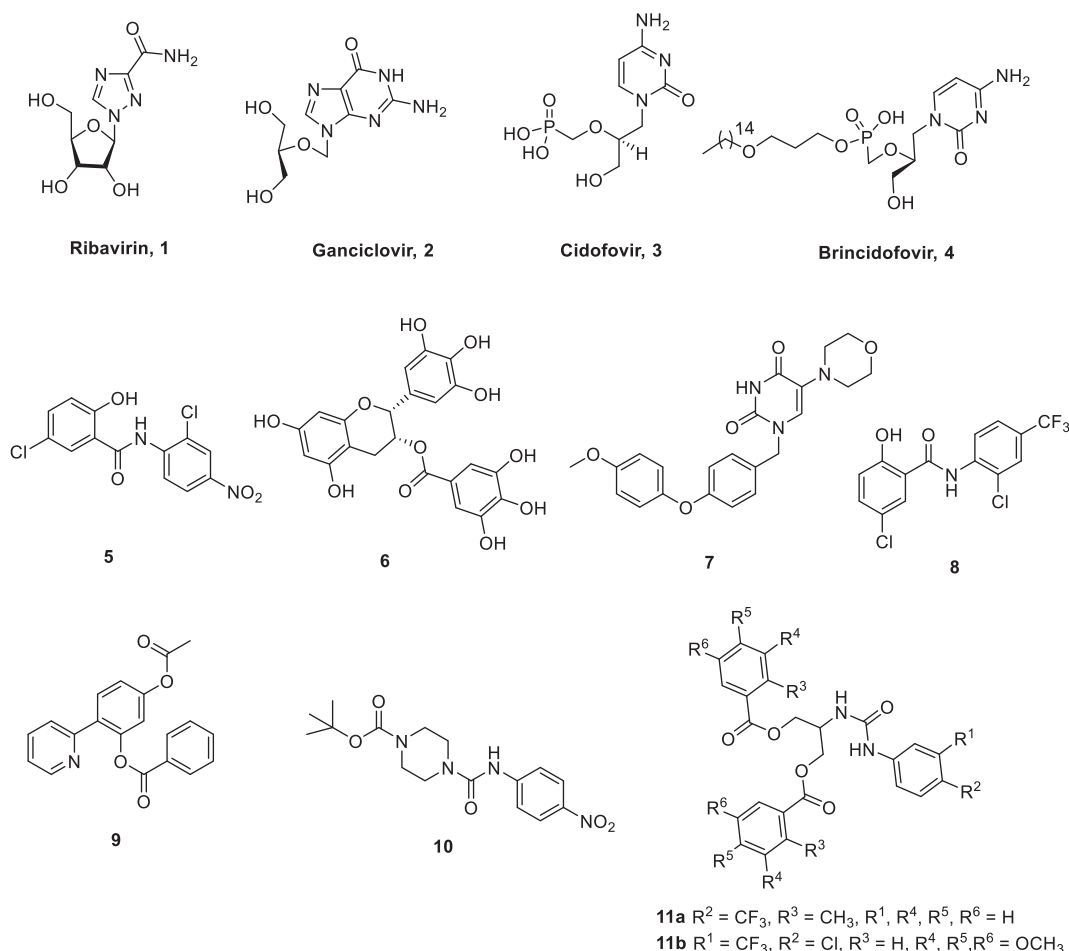


Fig. 1. Current drugs employed for severe HAdV infections and novel compounds with *in vitro* anti-HAdV activity.

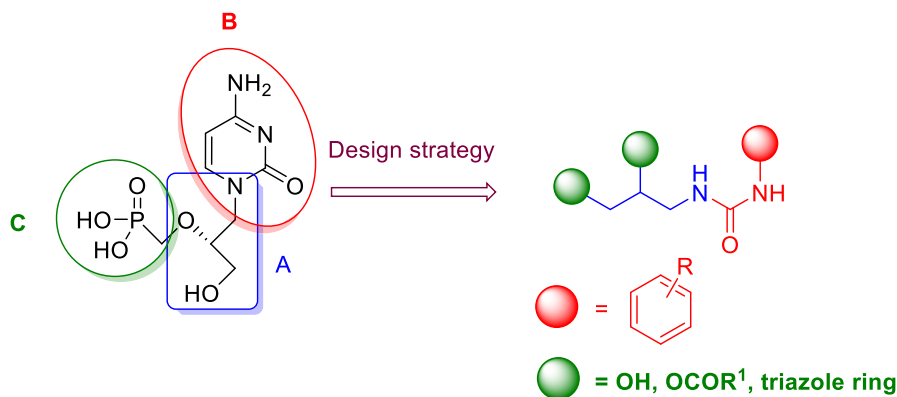


Fig. 2. Analysis of the CDV structure and following design strategy.

general backbone. Our main purposes were: mono or diacylation of the hydroxyls (benzoic acid esters) and their replacement by 1,2,3-triazole rings.

Based on the relevance of aromatic esters as privileged functional groups for anti-HAdV activity [18,21] and on the promising results demonstrated by some serinol-derived aromatic diesters in the inhibition of HAdV infection [25], firstly a set of diester derivatives from the isomeric 3-amino-1,2-propanediol (core present in antiviral compounds [27,28]) was designed, in order to explore the effect of this different skeleton on the anti-HAdV activity. Our attention was also focused on di- and trimethoxy substitutions, frequently present in anticancer and antiviral compounds [29–31]. In this sense and aiming to further explore the presence of methoxy groups, a trimethoxycinnamic moiety was also inserted, as it is a privileged structural scaffold broadly distributed in natural products (esters and amides derivatives) with diverse and important biological functions, included antiviral activities [32].

To evaluate the impact of the presence of a free hydroxyl group, as in CDV, in providing active compounds, a small collection of monoester derivatives of 3-amino-1,2-propanediol, in position 1 and 2, was designed.

1,2,3-Triazole ring is a well-known scaffold that has widespread presence in different compounds characterized by several biological activities; antiviral, antibacterial, antitumoral, among others [33–35].

Application of bioisosteric substitution is a common technique in the structural modification of active compounds to design analogues. In addition, triazoles are among the most common amide bond isosteres and have been widely employed in the peptidomimetics field as well as in the design of new analogues of bioactive compounds [36–39].

Related to our work, we focused on their use as ester isosteres, in an attempt to obtain analogues with significant anti-HAdV activity. In case they generated promising derivatives, these would be expected to have reduced *in vivo* susceptibility to enzymatic degradation, compared to the ester prototypes [36].

2.1.2. Synthesis

Based on this design, the first structural modification was the introduction of the aryl urea moiety at the nitrogen with different substituents on the phenyl ring. The synthesis of these compounds was carried out by reaction between 3-amino-1,2-propanediol (12), commercially available, and the appropriate phenyl isocyanate, using three different substituted

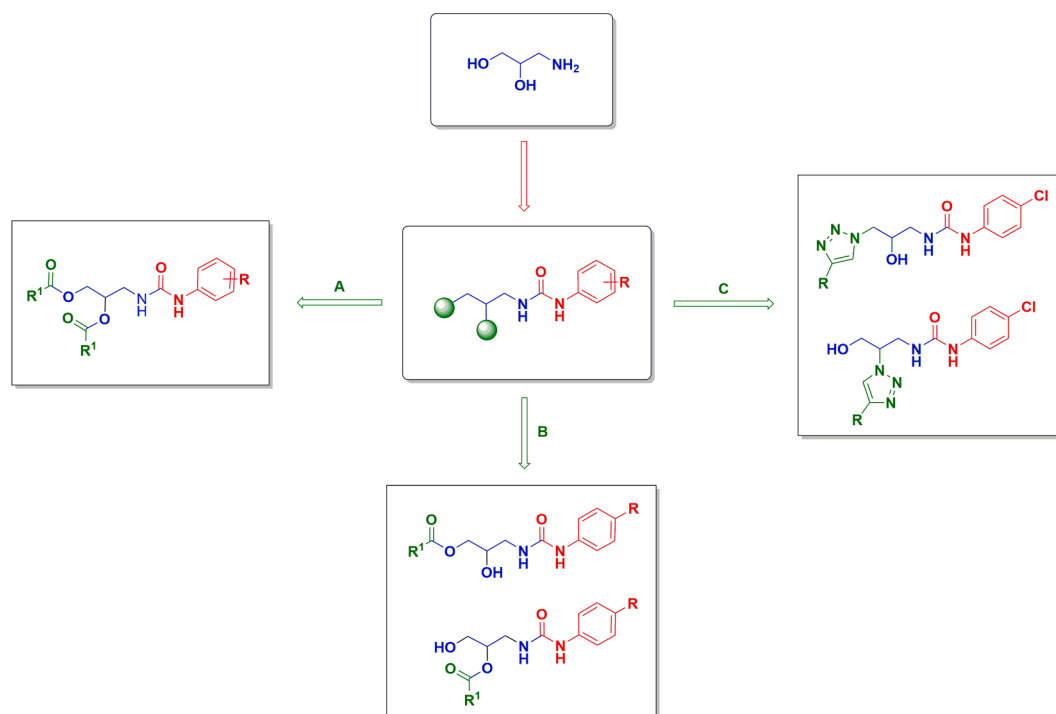


Fig. 3. Three different approaches for the introduction of chemical diversity.

phenyl isocyanates (*p*-CF₃, *p*-Cl and *p*-CH₃ as models of electron withdrawing and electron-releasing groups) (Scheme 1).

Once these urea derivatives (13–17) were prepared, three different approaches were carried out to generate final compounds (Fig. 3).

Route A, the preparation of a set of diester derivatives.

Route B, the selective monoacylation of hydroxyl groups of the aminoalcohol chain.

Route C, the introduction of 1,2,3-triazole rings, located at position 1 or 2 of the aminoalcohol chain.

2.1.2.1. Route A. Synthesis of *N*-phenylaminocarbonyl diester derivatives.

Diester derivatives (18–46) were synthesized by an acylation reaction of both hydroxyl groups of the urea intermediate (13–17), with the corresponding acyl chloride or carboxylic acid to give the final product in a good yield (Scheme 1, Table 1).

At this step, the structural variability on benzoyl moiety was examined as follows: methyl and methoxy groups as representative electron releasing substituents, and CN, NO₂ and CF₃ as electron-withdrawing groups (to explore the effects of the electronic properties on the antiviral activity) as well as di- and trimethoxy substitutions. The trimethoxycinnamoyl derivatives were prepared.

2.1.2.2. Route B. Synthesis of *N*-phenylaminocarbonyl monoester and carbamate derivatives.

Two different synthetic approaches were employed for the generation of monoester derivatives from ureas 13 and 14, depending on the position of the acyl function on the aminoalcohol skeleton. For the preparation of acylated derivatives at primary position (47–49, Table 2), a selective *O*-acylation reaction of primary alcohol group of 13 was performed. The reaction was carried out in dichloromethane (DCM) at –40 °C by controlling the stoichiometric conditions, using the appropriate acylating agent (*p*- or *o*-CH₃, *p*-CF₃ benzoyl chlorides) and pyridine (Scheme 2).

The introduction of the ester function on the secondary alcohol required an acyl protection and deprotection strategy. In the first step, the monoacylation of primary hydroxyl of the urea derivative (13, 14) proceeded following the same reaction condition described above, but using chloroacetyl ester as protecting group (50 and 51). During the subsequent step, the intermediates 52–57 were generated by the introduction of the desired benzoyl ester function at secondary position. Finally, the deprotection of position 1 through the reaction with thio-urea in CH₃CN-H₂O at 60 °C removed the chloroacetyl ester, giving the monoacylated compounds 59–64 in good yields. For the synthesis of

monocarbamate 65 the same synthetic methodology was employed, except for the acylation of secondary alcohol that was performed using the appropriate phenyl isocyanate in the presence of 4-dimethylamino-pyridine (DMAP) (Scheme 2, Table 2).

At this point it should be noticed that during the preparation of the trimethoxycinnamic diester analogue 45, the monoester derivative at primary position was isolated, compound 66 (Table 2).

2.1.2.3. Route C. Synthetic route for the preparation of *N*-phenylaminocarbonyl 1,2,3-triazole derivatives.

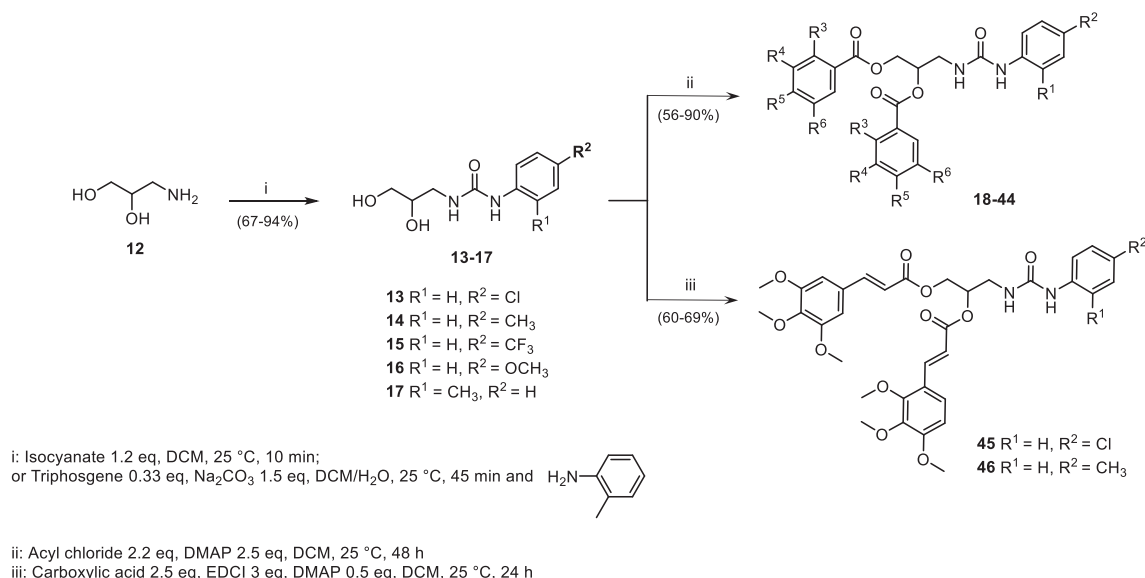
We generated a set of 4-substituted-1,2,3-triazole derivatives following two different methodologies for the introduction of the triazole moiety at both positions of the carbon chain.

For the preparation of compounds 71–76 (Table 3), in which the heterocyclic nucleus is located at primary position, we employed allylamine as the starting material for the synthetic procedure (67). Once the *p*-Cl substituted urea derivative 68 was prepared, an oxidation reaction of olefin, using *meta*-chloroperbenzoic acid (*m*CPBA) in dry tetrahydrofuran (THF), furnished the corresponding oxirane 69. In the next step, the acid-catalysed ring opening reaction using NH₄Cl and sodium azide under ethanol reflux, gave the azide derivative 70. Finally, the synthesis of 1,2,3-triazole ring (1,4 adduct) was performed through a click chemistry approach, the copper(I)-catalysed alkyne-azide 1,3-dipolar cycloaddition (CuAAC) reaction (Scheme 3). The reaction proceeded using the appropriate terminal alkyne, CuSO₄ as a source of pre-catalyst Cu^{II} and sodium ascorbate as reducing agent, in *t*-BuOH-H₂O at room temperature. This reaction represents the most used “click” reaction to obtain 1,2,3-triazole, due to its reliability, specificity, and biocompatibility [40,41].

For the introduction of the triazole ring at secondary position more steps were required and are depicted in Scheme 4. From the urea derivative (*p*-Cl, 13) the first step involved the selective protection of the primary alcohol with the benzoyl group (77). The acylated product 77 was mesylated in THF (78) for the subsequent nucleophilic substitution with sodium azide (in dimethylformamide, DMF, at 85 °C), furnishing the introduction of the azide group in position 2 (79). The click chemistry reaction between deprotected azide derivative 80 and the appropriate substituted alkyne, in the same conditions described above, afforded final 1,2,3-triazole derivatives 81–86 (Table 3).

Compounds 71–76 and 81–86 were fully characterized by NMR spectroscopy (see Experimental Section).

To establish the regiochemistry of the click reaction heteronuclear



Scheme 1. Synthesis of *N*-phenylaminocarbonyl diester derivatives 18–46.

Table 1
Benzoic acid and cinnamic acid diesters **18–46** from route A.

Percentage of plaque formation inhibition (%)^a

Compound							CC ₅₀ (μM) ^b
	R ¹	R ²	R ³	R ⁴	R ⁵	R ⁶	
18 (A)	H	Cl	H	H	H	H	0.00 ± 0.00
19 (A)	H	Cl	H	H	CH ₃	H	59.84 ± 29.71
20 (A)	H	Cl	CH ₃	H	H	H	75.08 ± 15.71
21 (A)	H	Cl	H	H	OCH ₃	H	0.00 ± 0.00
22 (A)	H	Cl	H	H	CN	H	0.00 ± 0.00
23 (A)	H	Cl	H	H	NO ₂	H	0.00 ± 0.00
24 (A)	H	Cl	H	H	CF ₃	H	26.47 ± 8.32
25 (A)	H	Cl	OCH ₃	H	OCH ₃	H	49.70 ± 6.77
26 (A)	H	Cl	H	OCH ₃	OCH ₃	OCH ₃	60.22 ± 8.43
27 (A)	H	CH ₃	H	H	CH ₃	H	31.00 ± 10.43
28 (A)	H	CH ₃	CH ₃	H	H	H	40.25 ± 5.27
29 (A)	H	CH ₃	H	H	OCH ₃	H	53.07 ± 16.18
30 (A)	H	CH ₃	H	H	CN	H	4.43 ± 6.26
31 (A)	H	CH ₃	H	H	NO ₂	H	40.25 ± 5.27
32 (A)	H	CH ₃	H	H	CF ₃	H	21.79 ± 30.81
33 (A)	H	CH ₃	OCH ₃	H	OCH ₃	H	47.01 ± 8.79
34 (A)	H	CH ₃	H	OCH ₃	OCH ₃	OCH ₃	81.29 ± 1.10
35 (A)	H	CF ₃	H	H	CH ₃	H	0.00 ± 0.00
36 (A)	H	CF ₃	CH ₃	H	H	H	7.30 ± 11.04
37 (A)	H	CF ₃	H	H	OCH ₃	H	18.51 ± 1.92
38 (A)	H	CF ₃	H	H	CN	H	40.41 ± 13.31
39 (A)	H	CF ₃	H	H	NO ₂	H	2.12 ± 3.00
40 (A)	H	CF ₃	H	H	CF ₃	H	26.83 ± 24.33
41 (A)	H	CF ₃	OCH ₃	H	OCH ₃	H	46.69 ± 3.36
42 (A)	H	CF ₃	H	OCH ₃	OCH ₃	OCH ₃	57.85 ± 22.21
43 (A)	CH ₃	H	H	OCH ₃	OCH ₃	OCH ₃	20.29 ± 2.82
44 (A)	H	OCH ₃	H	OCH ₃	OCH ₃	OCH ₃	99.86 ± 0.13
45 (B)	H	Cl	–	–	–	–	0.00 ± 0.00
46 (B)	H	CH ₃	–	–	–	–	0.00 ± 0.00
Cidofovir^c	–	–	–	–	–	–	3.51 ± 4.97
							179.09 ± 35.10

^a Percentage of control HAdV5-GFP inhibition in a plaque assay at 10 μM using the 293 β5 cell line. See Experimental Section

^b Cytotoxic concentration 50%. The results represent means ± SD of triplicate samples from three independent experiments.

^c Data of cidofovir, as positive clinical drug candidate, have been listed.

2D NMR experiments were performed with compounds **74** and **84**, both 4-fluorophenyl triazole derivatives, as models [34].

The formation of the triazole ring was confirmed through the presence of a single signal of the triazolyl proton at $\delta = 8.52$ ppm (**74**) and 8.65 ppm (**84**). Firstly, the presence of the 1,4-adduct was confirmed using the heteronuclear multiple bond correlation (HMBC) experiment to identify long-range coupling (three bonds) between protons and carbons. In compound **74**, the 1,4-substitution was proven because the terminal CH₂ signals (δ 4.71 and 4.32 ppm) showed a cross-peak with the CH of the triazole ring (δ 122.1 ppm). Compound **84** showed similar coupling profile, between CH signal (4.69–4.62 ppm) of the central chain with the CH-triazole (120.8 ppm) (Fig. 4 A). To confirm the 1,4-adduct formation, NOESY experiments were performed. The NOESY spectrum showed correlation between the proton of the triazole ring and both CH₂ groups, those next to the triazole ring (blue arrows) and those next to the urea function (little correlation, green arrows); and between CH protons (red arrow) of the aliphatic chain for compound **74**. For compound **84**, correlation between the triazole proton and the CH₂ terminal (blue arrows), CH (red arrow) and one of the CH₂ linked to the urea group (green arrow) was observed (Fig. 4 B) (see Supplementary Material).

For the synthesis of 1,2,3-triazole derivatives (1,4 adduct), six different terminal alkynes were employed but only four of them were commercially available (propargyl alcohol, 4-ethynylanisole, 1-ethynyl-4-fluorobenzene and 2-ethynylbenzaldehyde). With the aim to introduce an aromatic acid function, the ring-opening of phthalic anhydride were performed by an aminolysis reaction with propargyl amine, in THF

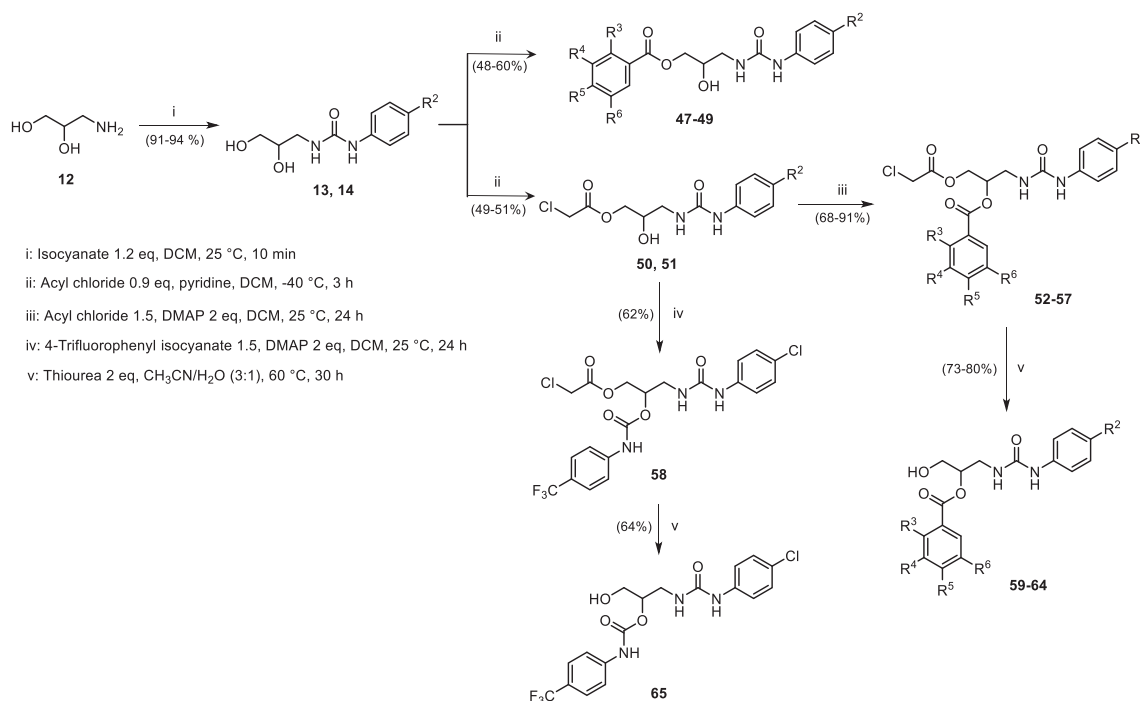
at room temperature (**87**). For the preparation of alkynyl phosphonate **88** the propargyl alcohol reacted with the diethyl (tosyloxy)methylphosphonate in basic condition of NaH at 25 °C (Scheme 5). Both compounds were characterized by NMR spectroscopy (see Experimental Section).

2.2. Biological evaluation

2.2.1. In vitro evaluation of HAdV infection inhibition and cellular viability

As the first step in the biological evaluation, the anti-HAdV activity of the new derivatives from the three routes was evaluated in plaque assay at 10 μM, quantifying HAdV plaque formation in the presence of the candidate molecules. Their effect on cellular viability was also carried out and the 50% cytotoxic concentration (CC₅₀) determined for those compounds that reached a percentage of inhibition in the plaque assay > 60% (Tables 1-3). Since CDV currently represents the drug of choice to treat HAdV infections, it was also evaluated following our own methodologies and compared to our results.

The analysis of the evaluation of the diester derivatives (**18–46**, Table 1) showed, from a structure–activity relationship (SAR) point of view, that the impact of electron-withdrawing substituents of the aromatic acyl moiety (CN, NO₂ and CF₃) was generally detrimental for the antiviral activity. For *p*-Cl substituted phenyl urea derivatives (**22–24**) the plaque formation inhibition range was from 0% to 25.83%, slightly higher than *p*-CF₃ phenyl ureas (**38–40**) and *p*-CH₃ analogues (**30–32**), with 2.12% to 44.65% range values. Compounds **31** (*p*-NO₂ with *p*-CH₃ substituted phenyl urea) and **38** (*p*-CN with *p*-CF₃ substituted phenyl



Scheme 2. Synthesis of *N*-phenylaminocarbonyl monoester and its derivatives. Percentage of plaque formation inhibition^a

Table 2
 Benzoic monoacylated derivatives **47–49** and **59–66** from route B.

Compound						CC ₅₀ (μM) ^b	
	R ²	R ³	R ⁴	R ⁵	R ⁶		
47 (A)	Cl	H	H	CH ₃	H	15.20 ± 1.39	–
48 (A)	Cl	CH ₃	H	H	H	25.99 ± 3.65	–
49 (A)	Cl	H	H	CF ₃	H	5.70 ± 8.06	–
59 (B)	Cl	H	H	CH ₃	H	20.92 ± 10.17	–
60 (B)	Cl	H	H	CF ₃	H	100.00 ± 0.00	> 200
61 (B)	Cl	H	H	NO ₂	H	0.00 ± 0.00	–
62 (B)	Cl	H	OCH ₃	OCH ₃	OCH ₃	48.03 ± 6.79	–
63 (B)	CH ₃	H	OCH ₃	OCH ₃	OCH ₃	0.00 ± 0.00	–
64 (B)	CH ₃	H	H	CF ₃	H	40.21 ± 7.11	–
65 (C)	Cl	H	H	CF ₃	H	19.57 ± 2.84	–
66 (D)	Cl	–	–	–	–	75.04 ± 9.54	174.32 ± 4.52
Cidofovir^c	–	–	–	–	–	3.51 ± 4.97	179.09 ± 35.10

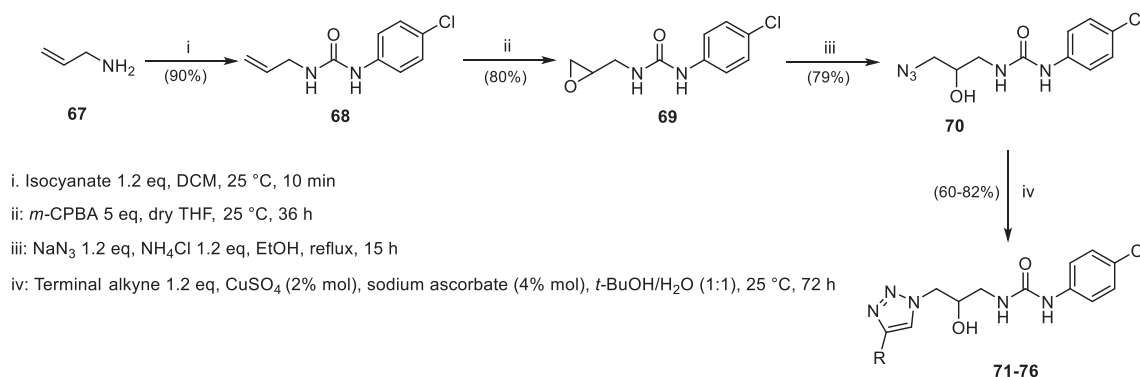
^a Percentage of control HAdV5-GFP inhibition in a plaque assay at 10 μM using the 293 β5 cell line. See Experimental Section.

^b Cytotoxic concentration 50%. The results represent means ± SD of triplicate samples from three independent experiments.

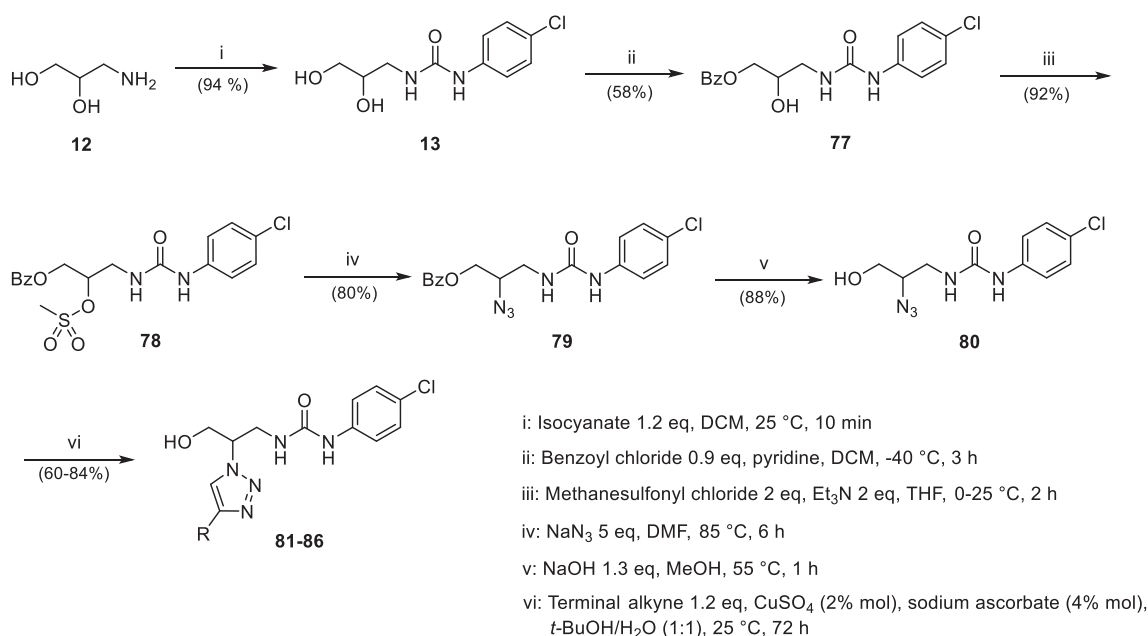
^c Data of cidofovir, as positive clinical drug candidate, have been listed.

urea) showed a moderate activity (44.65% and 40.41%, respectively). For electron donor groups at *para* position of the acyl function (methyl and methoxy) the levels of inhibition depended on the urea. *p*-CF₃ substituted ureas (**35–37**) showed almost no activity (0.00–18.51%), similarly to *p*-Cl phenyl urea derivatives (**19** and **21**, no inhibition). Higher levels of inhibition (31.00–60.70%) were found with *p*-CH₃ phenyl urea derivatives (**27–29**). Specifically, compounds with a methyl group in *ortho* position on the aromatic ester with *p*-Cl and *p*-CH₃ phenyl

urea (**20** and **28**), demonstrated significant antiviral activity (75.08% and 60.70%, respectively). The dimethoxybenzoyl derivatives (**25**, **33** and **41**) gave similar percentage of plaque formation inhibition (29.70%, 47.01%, 46.69%, respectively), regardless of the type of substituent on the phenylaminocarbonyl function, indicating the relevance of this group for the activity. The introduction of an additional methoxy group (**26**, **34** and **42**, trimethoxybenzoyl derivatives) provided an improved antiviral activity, inhibiting HAdV plaque formation from



Scheme 3. Synthetic route for the preparation of *N*-phenylaminocarbonyl-1,2,3-triazole derivatives at primary position (71–76).



Scheme 4. Synthetic route for the preparation of *N*-phenylaminocarbonyl 1,2,3-triazole derivatives at secondary position (81–86).

57.85% to 81.29%, higher than the corresponding dimethoxy analogues. Compound 34 (*p*-methyl phenyl urea) resulted the most active diester derivative, with 81.29% inhibition of HAdV plaque formation. As *p*-Cl and *p*-CH₃ urea derivatives gave, in general terms, higher activity than *p*-CF₃, they were employed for the preparation of the trimethoxycinnamoyl derivatives 45 and 46, which did not show activity (0% plaque formation inhibition). This modification did not lead to potentially interesting analogues. Finally, the unsubstituted benzoyl diester derivative (18) was also not active.

Considering the *in vitro* inhibition demonstrated by compound 34, the preparation of analogues with different substituted phenyl urea was the natural evolution. Two modifications were designed: the position isomer analogue (*o*-methyl substituted urea, 43) and another electron donor group at *para* position (*p*-OCH₃ phenyl urea, 44). They gave 20.29% and 99.86% of inhibition, respectively. These results suggest the relevance of *para* substitution for the biological activity.

At this point, it is important to note that the urea derivatives 13–16 used as precursors were also evaluated, yielding percentages inhibition values between 0.00% and 59%. However, compound 17 (*o*-CH₃ phenyl urea) gave 82.52% of inhibition, becoming an interesting potential anti-HAdV agent. For this compound the CC₅₀ was 139.95 μM.

As can be seen in Table 1, for compounds 20, 26, 34 and 44, the CC₅₀ values were determined and they were selected for further biological

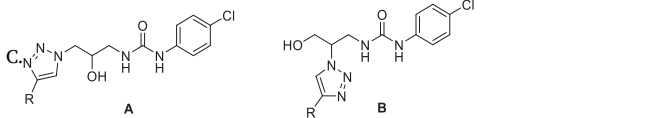
evaluations, together with compound 17, to gain some mechanistic understanding for their mode of action.

The evaluation of the antiviral activity of the monoester derivatives at the primary alcohol showed that they lacked significant anti-HAdV activity, giving percentages of plaque formation inhibition from 0% to 25.99%, (compounds 47–49). It is worth to mention the drastic reduction on antiviral activity for the *o*-methyl benzoyl derivative 48 (25.99%) compared to its diester analogue 20 (75.08%) (Table 2)

The urea 13 gave the monoesters at secondary position 59 and 60 with *p*-CH₃ and *p*-CF₃ in order to compare their biological results with the analogues 47 and 49, displaying a slight higher inhibition for the *p*-CH₃ benzoyl derivative (20.92% inhibition for compound 59 versus 15.20% inhibition for compound 47). However, for *p*-CF₃ analogue 60, a complete plaque formation inhibition (100%) was observed, unlike the regioisomer 49 (5.70%). As CF₃ is an electron withdrawing group, *p*-NO₂ benzoyl analogue (61) was prepared and evaluated, in order to explore the role of this electronic property (no inhibition observed). In the same way, the trimethoxy derivative was also synthesized (62), showing a reduced antiviral activity compared to the diester analogue (26) (48.03% versus 60.22%). Same activity behaviour was observed for monoester of *p*-methyl urea derivative 63 (no inhibition) in contrast to its diester analogue (34) with 81.29% of inhibition (Table 2).

Other attempt to obtain active compounds started from compound

Table 3
1,2,3-Triazole derivatives **71–76** and **81–86** from route



Comp.	R	Percentage of plaque formation inhibition (%) ^a	CC ₅₀ (μM) ^b
71 (A)		10.77 ± 15.23	–
81 (B)		5.80 ± 15.48	–
72 (A)		4.78 ± 74.93	–
82 (B)		0.00 ± 0.00	–
73 (A)		33.33 ± 6.10	91.24 ± 4.89
83 (B)		0.00 ± 0.00	–
74 (A)		21.54 ± 26.11	174.34 ± 15.57
84 (B)		37.45 ± 0.56	30.93 ± 2.08
75 (A)		0.00 ± 0.00	–
85 (B)		21.57 ± 4.21	175.46 ± 2.97
76 (A)		0.00 ± 0.00	–
86 (B)		12.63 ± 7.36	–
Cidofovir^c		3.51 ± 4.97	179.09 ± 35.10

^a Percentage of control HAdV5-GFP inhibition in a plaque assay at 10 μM using the 293β5 cell line. See Experimental Section.

^b Cytotoxic concentration 50%. The results represent means ± SD of triplicate samples from three independent experiments.

^c Data of cidofovir, as positive clinical drug candidate, have been listed.

60, which demonstrated the highest level of inhibition. Two structural modifications were introduced on it. Related to the urea function, the preparation of the analogue with *p*-CH₃ phenyl urea (**64**) gave less activity than **60** (40.21%). The second one was the replacement of the ester function with a carbamate one (**65**), which also resulted in a decreased antiviral activity (19.57%) (Table 2).

The evaluation of the trimethoxycinnamic monoester **66** gave 75.04% of plaque inhibition and CC₅₀ of 174.32 μM. From this group, compounds **60** and **66** (as prototypes of monoester at secondary and primary position respectively) were selected for further biological studies.

The biological evaluation of the synthesized 1,2,3-triazole derivatives at both positions, **71–76** and **81–86**, did not offer a suitable inhibitory activity (Table 3). Among triazole derivatives at the primary position, compound **73** (phosphonate group) showed moderate activity, with 33.33% of plaque formation inhibition (the highest one), while its analogue at secondary position was not active. For triazole derivatives with a phenyl ring, those with the heterocycle at secondary position displayed higher values of inhibition than those with the triazole at primary one, *p*-fluorophenyl ring derivatives (37.45% compound **84** versus 21.54% compound **74**), *p*-methoxyphenyl ring triazole derivatives (21.57% compound **85** versus 0% compound **75**). Their CC₅₀ was also determined and high values were observed. They become interesting compounds for further optimization process, in the search for new scaffolds, by acting on the urea portion of the main chain, and also by the generation of different substituted phenyl ring at the triazole moiety.

From this screening we selected 7 compounds which were able to inhibit HAdV infection in more than 60% compared to a control infection. First, we assayed these compounds with the aim to determine their

specificity through the selectivity index (SI), measured as the ratio between their half maximal inhibitory concentration (IC₅₀) and their 50% cytotoxic concentration (CC₅₀).

All compounds showed a dose-dependent inhibition of HAdV5 infection (Figure S62, Supplementary Material), showing IC₅₀ values significantly lower than CDV [42]. These IC₅₀ values ranged from 2.47 μM to 5.75 μM. Their CC₅₀ were at least 10 times over their IC₅₀ values with SI between 11.63 and 66.23 (Table 4). We next evaluated the effect of these compounds on HAdV replication measuring their effectiveness in blocking the production of new virus particles using a virus burst size assay. Treatment with the compounds was associated with overall reductions in virus yield in the range 1.52–48.18-fold, but only compounds **34** (194.61) and **44** (285.65) showed a significant reduction (Table 4).

In our previous work we identified a set of serinol derivatives with significant anti-HAdV activity [25]. Compound **11b** (Fig. 1) was found to show high antiviral potency (IC₅₀ 3.67 μM) and safety (SI 17.37). In the present work, aminoglycerol derivatives **26**, **34** and **44**, also being trimethoxy benzoyl diesters as **11b**, not only provided the same antiviral potency, but also improved the safety (in consequence the SI) and increased the reduction in virus yield. The combination of electron-releasing groups (*p*-OCH₃ and *p*-CH₃) with the presence of trimethoxy benzoyl groups in compounds **34** and **44** respectively seems to be associated with dramatic reductions in virus yield compare with the rest of the selected aminoglycerol derivatives or those previously described serinol derivatives.

2.2.2. Antiviral mechanism of action studies

2.2.2.1. Time of addition assay.

HAdV replicative cycle is a well-known coordinated process, beginning with the binding of HAdV fiber to its cellular receptors in the plasma membrane of the cell-host and subsequent entry into the cell by clathrin-mediated endocytosis or macropinocytosis taking 5 min after binding [43–45]. Using the endocytic network, HAdV virions force the lysis of the endosomal membrane after 15 min and are transported along the microtubules network to the nuclear pore complex (NPC) where they attach after 35–45 min and the viral genome is released into the nucleus [45,46].

In order to determine at what point, during the HAdV replicative cycle, these compounds could be exerting their antiviral activity, we next evaluated their antiviral activity in a time of addition assay (Fig. 5).

All compounds showed a time-decrease inhibitory effect, following a similar pattern with minimal differences. Compounds **20** and **60** showed an inhibition > 60% when they were either preincubated with the virus prior to their addition to cells or added at the beginning of the incubation (60 min and 0 min), but they lacked that activity at further time points. Compounds **17**, **26**, **34** and **66** did not show a significant decrease in their inhibition effect during the whole time. Compound **44** did not show an inhibition higher than 50% at any time point, however, a decrease in that effect was observed from the 5 min time-point to the 120 min time-point.

Based on these results, it was difficult to establish the specific step in the HAdV replicative cycle at which these molecules could be acting. Thus, our next step was to evaluate the effect of these compounds on the viral DNA access to the nucleus cell (Fig. 6).

Once HAdV particles leave the endosome after the lysis mediated by HAdV protein VI, the partially uncoated capsids are transported to the nuclear membrane via the microtubule network. Then, the HAdV genome is imported into the nucleus via the nuclear pore complex [47]. Our hypothesis was that if these derivatives inhibited any of the steps of the HAdV entry, this would be reflected in the quantification of HAdV genomes at the host nucleus after a synchronized infection.

As shown in Fig. 6, we did not find statistical differences in the percentage of nuclear-associated HAdV genomes between the control sample with DMSO and evaluated compounds. Together, these results

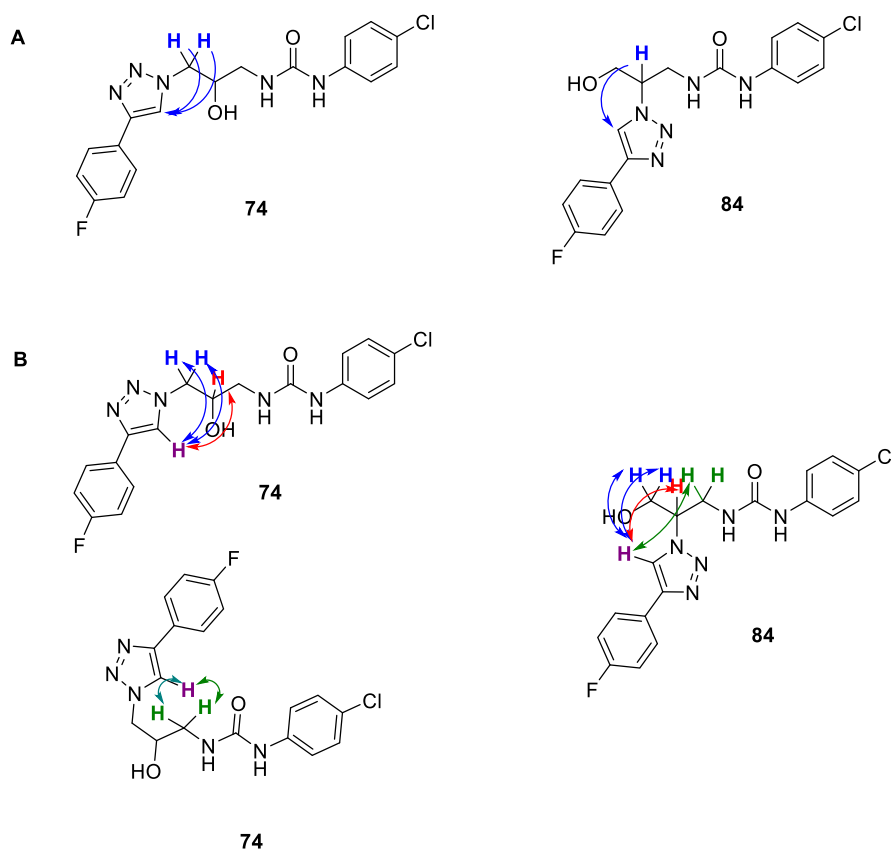
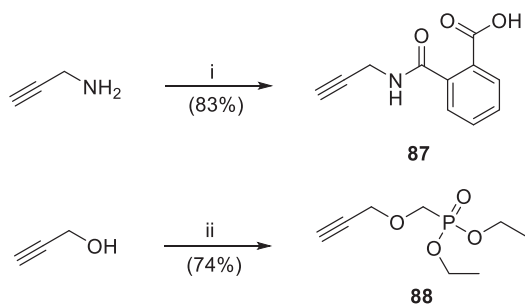


Fig. 4. A) ^1H , ^{13}C -HMBC correlations for compounds **74** and **84**, B) ^1H , ^1H -NOESY correlations for compounds **74** and **84**.



i: Phthalic anhydride 1 eq, dry THF, rt, 18 h

ii: NaH 1.1 eq, diethyl (tosyloxy)methyl phosphonate 1.3 eq, dry THF, 0-25 °C, 24 h

Scheme 5. Synthesis of terminal alkynes **87** and **88**.

suggested that any of these compounds seemed to be blocking any of the steps covering from the binding of the viral particles to the host cell until the arrival of HAdV genomes into the nucleus. This result agrees on the result obtained for the serinol derivative, where none of them showed a significant inhibition of the HAdV genomes accessibility into the nucleus [25].

2.2.2.2. Impact on HAdV DNA replication. We next considered if they might be acting at the HAdV DNA replication process once the HAdV genomes get into the cell nucleus. In this sense we quantified the HAdV DNA replication in the presence of the compounds by quantitative real-time PCR after extracting the DNA from cells after 16 h of incubation as a measure of the DNA replication efficiency.

Since compounds **17**, **20**, **34** and **60** showed no significant inhibition

Table 4

IC₅₀, CC₅₀, SI, and virus yield reduction values for selected compounds and for cidofovir as approved clinical drug^a.

Comp.	IC ₅₀ (μM) ^b	CC ₅₀ (μM) ^c	SI ^d	Yield reduction (fold-reduction) ^e
17	5.75 ± 1.01	139.95 ± 31.13	24.34	48.18 ± 25.03
20	2.47 ± 0.07	28.70 ± 3.10	11.63	11.54 ± 4.23
26	4.19 ± 2.59	97.25 ± 16.56	23.20	19.46 ± 3.69
34	2.79 ± 0.29	175.16 ± 2.97	62.68	194.61 ± 36.89
44	4.67 ± 0.05	136.62 ± 6.54	29.25	285.65 ± 54.15
60	3.02 ± 0.08	>200	66.23	17.80 ± 5.35
66	3.12 ± 0.44	174.32 ± 4.52	55.87	1.52 ± 0.79
Cidofovir	24.06 ± 5.9	179.09 ± 35.10	7.5	82.5 ± 21.4

^a All results are shown as means ± SD of duplicate samples from two independent experiments.

^b Inhibitory concentration 50 obtained in a plaque assay.

^c Cytotoxic concentration 50.

^d Selectivity index value was determined as the ratio of IC₅₀ and CC₅₀.

^e Fold-reduction in virus yield as the ratio of particles produced in the presence of DMSO divided by the yield in the presence 10-fold IC₅₀ concentration obtained in the plaque assay of each compound.

of the HAdV DNA replication comparing to the DMSO control (Fig. 7), their mechanism of action must be related with viral processes beyond the HAdV DNA replication as for example, viral proteins maturation or viral capsid assembly. On the other hand, the presence of compounds **26**, **44** and **66** resulted in a significant reduction in the number of HAdV

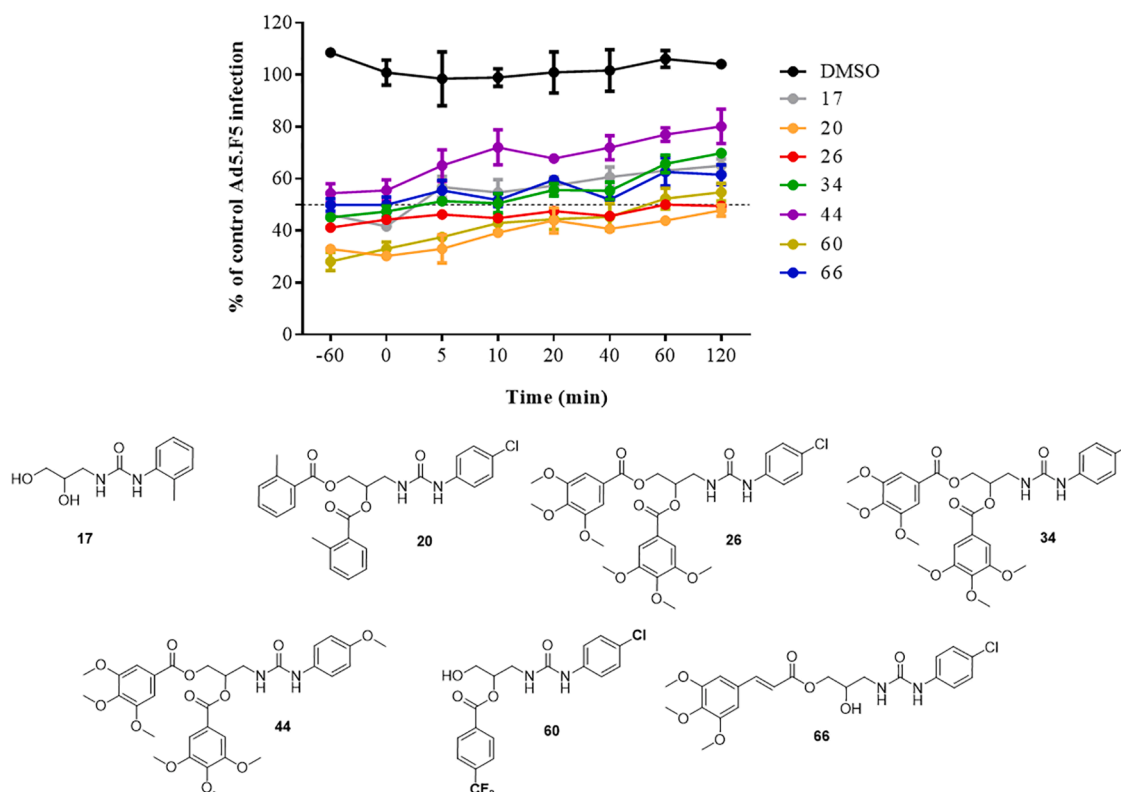


Fig. 5. Time-dependence curve assay. Effect of selected compounds on HAdV infection at different time points at 10-fold the IC_{50} concentration obtained in the plaque assay of each compound. The line chart represents mean \pm SD of duplicate samples.

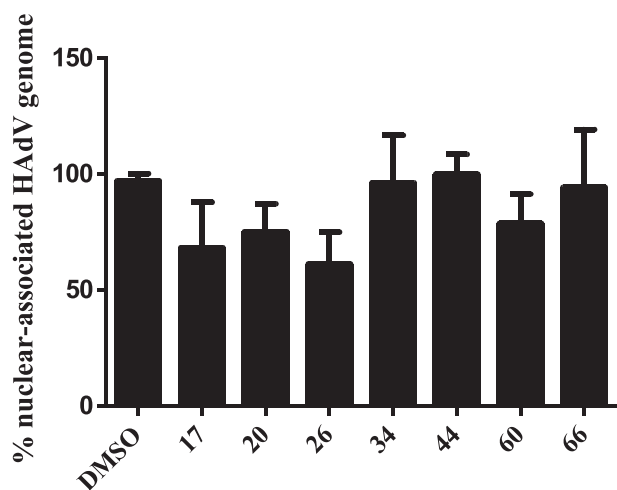


Fig. 6. Percentage of the nuclear-associated HAdV genome of selected compounds. Compounds were added at 10-fold the IC_{50} concentration obtained in the plaque assay of each compound. Each bar represents mean \pm SD of duplicate samples.

copies comparing with DMSO. Thus, since they did not block genome accessibility to the nucleus we value two possible scenarios for this results; i) these three compounds could be targeting any of the viral proteins involved in the HAdV DNA replication, such as the terminal protein (pTP), the HAdV DNA polymerase or the DNA-binding protein (DBP); ii) they could be targeting the transcription of HAdV immediately early proteins, a process occurring once the HAdV genomes access the cell nucleus and essential for the subsequent initiation of the HAdV DNA replication.

To assay the inhibition of HAdV mRNA transcription by these three

derivatives, we infected A549 cells in the presence of these compounds at the specified concentrations for 6 h. Then, we quantified the mRNA copy number of the HAdV immediately early genes E1A and E2B, using quantitative reverse transcription (RT-PCR). As shown in Fig. 8, only compound 66 reduced significantly the copy number of the E1A mRNA at 6 h post-infection compared to the DMSO control. The ability of compound 66 to reduce the expression of HAdV E1A gene transcription would explain the inhibitory effect observed on HAdV DNA replication. However, in case of compounds 26 and 44, the reduction of HAdV DNA quantified by qPCR seemed to be related to a direct inhibition of the HAdV DNA replication process rather than to the inhibition of either E1A or E2B genes transcription.

It is worth it to mention that in our previous work any of the monoester derivatives were found to have anti-HAdV activity while compound 66, not only showed significant antiviral activity at low micromolar concentration but also, this activity seems to be associated with the inhibition of the HAdV E1A gene expression [25].

2.2.3. Synergistic activity of the selected derivatives

As three different potential mechanisms of action were identified, we decided to evaluate the antiviral activity of the combination of three representative compounds for each mechanism with the hypothesis that their combination would result in an improved antiviral activity due to their synergistic effect activity. The selected compounds for this assay were compound 44, targeting specifically the HAdV DNA replication process, compound 66 that targeted HAdV E1A mRNA transcription, and compound 20 whose mechanism of action was associated with later steps after HAdV DNA replication. We employed a combination study based on the Chou – Talalay method for drug combination using CalcuSyn software [48] and plaque assay starting from $2 \times IC_{50}$ and in serial 2-fold dilutions. The constant ratio for each combination was selected based on the IC_{50} values for each drug. The data for all the combinations showed good conformity with the mass action law principle ($r =$

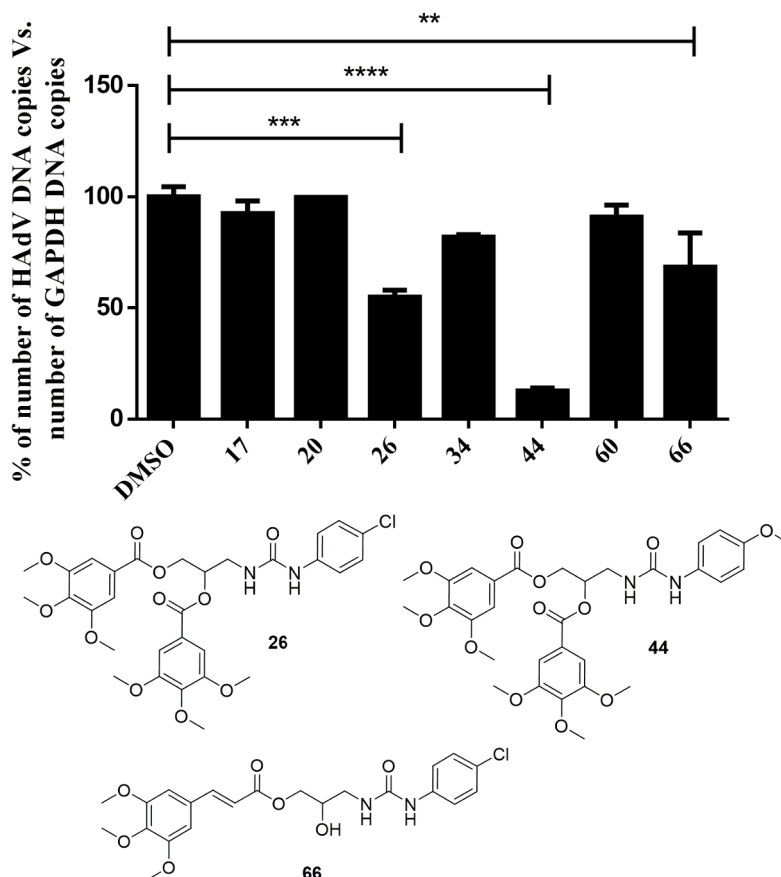


Fig. 7. Effect of selected compounds on HAdV DNA replication. Compounds were added at 10-fold the IC_{50} concentration obtained in the plaque assay of each compound. Results are expressed as the relative copy number of HAdV DNA normalized to GAPDH copy number. Each bar represents mean \pm SD of duplicate samples. Statistical significance is pointed as $**p \leq 0.01$, $***p \leq 0.001$, and $****p \leq 0.0001$.

0.97–0.99). Only the combination between compounds **66** and **44** (ratio 1:1.498) resulted in a nearly additive effect at all effective dose values. The combinations that included compounds **20** and **44** (ratio 1:1.891) were classified as slightly antagonistic at their ED_{50} , antagonistic at the ED_{75} and strongly antagonistic at their ED_{90} . As for the combinations between compounds **20** and **66** (ratio 1:1.263) they resulted in all cases as slightly antagonistic. In case of combination between **20** and **66**, all ED values maintained a slight antagonistic effect (Table 5).

2.3. *In silico* prediction of drug-likeness and pharmacokinetics properties

Since many potential therapeutic candidates fail to reach the clinic because of their unfavorable ADME behaviours, the estimation of physicochemical and pharmacokinetics properties in early stages of the drug discovery process is an important tool for decreasing the fraction of these failures in later phases of development.

Firstly, the physico-chemical parameters of the selected compounds were predicted by the use of Molsoft software (<https://www.molsoft.com>) [49,50] to assess their compliance with the Lipinski's rule of five, the theoretical agreement for a molecule to become an oral drug with respect to bioavailability.

The obtained results illustrated in Table 6, showed that compounds **17**, **20**, **60** and **66** are in agreement with Lipinski's rule (with only one violation $\text{Log P} > 5$ for compound **20**). However, compounds **26**, **34** and **44** failed with two violations, Log P and Molecular Weight values, exceeding the accepted ranges. In addition, topological polar surface area PSA (a criteria that allows the prediction of transport properties of polar atoms through membranes) was also predicted (all the tested compounds had TPSA values $< 140 \text{ \AA}^2$), and used to calculate the percentage of oral absorption (%ABS) by the following equation: (%ABS

= $109 - (0.345 \text{ TPSA})$ [51]. Not only those compounds that confirmed Lipinski's rule exhibited high oral absorption (%ABS of 85.82, 83.15, 84.44 and 76.57, respectively), but also compounds **26**, **34** and **44** (those failed Lipinski's rule) showed moderate-high %ABS (in an accepted value range 65–67%). Drug likeness is a complex balance between various molecular properties like molecule size, hydrogen bonding characters, electronic distribution and hydrophobicity [52]. The more positive drug likeness score values, the more likely the compound was expected to be as a promising therapeutic pharmacophore [53]. A positive model score was attributed for all compounds excepting **17**, which stranded for good drug likeness behaviour, especially compounds **20**, **26**, **44** and **66** (score ≥ 1) (Supplementary Material, S63).

Secondly, predicted absorption, distribution, metabolism and excretion (ADME) data were calculated for the most active compounds using preADMET software (<https://preadmet.bmdrc.kr>) and results are presented in Table 7.

Absorption refers to the process by which the drug can go to the systemic circulation through the organs of the body. Several routes for absorption such as oral absorption (human intestinal absorption, HIA), skin permeability (SP, log Kp), and permeability through certain cells such as Caco2 (a human colon epithelial cancer cell line that differentiates to form tight junctions between cells to serve as a model of paracellular movement of compounds across the monolayer) and MDCK cells (MDCK permeability coefficient provided helpful *in vitro* tools to assess a drug's permeability and transporter interactions during drug discovery and development) were measured [53].

By inspecting results recorded in Table 7, it was found that all compounds showed good intestinal absorption, six out of seven $> 90\%$ (normal range for well absorbed compounds 70–100% abs). Moderate permeability through *in vitro* Caco2 cells ranged from 15.40 to 40.88

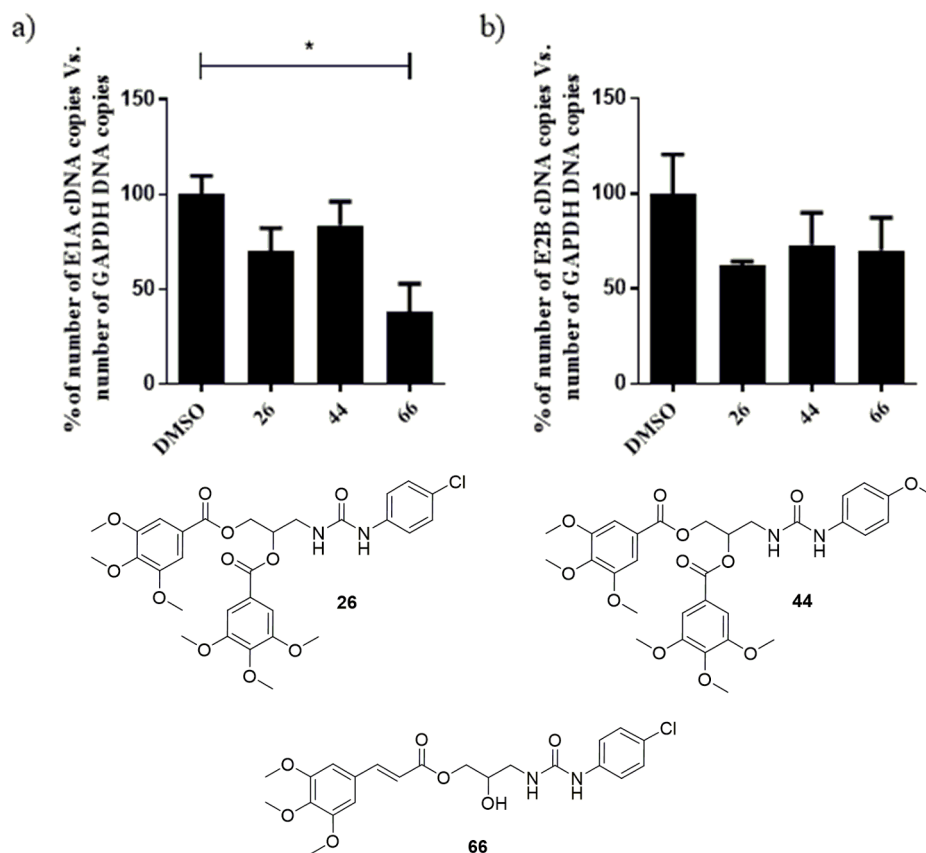


Fig. 8. Effect of the selected compounds on HAdV E1A (a) and E2B (b) gene expression. Compounds were tested at 10-fold the IC_{50} concentration obtained in the plaque assay of each compound. Results are expressed as the relative copy number of HAdV E1A or E2B mRNA normalized to GAPDH copy number. Each bar represents mean \pm SD of duplicate samples. Statistical significance is pointed as $*p \leq 0.05$.

Table 5

IC_{50} values in a plaque assay for each compound and its combination with the combination index value calculated with CalcuSyn software.

Combination (Ratio)	Compound	IC_{50} single	IC_{50} combination	Combinatory index (CI) values in Plaque assay			
				ED_{50}	ED_{75}	ED_{90}	r
20 & 44 (1:1.891)	20	2.47 ± 0.07	2.1 ± 0.04	1.19	1.46	1.81	0.99
	44	4.67 ± 0.05	3.96 ± 0.07				
20 & 66 (1:1.263)	20	2.47 ± 0.07	2.08 ± 0.37	1.15	1.12	1.11	0.98
	66	3.12 ± 0.44	2.26 ± 0.43				
66 & 44 (1:1.498)	66	3.12 ± 0.44	1.65 ± 0.09	0.97	1.03	1.10	0.97
	44	2.47 ± 0.07	2.46 ± 0.14				

Table 6

Calculated parameters of Lipinski's rule for selected compounds.

Compound	Parameter							
	MW	LogP	HBD	HBA	nVs	MolPSA	%ABS	Drug-likeness score
AR	≤ 500	≤ 5	≤ 5	≤ 100	≤ 1	≤ 140	–	–
17	224.12	0.32	4	3	0	67.17	85.82	–0.08
20	480.15	6.11	2	5	1	74.92	83.15	1.27
26	632.18	4.74	2	11	2	120.88	67.29	1.20
34	612.23	4.59	2	11	2	120.88	67.29	0.88
44	628.23	4.10	2	12	2	128.42	64.69	1.00
60	416.08	4.25	3	4	0	71.18	84.44	0.26
66	464.14	3.78	3	7	0	94.00	76.57	0.93

AR: accepted range; MW, Molecular weight; LogP, lipophilicity (O/W); HBD, Number of hydrogen bond donors; HBA, Number of hydrogen bond acceptors; nVs, Number of Lipinski rule violations; MolPSA, molecular polar surface area (PSA) (\AA^2); %ABS, percentage of oral absorption.

Table 7
Predicted ADMET properties of selected compounds.

Parameter	Compound						
	17	20	26	34	44	60	66
Absorption							
HIA (%)	72.97	95.62	96.73	95.86	94.63	91.65	92.40
Caco2 (nm/sc)	15.40	26.19	33.73	39.62	40.88	18.80	22.07
SP LogP (cm/h)	-4.16	-2.16	-2.90	-2.89	-3.05	-2.74	-3.17
MDCK (nm/sc)	12.84	0.04	0.04	0.04	0.04	0.12	0.06
Distribution							
BBB	0.27	1.03	0.02	0.02	0.03	1.16	0.11
PPB (%)	20.26	89.45	89.63	89.75	88.01	86.46	84.31
Metabolism (CYP) and excretion							
CYP2C19 inhibitor	no	no	no	no	no	no	no
CYP2D6 inhibitor	no	no	no	no	no	no	no
CYP3A4 inhibitor	no	no	yes	yes	yes	no	no
Pgp inhibitor	no	yes	yes	yes	yes	no	no

HIA: Intestinal absorption; Caco2: permeability through cells derived from human colon adenocarcinoma; SP LogP: skin permeability; MDCK: permeability through Madin-Darby canine kidney cells; BBB: Blood-Brain Barrier; PPB: Plasma-protein binding; CYP: cytochrome P450; Pgp: P-glycoprotein.

nm/sc was observed (normal range 4–70 nm/s); the skin permeability was found to be slightly less than acceptable range (-2.5 logKp), while low values were detected for *in vitro* MDCK cells.

Two parameters, blood brain barrier (BBB) and plasma binding protein (PPB), were measured to predict the distribution of molecules from one organ to another. BBB permits the diffusion to the brain for small hydrophobic molecules; this parameter evaluates whether compounds pass across the blood–brain barrier. The measurement of the percentage of a molecule bound to plasma protein (PPB%) is also helpful in estimation of the novel target compounds distribution (only the unbound fraction is available to pass across membranes and for the interaction with the target). Results showed that most of the tested compounds displayed high PPB values (84.31–89.75), quite close to that what it is consider strong bound to plasma proteins (>90%). Only compound **17** showed weak bound (PPB 20.26%). BBB was low (<0.1) for compounds **26**, **34** and **44**, and medium (normal medium range ≤ 0.1–2) for **17**, **20**, **60** and **66**. Two compounds, **20** and **60**, are in the acceptable range to be central nervous systems active compounds (>0.4) with BBB values 1.03 and 1.16 respectively.

Cytochrome P450 isoforms predicts the ability of compounds to be inhibitors for drug metabolizing enzymes such as CYP2C19, CYP2D6 and CYP3A4. In this study, the tested compounds did not show inhibition behaviour for CYP2C19 and CYP2D6. An inhibitory effect on Pgp was detected in four compounds (**20**, **26**, **34** and **44**), while inhibitory behaviour on CYP3A4 was detected for compounds **26**, **34** and **44**.

3. Conclusion

To sum up, a set of new compounds derived from 3-amino-1,2-propanediol, in which the nitrogen was functionalized as phenyl urea and hydroxyl groups as substituted benzoyl esters or triazoles, has been designed, synthesized, and the antiviral activity against HAdV was evaluated. Seven selected compounds showed significant anti-HAdV activity within low micromolar ranges, with low cytotoxicity. Our mechanistic studies suggest that compounds **26** and **44** target the replication of HAdV DNA by interfering with some of the viral proteins involved in this process. Compound **66** would block the transcription of the HAdV E1A gene which is essential to subsequently carry out HAdV DNA replication, and compounds **17**, **20**, **34** and **60** would interfere with later steps of HAdV life cycle after DNA replication, although further evaluations will be needed for deeper characterization of their precise mechanism of action. Physicochemical properties, drug likeness scores and pharmacokinetic profiles were predicted for the seven selected compounds. While compounds **17**, **20**, **60** and **66** resulted to be in agreement with Lipinski's rule of five (showing high oral absorption), compounds **26**, **34** and **44** failed with two violations (moderate-high oral absorption). In general, all of the selected compounds exhibited

acceptable physicochemical properties, favourable oral bioavailability and good drug-likeness scores (most of them).

Although further rounds of optimization as well as a better understanding of their mode of action will be required, these molecules, inspired by the aminoglycerol backbone, represent a promising starting point for the development of a new class of antiviral compounds.

4. Experimental Section

4.1. Chemistry

4.1.1. General chemistry methods

All reagents, solvents, and starting materials were obtained from commercial suppliers and were used without further purification. The crude reaction mixtures were concentrated under reduced pressure by removing the organic solvents in a rotary evaporator. Reactions were monitored by thin layer chromatography (TLC) using Kieselgel 60 F₂₅₄ (E. Merck) plates and UV detector for visualization. Flash column chromatography was performed on Silica Gel 60 (E. Merck). All reported yields are of purified products. Melting points were obtained on a Stuart Melting Point Apparatus SMP 10 and are uncorrected. Mass spectra were recorded on a Micromass AUTOSPECQ mass spectrometer: CI at 150 eV, HR mass measurements with resolutions of 10,000. FAB mass spectra were recorded using a thioglycerol matrix. NMR spectra were recorded at 25 °C on a Bruker AV500 spectrometer at 500 MHz for ¹H and 125 MHz for ¹³C. COSY, DEPT, HSQC, and HMBC experiments were performed to assign the signals in the NMR spectra. The chemical shifts (δ) reported are given in parts per million (ppm) on the δ scale relative to TMS, and the coupling constants (J) are in hertz (Hz). ¹H chemical shift values (δ) are referenced to the residual nondeuterated components of the NMR solvents ($\delta = 2.54$ ppm for DMSO, $\delta = 7.26$ ppm for CDCl₃). The ¹³C chemical shifts (δ) are referenced to deuterated solvent (central peak, $\delta = 39.5$ ppm for DMSO and 49.15 ppm for MeOD) as the internal standard. The spin multiplicities are reported as s (singlet), d (doublet), t (triplet), q (quadruplet), m (multiplet), or br s (broad singlet). The purity of final compounds was evaluated by elemental analysis (C, H, and N). The purity of all the final compounds was confirmed to be $\geq 95\%$ by combustion.

4.1.2. General procedure for the synthesis of urea derivatives (**13**–**17**, and **68**)

To a solution of the appropriate isocyanate (3.6 mmol) in dry DCM (20 mL), a solution of the aminoalcohol **12** (3.0 mmol) in methanol (1 mL) was added dropwise. A white precipitate appeared that was filtered at *vacuum* and washed with fresh DCM to give urea derivative.

4.1.2.1 *N*-(4-Chlorophenyl)-*N'*-(2,3-dihydroxypropyl)urea (**13**). The product was obtained as a white solid (690 mg, 94% yield), mp

160–161 °C. ^1H NMR (500 MHz, DMSO- d_6) δ 8.76 (s, 1H, NHAr), 7.37–7.35 (m, 2H, Ar), 7.25–7.23 (m, 2H, Ar), 6.19 (t, J = 5.5 Hz, 1H, CH_2NH), 5.01 (d, J = 4.9 Hz, 1H, CHOH), 4.82 (t, J = 5.2 Hz, 1H, CH_2OH), 3.56–3.50 (m, 2H, CH_2OH), 3.38–3.30 (m, 2H, CH_2NH), 3.03–2.98 (m, 1H, CH). ^{13}C NMR (125 MHz, DMSO- d_6) δ 155.6, 139.1, 128.4, 124.8, 119.4, 70.5, 63.5, 42.4. HRMS (m/z): calcd for $\text{C}_{10}\text{H}_{13}\text{ClN}_2\text{O}_3\text{Na}$ 267.0507 [$\text{M} + \text{Na}$] $^+$; found 267.0501. Anal. Calcd for $\text{C}_{10}\text{H}_{13}\text{ClN}_2\text{O}_3$: C, 49.09; H, 5.36; N, 11.45. Found: C, 49.51; H, 5.66; N, 11.34.

4.1.2.2 *N*-(2,3-Dihydroxypropyl)-*N'*-(4-methylphenyl)urea (14). The product was obtained as a white solid (615 mg, 91% yield), mp 147–148 °C. ^1H NMR (500 MHz, DMSO- d_6) δ 8.48 (s, 1H, NHAr), 7.26 (d, J = 8.5 Hz, 2H, Ar), 7.03 (d, J = 8.2 Hz, 2H, Ar), 6.10 (t, J = 5.6 Hz, 1H, CH_2NH), 4.85 (d, J = 4.9 Hz, 1H, CHOH), 4.60 (t, J = 5.7 Hz, 1H, CH_2OH), 3.51 (sex, J = 5.6 Hz, 1H, CH), 3.32–3.27 (m, 2H, CH_2OH), 3.01–2.95 (m, 2H, CH_2NH), 2.22 (s, 3H, CH_3). ^{13}C NMR (125 MHz, DMSO- d_6) δ 155.6, 138.1, 129.6, 129.0, 117.6, 70.7, 63.7, 42.5, 20.3. HRMS (m/z): calcd for $\text{C}_{11}\text{H}_{16}\text{N}_2\text{O}_3\text{Na}$ 247.1064 [$\text{M} + \text{Na}$] $^+$; found 247.1056. Anal. Calcd for $\text{C}_{11}\text{H}_{16}\text{N}_2\text{O}_3$: C, 58.91; H, 7.19; N, 12.49. Found: C, 58.53; H, 7.03; N, 12.16.

4.1.2.3 *N*-(2,3-Dihydroxypropyl)-*N'*-[4-(trifluoromethyl)phenyl]urea (15). The product was obtained as a white solid (673 mg, 80% yield), mp 135–136 °C. ^1H NMR (500 MHz, DMSO- d_6) δ 9.04 (s, 1H, NHAr), 7.60–7.57 (m, 4H, Ar), 6.30 (t, J = 5.3 Hz, 1H, CH_2NH), 4.88 (d, J = 5.0 Hz, 1H, CHOH), 4.61 (t, J = 5.6 Hz, 1H, CH_2OH), 3.57–3.51 (m, 1H, CH), 3.35–3.30 (m, 2H, CH_2OH), 3.04–2.99 (m, 2H, CH_2NH). ^{13}C NMR (125 MHz, DMSO- d_6) δ 155.0, 144.2, 125.9, 121.0, 120.8, 117.1, 70.5, 63.7, 42.5. HRMS (m/z): calcd for $\text{C}_{11}\text{H}_{13}\text{F}_3\text{N}_2\text{O}_3\text{Na}$ 301.0770 [$\text{M} + \text{Na}$] $^+$; found 301.0769. Anal. Calcd for $\text{C}_{11}\text{H}_{13}\text{F}_3\text{N}_2\text{O}_3$: C, 47.49; H, 4.71; N, 10.07. Found: C, 49.51; H, 5.66; N, 11.34.

4.1.2.4 *N*-(2,3-Dihydroxypropyl)-*N'*-(4-methoxyphenyl)urea (16). The product was obtained as a white solid (635 mg, 88% yield), mp 155–156 °C. ^1H NMR (300 MHz, DMSO- d_6) δ 8.39 (s, 1H, NHAr), 7.28 (d, J = 6.8 Hz, 2H, Ar), 6.81 (d, J = 6.8 Hz, 2H, Ar), 6.03 (t, J = 5.5 Hz, 1H, CH_2NH), 4.85 (d, J = 4.8 Hz, 1H, CHOH), 4.60 (t, J = 5.7 Hz, 1H, CH_2OH), 3.69 (s, 3H, OCH_3), 3.53–3.44 (m, 1H, CH), 3.38–3.23 (m, 2H, CH_2OH), 3.02–2.92 (m, 2H, CH_2NH). ^{13}C NMR (125 MHz, DMSO- d_6) δ 156.2, 154.1, 134.2, 119.7, 114.3, 71.2, 64.1, 55.6, 43.1. HRMS (m/z): calcd for $\text{C}_{11}\text{H}_{16}\text{N}_2\text{O}_4\text{Na}$ 263.1002 [$\text{M} + \text{Na}$] $^+$; found 263.1003.

4.1.2.5 *N*-Allyl-*N'*-(4-chlorophenyl)urea (68). The product was obtained as a white solid and purified by column chromatography using dichloromethane-methanol (140:1) as eluent (570 mg, 90% yield). ^1H NMR (500 MHz, DMSO- d_6) δ 8.66 (s, 1H, NHAr), 7.46 (d, J = 8.3 Hz, 2H, Ar), 7.30 (d, J = 8.7 Hz, 2H, Ar), 6.32 (t, J = 5.3 Hz, 1H, CH_2NH), 5.91–5.87 (m, 1H, $\text{CH}_2 = \text{CH}$), 5.23–5.18 (m, 1H, $\text{CH}_2 = \text{CH}$), 5.13–5.08 (m, 1H, $\text{CH}_2 = \text{CH}$), 3.77 (t, J = 5.4 Hz, 1H, CH_2NH). ^{13}C NMR (125 MHz, DMSO- d_6) δ 154.9, 139.4, 136.2, 128.6, 128.4, 124.5, 119.8, 119.1, 114.7, 41.4. HRMS (m/z): calcd for $\text{C}_{10}\text{H}_{12}\text{ClN}_2\text{O}$ 211.0633 [$\text{M} + \text{H}$] $^+$; found 211.0633. Anal. Calcd for $\text{C}_{10}\text{H}_{11}\text{ClN}_2\text{O}$: C, 57.02; H, 5.26; N, 13.30. Found: C, 56.79; H, 5.03; N, 12.86.

4.1.2.6 *N*-(2,3-Dihydroxypropyl)-*N'*-(2-methylphenyl)urea (17). According to the published procedure [54], a solution of *o*-methyl aniline (1.2 mmol) in DCM (25 mL) was added to a solution of Na_2CO_3 (1.9 mmol) in water (25 mL) and the reaction mixture was vigorously stirred for 5 min at rt; then triphosgene (0.39 mmol) was added and the solution was stirred for additional 30 min. After this time, 3-amino-1,2-propanediol (**11**, 1.8 mmol) was added dropwise to the flask and the solution was stirred at rt until TLC showed the full consumption of the starting material (2 h). The mixture was separated and the inorganic layer was extracted with ethyl acetate (3 \times 40 mL). The combined organic layers were dried (MgSO_4), filtered and evaporated *in vacuo* to obtain the compound as a white resin. (455 mg, 67% yield). ^1H NMR (300 MHz, DMSO- d_6) δ 7.87–7.77 (m, 2H, NHAr, Ar), 7.13–7.04 (m, 1H, Ar), 6.85 (t, J = 7.3 Hz, 2H, Ar), 6.63 (t, J = 5.2 Hz, 1H, CH_2NH), 4.89–4.84 (m, 1H, CHOH), 4.63–4.56 (m, 1H, CH_2OH), 3.55–3.46 (m, 1H, CH), 3.33–3.25 (m, 2H, CH_2OH), 3.03–2.93 (m, 2H, CH_2NH), 2.18 (s, 3H, CH_3). ^{13}C NMR (125 MHz, DMSO- d_6) δ 156.2, 138.7, 130.5, 127.0,

126.5, 122.2, 120.8, 71.3, 64.1, 42.9, 18.4. HRMS (m/z): calcd for $\text{C}_{11}\text{H}_{16}\text{N}_2\text{O}_3\text{Na}$ 247.1053 [$\text{M} + \text{Na}$] $^+$; found 247.1055. Anal. Calcd for $\text{C}_{11}\text{H}_{16}\text{N}_2\text{O}_3$: C, 58.91; H, 7.19; N, 12.49. Found: C, 58.67; H, 7.21; N, 12.49.

4.1.3. General procedure for the synthesis of diester derivatives by reaction with acyl chlorides (18–44)

To a solution of the urea derivative (13–17) (0.54 mmol) in dry DCM (20 mL) and DMAP (1.3 mmol), the appropriate acylating agent (1.1 mmol) in dry DCM (5 mL) was added. The reaction mixture was stirred at rt until TLC showed that all the starting material had reacted (24 h), then was washed with 1 N aqueous solution of HCl (2 \times 20 mL), saturated solution of NaHCO_3 (2 \times 20 mL) and brine (20 mL). The organic layer was dried (Na_2SO_4), filtered and evaporated under reduced pressure. The compound was further purified by flash column chromatography on silica gel using the appropriate eluent.

4.1.3.1 *N*-[2,3-Bis(benzoyloxy)propyl]-*N'*-(4-chlorophenyl)urea (18). The product was obtained as a white solid and purified by column chromatography using hexane–ethyl acetate (1:1) as eluent (160 mg, 70% yield), mp 130–131 °C. NMR (500 MHz, DMSO- d_6) δ 8.72, (s, 1H, NHAr), 8.02 (d, J = 7.5 Hz, 2H, Ar), 7.95 (d, J = 7.5 Hz, 2H, Ar), 7.60–7.52 (m, 2H, Ar), 7.55–7.49 (m, 4H, Ar), 7.43 (d, J = 8.8 Hz, 2H, Ar), 7.28 (d, J = 8.7 Hz, 2H, Ar), 6.50 (t, J = 5.9 Hz, 1H, CH_2NH), 5.52–5.45 (m, 1H, CH), 4.67 (dd, J = 3.4 Hz, J = 12.0 Hz, 1H, CH_2O), 4.52 (dd, J = 6.6 Hz, J = 12.0 Hz, 1H, CH_2O), 3.70–3.58 (m, 2H, CH_2NH). ^{13}C NMR (125 MHz, DMSO- d_6) δ 165.4, 165.3, 155.2, 139.3, 133.4, 129.6, 129.4, 129.3, 129.1, 128.7, 128.6, 128.4, 124.7, 119.2, 71.0, 63.7, 39.5. HRMS (m/z): calcd for $\text{C}_{24}\text{H}_{21}\text{ClN}_2\text{O}_5\text{Na}$ 475.1031 [$\text{M} + \text{Na}$] $^+$; found 475.1026.

4.1.3.2 *N*-[2,3-Bis(4-methylbenzoyloxy)propyl]-*N'*-(4-chlorophenyl)urea (19). The product was obtained as a colourless oil and purified by column chromatography using hexane–ethyl acetate (1.5:1) as eluent (205 mg, 85% yield). MS (FAB): m/z 503 (100%) [$\text{M} + \text{Na}$] $^+$. ^1H NMR (500 MHz, DMSO- d_6) δ 8.72, (s, 1H, NHAr), 7.89–7.87 (m, 2H, Ar), 7.83–7.81 (m, 2H, Ar), 7.42–7.40 (m, 2H, Ar), 7.33–7.29 (m, 4H, Ar), 7.27–7.25 (m, 2H, Ar), 6.28 (t, J = 5.8 Hz, 1H, CH_2NH), 5.46–5.41 (m, 1H, CH), 4.61 (dd, J = 4.1 Hz, J = 12.0 Hz, 1H, CH_2O), 4.46 (dd, J = 6.0 Hz, J = 11.6 Hz, 1H, CH_2O), 3.62–3.54 (m, 2H, CH_2NH), 2.38 (s, 3H, CH_3), 2.37 (s, 3H, CH_3). ^{13}C NMR (125 MHz, DMSO- d_6) δ 165.4, 165.2, 155.1, 143.8, 143.6, 139.3, 129.4, 129.3, 129.2, 129.1, 128.4, 126.8, 124.4, 119.2, 71.3, 65.7, 30.7, 21.2, 21.1. Anal. Calcd for $\text{C}_{26}\text{H}_{25}\text{ClN}_2\text{O}_5$: C, 64.93; H, 5.24; N, 5.82. Found: C, 64.82; H, 5.76; N, 5.74.

4.1.3.3 *N*-[2,3-Bis(2-methylbenzoyloxy)propyl]-*N'*-(4-chlorophenyl)urea (20). The product was obtained as a colourless oil and purified by column chromatography hexane–ethyl acetate (1.5:1) as eluent (216 mg, 90% yield). MS (FAB): m/z 503 (100%) [$\text{M} + \text{Na}$] $^+$. ^1H NMR (500 MHz, DMSO- d_6) δ 8.72, (s, 1H, NHAr), 7.88–7.86 (m, 1H, Ar), 7.83–7.81 (m, 1H, Ar), 7.50–7.46 (m, 2H, Ar), 7.43–7.41 (m, 2H, Ar), 7.43–7.27 (m, 6H, Ar), 6.48 (t, J = 6.0 Hz, 1H, CH_2NH), 5.50–5.45 (m, 1H, CH), 4.63 (dd, J = 3.4 Hz, J = 12.0 Hz, 1H, CH_2O), 4.48 (dd, J = 6.5 Hz, J = 12.0 Hz, 1H, CH_2O), 3.64–3.55 (m, 2H, CH_2NH), 2.49 (s, 3H, CH_3), 2.48 (s, 3H, CH_3). ^{13}C NMR (125 MHz, DMSO- d_6) δ 167.0, 166.8, 155.6, 139.8, 139.7, 139.6, 132.8, 132.7, 132.1, 132.0, 130.7, 130.6, 129.9, 129.5, 128.9, 126.5, 126.3, 125.2, 119.8, 71.8, 64.1, 31.2, 21.5, 21.4. Anal. Calcd for $\text{C}_{26}\text{H}_{25}\text{ClN}_2\text{O}_5$: C, 64.93; H, 5.24; N, 5.82. Found: C, 64.75; H, 5.58; N, 5.60.

4.1.3.4 *N*-[2,3-Bis(4-methoxybenzoyloxy)propyl]-*N'*-(4-chlorophenyl)urea (21). The product was obtained as a white solid and purified by column chromatography using hexane–ethyl acetate (1:1) as eluent (190 mg, 74% yield), mp 202–203 °C. ^1H NMR (500 MHz, DMSO- d_6) δ 8.71, (s, 1H, NHAr), 7.96–7.94 (m, 2H, Ar), 7.90–7.88 (m, 2H, Ar), 7.44–7.42 (m, 2H, Ar), 7.27–7.25 (m, 2H, Ar), 7.04–7.01 (m, 4H, Ar), 6.48 (t, J = 5.7 Hz, 1H, CH_2NH), 5.45–5.41 (m, 1H, CH), 4.59 (dd, J = 3.5 Hz, J = 12.1 Hz, 1H, CH_2O), 4.46 (dd, J = 6.7 Hz, J = 11.8 Hz, 1H, CH_2O), 3.63–3.55 (m, 2H, CH_2NH), 3.83 (s, 3H, OCH_3), 3.82 (s, 3H, OCH_3). ^{13}C NMR (125 MHz, DMSO- d_6) δ 165.1, 165.0, 163.3, 163.2,

155.1, 139.3, 131.4, 131.3, 128.4, 124.7, 121.8, 121.5, 119.2, 114.0, 113.9, 71.2, 63.4, 55.5, 55.4, 31.2. HRMS (*m/z*): calcd for $C_{26}H_{25}ClN_2O_7Na$ 535.1242 [$M + Na$]⁺; found 535.1247.

4.1.3.5. *N*-[2,3-Bis(4-cyanobenzoyloxy)propyl]-*N'*-(4-chlorophenyl)urea (**22**). The product was obtained as a white solid and purified by column chromatography using hexane–ethyl acetate (1.5:1) as eluent (150 mg, 60% yield), mp 205–206 °C. ¹H NMR (500 MHz, DMSO-*d*₆) δ 8.70, (s, 1H, NHAr), 8.13–8.12 (m, 2H, Ar), 8.08–8.06 (m, 2H, Ar), 8.01–7.99 (m, 4H, Ar), 7.40–7.38 (m, 2H, Ar), 7.26–7.23 (m, 2H, Ar), 6.51 (t, *J* = 5.7 Hz, 1H, CH₂NH), 5.50–5.47 (m, 1H, CH), 4.70 (dd, *J* = 3.3 Hz, *J* = 12.4 Hz, 1H, CH₂O), 4.56 (dd, *J* = 6.6 Hz, *J* = 12.0 Hz, 1H, CH₂O), 3.67–3.60 (m, 2H, CH₂NH). ¹³C NMR (125 MHz, DMSO-*d*₆) δ 164.3, 164.2, 155.2, 139.2, 133.5, 133.2, 132.8, 132.7, 129.9, 129.8, 128.4, 124.7, 119.3, 118.0, 117.9, 115.6, 7.23, 64.3. HRMS (*m/z*): calcd for $C_{26}H_{19}ClN_4O_5Na$ 525.0936 [$M + Na$]⁺; found 525.0933. Anal. Calcd for $C_{26}H_{19}ClN_4O_5$: C, 62.09; H, 3.82; N, 11.14. Found: C, 62.25; H, 3.81; N, 11.00.

4.1.3.6. *N*-[2,3-Bis(4-nitrobenzoyloxy)propyl]-*N'*-(4-chlorophenyl)urea (**23**). The product was obtained as a yellow solid and purified by column chromatography using hexane–ethyl acetate (1:1) as eluent (244 mg, 90% yield), mp 216–217 °C. mp 216–217 °C. MS (FAB): *m/z* 565 (100%) [$M + Na$]⁺. ¹H NMR (500 MHz, DMSO-*d*₆) δ 8.70, (s, 1H, NHAr), 8.35–8.33 (m, 4H, Ar), 8.23–8.21 (m, 2H, Ar), 8.18–8.16 (m, 2H, Ar), 7.41–7.38 (m, 2H, Ar), 7.26–7.23 (m, 2H, Ar), 6.53 (t, *J* = 6.01 Hz, 1H, CH₂NH), 5.55–5.51 (m, 1H, CH), 4.74 (dd, *J* = 3.3 Hz, *J* = 12.2 Hz, 1H, CH₂O), 4.60 (dd, *J* = 6.7 Hz, *J* = 12.2 Hz, 1H, CH₂O), 3.70–3.60 (m, 2H, CH₂NH). ¹³C NMR (125 MHz, DMSO-*d*₆) δ 164.1, 163.0, 155.2, 150.4, 150.3, 139.2, 134.9, 134.7, 130.8, 130.6, 128.4, 124.7, 123.9, 123.8, 119.2, 72.5, 64.4.

4.1.3.7. *N*-[2,3-Bis[(4-trifluoromethyl)benzoyloxy]propyl]-*N'*-(4-chlorophenyl)urea (**24**). The product was obtained as a white solid and purified by column chromatography using hexane–ethyl acetate (2:1) as eluent (198 mg, 67% yield), mp 156–157 °C. ¹H NMR (500 MHz, DMSO-*d*₆) δ 8.73, (s, 1H, NHAr), 8.21 (d, *J* = 8.53 Hz, 2H, Ar), 8.16 (d, *J* = 8.62 Hz, 2H, Ar), 7.93–7.88 (m, 4H, Ar), 4.43–4.41 (m, 2H, Ar), 7.28–7.24 (m, 2H, Ar), 6.54 (t, *J* = 5.90 Hz, 1H, CH₂NH), 5.57–5.52 (m, 1H, CH), 4.74 (dd, *J* = 3.6 Hz, *J* = 12.3 Hz, 1H, CH₂O), 4.61 (dd, *J* = 6.6 Hz, *J* = 12.0 Hz, 1H, CH₂O), 3.72–3.62 (m, 2H, CH₂NH). ¹³C NMR (125 MHz, DMSO-*d*₆) δ 164.4, 164.3, 155.2, 139.2, 133.3, 133.1, 133.0, 132.9, 130.2, 130.0, 128.4, 125.8, 125.7, 125.6, 124.7, 122.6, 122.5, 119.2, 72.2, 64.2. HRMS (*m/z*): calcd for $C_{26}H_{19}ClF_6N_2O_5Na$ 611.0779 [$M + Na$]⁺; found 611.0771. Anal. Calcd for $C_{26}H_{19}ClF_6N_2O_5$: C, 53.03; H, 3.25; N, 4.76. Found: C, 52.75; H, 3.36; N, 4.77.

4.1.3.8. *N*-[2,3-Bis(2,4-dimethoxybenzoyloxy)propyl]-*N'*-(4-chlorophenyl)urea (**25**). The product was obtained as a white solid and purified by column chromatography using hexane–ethyl acetate (1:1.5) as eluent (235 mg, 82% yield), mp 113–114 °C. ¹H NMR (500 MHz, DMSO-*d*₆) δ 8.75, (s, 1H, NHAr), 7.78–7.72 (m, 2H, Ar), 7.45 (d, *J* = 8.5 Hz, 2H, Ar), 7.28 (d, *J* = 8.9 Hz, 2H, Ar), 6.65 (s, 2H, Ar), 6.62–6.57 (m, 2H, Ar), 6.42 (t, *J* = 5.7 Hz, 1H, CH₂NH), 5.35–5.30 (m, 1H, CH), 4.47 (dd, *J* = 3.2 Hz, *J* = 12.1 Hz, 1H, CH₂O), 4.37 (dd, *J* = 6.5 Hz, *J* = 12.2 Hz, 1H, CH₂O), 3.85 (d, *J* = 3.3 Hz, 6H, OCH₃), 3.80 (d, *J* = 4.5 Hz, 6H, OCH₃), 3.55 (t, *J* = 5.5 Hz, 2H, CH₂NH). ¹³C NMR (125 MHz, DMSO-*d*₆) δ 164.5, 164.1, 164.0, 163.9, 161.0, 160.9, 155.1, 139.3, 133.2, 133.1, 128.4, 124.6, 119.2, 111.6, 111.3, 105.3, 105.2, 98.9, 70.5, 62.9, 55.7, 55.5. HRMS (*m/z*): calcd for $C_{28}H_{29}ClN_2O_9Na$ 595.1454 [$M + Na$]⁺; found 595.1447. Anal. Calcd for $C_{28}H_{29}ClN_2O_9$: C, 58.69; H, 5.10; N, 4.89. Found: C, 58.25; H, 5.23; N, 4.44.

4.1.3.9. *N*-[2,3-Bis(3,4,5-trimethoxybenzoyloxy)propyl]-*N'*-(4-chlorophenyl)urea (**26**). The product was obtained as a white solid and purified by column chromatography using hexane–ethyl acetate (1:1.5) as eluent (248 mg, 78% yield), mp 163–164 °C. ¹H NMR (500 MHz, DMSO-*d*₆) δ 8.73 (s, 1H, NHAr), 7.41 (d, *J* = 8.7 Hz, 2H, Ar), 7.28–7.25 (m, 4H, Ar), 7.22 (s, 2H, Ar), 6.49 (t, *J* = 8.2 Hz, 1H, CH₂NH), 5.48–5.42 (m, 1H, CH), 4.65 (dd, *J* = 3.4 Hz, *J* = 11.9 Hz, 1H, CH₂O), 4.49–4.42 (m, 1H, CH₂O), 3.81–3.76 (m, 12H, OCH₃), 3.74–3.71 (m, 6H, OCH₃),

3.66–3.55 (m, 2H, CH₂NH). ¹³C NMR (125 MHz, DMSO-*d*₆) δ 165.0, 164.9, 155.2, 152.7, 152.6, 141.9, 141.8, 139.2, 129.2, 128.4, 124.7, 124.6, 124.3, 119.2, 106.8, 106.4, 71.7, 63.6, 60.1, 55.9, 55.8. HRMS (*m/z*): calcd. for $C_{30}H_{33}ClN_2O_{11}Na$ 655.1665 [$M + Na$]⁺; found 655.1653. Anal. Calcd for $C_{30}H_{33}ClN_2O_{11}$: C, 56.92; H, 5.25; N, 4.43. Found: C, 56.80; H, 5.25; N, 4.41.

4.1.3.10. *N*-[2,3-Bis(4-methylbenzoyloxy)propyl]-*N'*-(4-methylphenyl)urea (**27**). The product was obtained as a white solid and purified by column chromatography using hexane–ethyl acetate (2.5:1) as eluent (175 mg, 84% yield), mp 95–96 °C. ¹H NMR (500 MHz, DMSO-*d*₆) δ 8.44 (s, 1H, NHAr), 7.89 (d, *J* = 8.2 Hz, 2H, Ar), 7.82 (d, *J* = 8.2 Hz, 2H, Ar), 7.31 (t, *J* = 6.7 Hz, 4H, Ar), 7.27 (d, *J* = 8.4 Hz, 2H, Ar), 7.02 (d, *J* = 8.3 Hz, 2H, Ar), 6.39 (t, *J* = 6.0 Hz, 1H, CH₂NH), 5.44 (quint, *J* = 5.2 Hz, 1H, CH), 4.62 (dd, *J* = 3.5 Hz, *J* = 8.6 Hz, 1H, CH₂O), 4.47 (dd, *J* = 6.8 Hz, *J* = 5.2 Hz, 1H, CH₂O), 3.63–3.54 (m, 2H, CH₂NH), 2.37 (d, *J* = 4.0 Hz, 6H, CH₃), 2.22 (s, 3H, CH₃). ¹³C NMR (125 MHz, DMSO-*d*₆) δ 165.4, 165.3, 155.3, 143.8, 143.7, 137.7, 129.9, 129.4, 129.3, 129.2, 129.1 (2C), 128.9, 126.9, 126.7, 117.9, 71.4, 63.6, 26.8, 21.1, 20.3. HRMS (*m/z*): calcd for $C_{27}H_{28}N_2O_5Na$ 483.1890 [$M + Na$]⁺; found 483.1884. Anal. Calcd for $C_{27}H_{28}N_2O_5$: C, 70.42; H, 6.13; N, 6.08. Found: C, 69.40; H, 5.96; N, 5.89.

4.1.3.11. *N*-[2,3-Bis(2-methylbenzoyloxy)propyl]-*N'*-(4-methylphenyl)urea (**28**). The product was obtained as a white solid and purified by column chromatography using hexane–ethyl acetate (2.5:1) as eluent (168 mg, 74% yield), mp 116–117 °C. ¹H NMR (500 MHz, DMSO-*d*₆) δ 8.45 (s, 1H, NHAr), 7.87 (d, *J* = 7.7 Hz, 2H, Ar), 7.83 (d, *J* = 7.7 Hz, 2H, Ar), 7.51–7.46 (m, 2H, Ar), 7.34–7.25 (m, 6H, Ar), 7.03 (d, *J* = 8.0 Hz, 2H, Ar), 6.39 (t, *J* = 5.9 Hz, 1H, CH₂NH), 5.50–5.44 (m, 1H, CH), 4.63 (dd, *J* = 3.3 Hz, *J* = 12.1 Hz, 1H, CH₂O), 4.48 (dd, *J* = 6.8 Hz, *J* = 12.1 Hz, 1H, CH₂O), 3.63–3.53 (m, 2H, CH₂NH), 2.49 (s, 6H, CH₃), 2.22 (s, 3H, CH₃). ¹³C NMR (125 MHz, DMSO-*d*₆) δ 166.5, 166.3, 155.3, 139.2, 139.1, 137.7, 132.3, 132.2, 131.6, 131.5, 130.2, 130.1, 129.9, 129.3, 129.1, 129.0, 125.9, 125.8, 117.2, 71.3, 63.5, 21.0, 20.8, 20.2. HRMS (*m/z*): calcd for $C_{27}H_{28}N_2O_5Na$ 483.1890 [$M + Na$]⁺; found 483.1886.

4.1.3.12. *N*-[2,3-Bis(4-methoxybenzoyloxy)propyl]-*N'*-(4-methylphenyl)urea (**29**). The product was obtained as a solid and purified by column chromatography using hexane–ethyl acetate (2:1) as eluent (150 mg, 61% yield), mp 144–145 °C. ¹H NMR (500 MHz, DMSO-*d*₆) δ 8.42 (s, 1H, NHAr), 7.95 (d, *J* = 7.5 Hz, 2H, Ar), 7.89 (d, *J* = 9.1 Hz, 2H, Ar), 7.27 (d, *J* = 8.0 Hz, 2H, Ar), 7.05–7.00 (m, 6H, Ar), 6.37 (t, *J* = 6.0 Hz, 1H, CH₂NH), 5.43–5.39 (m, 1H, CH), 4.58 (dd, *J* = 3.8 Hz, *J* = 11.5 Hz, 1H, CH₂O), 4.45 (dd, *J* = 3.8 Hz, *J* = 11.5 Hz, 1H, CH₂O), 3.83 (s, 6H, OCH₃), 3.62–3.53 (m, 2H, CH₂NH), 2.22 (s, 3H, CH₃). ¹³C NMR (125 MHz, DMSO-*d*₆) δ 165.1, 164.9, 163.3, 155.3, 137.7, 131.4, 131.3, 129.9, 128.9, 121.8, 121.5, 117.9, 114.0, 113.9, 71.3, 63.5, 55.5, 55.4, 20.2. HRMS (*m/z*): calcd for $C_{27}H_{28}N_2O_7Na$ 515.1789 [$M + Na$]⁺; found 515.1783.

4.1.3.13. *N*-[2,3-Bis(4-cyanobenzoyloxy)propyl]-*N'*-(4-methylphenyl)urea (**30**). The product was obtained as a solid and purified by column chromatography using hexane–ethyl acetate (1:1) as eluent (155 mg, 64% yield), mp 181–182 °C. ¹H NMR (500 MHz, DMSO-*d*₆) δ 8.40 (s, 1H, NHAr), 8.13 (d, *J* = 8.2 Hz, 2H, Ar), 8.07 (d, *J* = 8.2 Hz, 2H, Ar), 8.03–7.98 (m, 4H, Ar), 7.23 (d, *J* = 8.4 Hz, 2H, Ar), 7.02 (d, *J* = 8.3 Hz, 2H, Ar), 6.40 (t, *J* = 6.0 Hz, 1H, CH₂NH), 5.51–5.47 (m, 1H, CH), 4.69 (dd, *J* = 3.5 Hz, *J* = 8.6 Hz, 1H, CH₂O), 4.56 (dd, *J* = 6.8 Hz, *J* = 5.2 Hz, 1H, CH₂O), 3.66–3.57 (m, 2H, CH₂NH), 2.22 (s, 3H, CH₃). ¹³C NMR (125 MHz, DMSO-*d*₆) δ 164.3, 164.2, 155.3, 137.6, 133.5, 133.2, 129.9, 129.8, 129.0, 117.9, 115.6, 72.4, 64.3, 39.5, 20.2. HRMS (*m/z*): calcd for $C_{27}H_{22}N_4O_5Na$ 505.1482 [$M + Na$]⁺; found 505.1476. Anal. Calcd for $C_{27}H_{22}N_4O_5$: C, 67.21; H, 4.60; N, 11.61. Found: C, 66.22; H, 4.47; N, 11.14.

4.1.3.14. *N*-[2,3-Bis(4-nitrobenzoyloxy)propyl]-*N'*-(4-methylphenyl)urea (**31**). The product was obtained as a light yellow solid and purified by column chromatography using hexane–ethyl acetate (2:1) as eluent (162 mg, 62% yield), mp 214–215 °C. ¹H NMR (500 MHz, DMSO-*d*₆) δ 8.45 (s, 1H, NHAr), 8.38–8.33 (m, 4H, Ar), 8.24 (d, *J* = 8.4 Hz, 2H, Ar),

8.19 (d, $J = 8.3$ Hz, 2H, Ar), 7.26 (d, $J = 6.0$ Hz, 2H, Ar), 7.03 (d, $J = 7.0$ Hz, 2H, Ar), 6.45 (t, $J = 5$ Hz, 1H, CH₂NH) 5.56–5.52 (m, 1H, CH), 4.75 (dd, $J = 3.5$ Hz, $J = 8.6$ Hz, 1H, CH₂O), 4.62 (dd, $J = 6.8$ Hz, $J = 5.2$ Hz, 1H, CH₂O), 3.71–3.61 (m, 2H, CH₂NH), 2.24 (s, 3H, CH₃). ¹³C NMR (125 MHz, DMSO-*d*₆) δ 164.0, 163.9, 155.3, 150.3, 137.6, 134.9, 134.6, 130.7, 130.6, 129.9, 128.9, 123.8, 117.8, 72.5, 64.4, 39.5, 20.2. HRMS (m/z): calcd for C₂₅H₂₂N₄O₉Na 545.1279 [M + Na]⁺; found 545.1274. Anal. Calcd for C₂₅H₂₂N₄O₉: C, 57.47; H, 4.24; N, 10.72. Found: C, 56.99; H, 4.20; N, 10.68.

4.1.3.15. *N*-[2,3-Bis[4-(trifluoromethyl)benzoyloxy]propyl]-*N'*-(4-methylphenyl) urea (**32**). The product was obtained as a white solid and purified by column chromatography using hexane–ethyl acetate (2:1) as eluent (179 mg, 63% yield), mp 137–138 °C. ¹H NMR (500 MHz, DMSO-*d*₆) δ 8.43 (s, 1H, NHAr), 8.20 (d, $J = 8.2$ Hz, 2H, Ar), 8.15 (d, $J = 8.2$ Hz, 2H, Ar), 7.92 (d, $J = 7.0$ Hz, 4H, Ar), 7.26 (d, $J = 8.4$ Hz, 2H, Ar), 7.04 (d, $J = 8.3$ Hz, 2H, Ar), 6.43 (t, $J = 6.1$ Hz, 1H, CH₂NH), 5.55–5.51 (m, 1H, CH), 4.74 (dd, $J = 3.4$ Hz, $J = 8.7$ Hz, 1H, CH₂O), 4.60 (dd, $J = 6.7$ Hz, $J = 5.4$ Hz, 1H, CH₂O), 3.70–3.60 (m, 2H, CH₂NH), 2.24 (s, 3H, CH₃). ¹³C NMR (125 MHz, DMSO-*d*₆) δ 164.4, 164.3, 155.4, 137.6, 133.3, 133.1, 133.0, 132.8, 132.6, 130.2, 130.0, 129.9, 129.0, 125.9, 125.8, 125.7, 125.6, 124.7, 122.6, 117.9, 72.3, 64.2, 20.2. HRMS (m/z): calcd for C₂₇H₂₂F₆N₂O₅Na 681.4719 [M + Na]⁺; found 681.4715. Anal. Calcd for C₂₇H₂₂F₆N₂O₅: C, 57.05; H, 3.90; N, 4.93. Found: C, 56.80; H, 3.88; N, 4.90.

4.1.3.16. *N*-[2,3-Bis(2,4-dimethoxybenzoyloxy)propyl]-*N'*-(4-methylphenyl)urea (**33**). The product was obtained as a white resin and purified by column chromatography using hexane–ethyl acetate (1:1.5) as eluent (169 mg, 61% yield). ¹H NMR (500 MHz, DMSO-*d*₆) δ 8.45 (s, 1H, NHAr), 7.75 (q, $J = 8.6$ Hz, 2H, Ar), 7.29 (d, $J = 8.0$ Hz, 2H, Ar), 7.04 (d, $J = 8.1$ Hz, 2H, Ar), 6.64 (s, 2H, Ar), 6.59 (t, $J = 8.5$ Hz, 2H, Ar), 6.32–6.28 (m, 1H, CH₂NH), 5.36–5.29 (m, 1H, CH), 4.51–4.43 (m, 1H, CH₂O), 4.37 (dd, $J = 6.5$ Hz, $J = 9.5$ Hz, 1H, CH₂O), 3.84–3.80 (m, 12H, OCH₃), 3.55–3.50 (m, 2H, CH₂NH), 2.24 (s, 3H, CH₃). ¹³C NMR (125 MHz, DMSO-*d*₆) δ 164.1, 164.0, 163.9, 160.9, 155.3, 137.8, 133.2, 133.1, 129.9, 129.0, 117.8, 111.7, 111.4, 105.3, 105.2, 98.9, 98.8, 70.6, 63.0, 55.5, 55.4, 20.2. HRMS (m/z): calcd for C₂₉H₃₂N₂O₉Na 575.2000 [M + Na]⁺; found 575.1993. Anal. Calcd for C₂₉H₃₂N₂O₉: C, 63.04; H, 5.84; N, 5.07. Found: C, 62.97; H, 5.81; N, 4.99.

4.1.3.17. *N*-[2,3-Bis(3,4,5-trimethoxybenzoyloxy)propyl]-*N'*-(4-methylphenyl)urea (**34**). The product was obtained as a white solid and purified by column chromatography using hexane–ethyl acetate (1:1.5) as eluent (267 mg, 87% yield), mp 151–152 °C. ¹H NMR (500 MHz, DMSO-*d*₆) δ 8.43 (s, 1H, NHAr), 7.26–7.24 (m, 4H, Ar), 7.22 (s, 2H, Ar), 7.02 (d, $J = 8.1$ Hz, 2H, Ar), 6.38 (t, $J = 8.5$ Hz, 1H, CH₂NH), 5.47–5.42 (m, 1H, CH), 4.65 (dd, $J = 3.6$ Hz, $J = 8.5$ Hz, 1H, CH₂O), 4.45 (dd, $J = 3.5$ Hz, $J = 8.4$ Hz, 1H, CH₂O), 3.82–3.72 (m, 18H, OCH₃) 3.63–3.55 (m, 2H, CH₂NH), 2.22 (s, 3H, CH₃). ¹³C NMR (125 MHz, DMSO-*d*₆) δ 165.0, 164.9, 155.4, 152.7, 152.6, 142.0, 141.9, 137.7, 130.0, 128.9, 124.7, 124.4, 117.9, 106.8, 106.6, 71.8, 63.7, 60.1, 55.9, 55.8, 39.5, 20.2. HRMS (m/z): calcd for C₃₁H₃₆N₂O₁₁Na 635.2211 [M + Na]⁺; found 635.2202. Anal. Calcd for C₂₅H₂₂N₄O₉: C, 60.78; H, 5.92; N, 4.57. Found: C, 60.90; H, 5.94; N, 4.58.

4.1.3.18. *N*-[2,3-Bis(4-methylbenzoyloxy)propyl]-*N'*-[4-(trifluoromethyl)phenyl] urea (**35**). The product was obtained as a white solid and purified by column chromatography using hexane–ethyl acetate (3:1) as eluent (217 mg, 84 %yield), mp 111–112 °C. ¹H NMR (500 MHz, DMSO-*d*₆) δ 9.00, (s, 1H, NHAr), 7.89 (d, $J = 8.2$ Hz, 2H, Ar), 7.83 (d, $J = 8.2$ Hz, 2H, Ar), 7.61–7.55 (m, 4H, Ar), 7.32–7.29 (m, 4H, Ar), 6.59 (t, $J = 5.9$ Hz, 1H, CH₂NH), 5.48–5.44 (m, 1H, CH), 4.63 (dd, $J = 3.3$ Hz, $J = 12.1$ Hz, 1H, CH₂O), 4.48 (dd, $J = 6.9$ Hz, $J = 12.1$ Hz, 1H, CH₂O), 3.67–3.58 (m, 2H, CH₂NH), 2.37, 2.36 (2 s, 6H, CH₃). ¹³C NMR (125 MHz, DMSO-*d*₆) δ 165.4, 165.2, 154.9, 144.0, 143.8, 143.7, 129.4, 129.3, 129.2, 129.1, 129.0, 126.8, 126.6, 125.8, 125.7, 117.3, 71.3, 63.5, 21.1, 21.0. HRMS (m/z): calcd for C₂₇H₂₅F₃N₂O₅Na: 537.1608 [M + Na]⁺; found 537.1600. Anal. Calcd for C₂₇H₂₅F₃N₂O₅: C, 63.03; H, 4.90; N, 5.44. Found: C, 62.88; H, 4.87; N, 5.38.

4.1.3.19. *N*-[2,3-Bis(2-methylbenzoyloxy)propyl]-*N'*-[4-(trifluoromethyl)

phenyl] urea (**36**). The product was obtained as a white solid and purified by column chromatography using hexane–ethyl acetate (2.5:1) as eluent (188 mg, 73% yield), mp 112–113 °C. ¹H NMR (500 MHz, DMSO-*d*₆) δ 9.05 (s, 1H, NHAr), 7.90 (d, $J = 8.2$ Hz, 1H, Ar), 7.85 (d, $J = 8.2$ Hz, 1H, Ar), 7.61 (q, $J = 8.7$ Hz, 4H, Ar), 7.52–7.47 (m, 2H, Ar), 7.35–7.28 (m, 4H, Ar), 6.63 (t, $J = 6.1$ Hz, 1H, CH₂NH), 5.54–5.50 (m, 1H, CH), 4.67 (dd, $J = 3.5$ Hz, $J = 11.8$ Hz, 1H, CH₂O), 4.52 (dd, $J = 6.8$ Hz, $J = 11.9$ Hz, 1H, CH₂O), 3.68–3.61 (m, 2H, CH₂NH), 2.51 (s, 3H, CH₃). ¹³C NMR (125 MHz, DMSO-*d*₆) δ 166.5, 166.3, 154.9, 143.9, 139.3, 139.2, 132.3, 132.2, 131.6, 131.5, 130.2, 130.1, 129.3, 128.9, 125.9, 123.5, 121.3, 117.4, 71.2, 63.5, 39.5, 21.0, 20.9. HRMS (m/z): calcd for C₂₇H₂₅F₃N₂O₅Na 515.1788 [M + Na]⁺; found 515.1782. Anal. Calcd for C₂₇H₂₅F₃N₂O₅: C, 63.03; H, 4.90; N, 5.44. Found: C, 62.52; H, 4.92; N, 5.49.

4.1.3.20. *N*-[2,3-Bis(4-methoxybenzoyloxy)propyl]-*N'*-[4-(trifluoromethyl)phenyl] urea (**37**). The product was obtained as a white solid and purified by column chromatography using hexane–ethyl acetate (1:1) as eluent (195 mg, 71% yield), mp 128–129 °C. ¹H NMR (500 MHz, DMSO-*d*₆) δ 9.01 (s, 1H, NHAr), 7.98–7.96 (m, 2H, Ar), 7.94–7.89 (m, 2H, Ar) 7.60 (q, $J = 8.0$ Hz, 4H, Ar), 7.07–7.03 (m, 4H, Ar), 6.60 (t, $J = 6.9$ Hz, 1H, CH₂NH), 5.47–5.43 (m, 1H, CH), 4.61 (dd, $J = 3.6$ Hz, $J = 11.8$ Hz, 1H, CH₂O), 4.48 (dd, $J = 7.0$ Hz, $J = 11.9$ Hz, 1H, CH₂O), 3.85 (s, 6H, OCH₃), 3.65–3.60 (m, 2H, CH₂NH). ¹³C NMR (125 MHz, DMSO-*d*₆) δ 165.1, 164.9, 163.3, 163.2, 154.9, 143.9, 132.6, 131.4, 131.2, 123.5, 121.7, 121.5, 117.3, 114.1, 114.0, 113.9, 113.8, 71.1, 63.4, 55.5, 39.5. HRMS (m/z): calcd for C₂₇H₂₅F₃N₂O₇Na 569.1506 [M + Na]⁺; found 569.1497. Anal. Calcd for C₂₇H₂₅F₃N₂O₇: C, 59.34; H, 4.61; N, 5.13. Found: C, 59.18; H, 4.57; N, 5.51.

4.1.3.21. *N*-[2,3-Bis(4-cyanobenzoyloxy)propyl]-*N'*-[4-(trifluoromethyl)phenyl]urea (**38**). The product was obtained as a white solid and purified by column chromatography using hexane–ethyl acetate (2:1) as eluent (205 mg, 76% yield), mp 170–171 °C. ¹H NMR (500 MHz, DMSO-*d*₆) δ 9.00, (s, 1H, NHAr), 8.14 (d, $J = 8.2$ Hz, 2H, Ar), 8.08 (d, $J = 8.2$ Hz, 2H, Ar), 8.02–7.99 (m, 4H, Ar), 7.56 (m, 4H, Ar), 6.63 (t, $J = 5.9$ Hz, 1H, CH₂NH), 5.53–5.49 (m, 1H, CH), 4.71 (dd, $J = 3.5$ Hz, $J = 12.1$ Hz, 1H, CH₂O), 4.57 (dd, $J = 6.7$ Hz, $J = 12.1$ Hz, 1H, CH₂O), 3.69–3.62 (m, 2H, CH₂NH). ¹³C NMR (125 MHz, DMSO-*d*₆) δ 164.3, 164.2, 155.0, 143.9, 133.4, 133.2, 132.8, 132.7, 130.0, 129.8, 125.9, 117.9, 117.4, 115.6, 72.2, 64.3. HRMS (m/z): calcd for C₂₇H₁₉F₃N₄O₅Na: 559.1200 [M + Na]⁺; found 559.1192. Anal. Calcd for C₂₇H₁₉F₃N₄O₅: C, 60.45; H, 3.57; N, 10.44. Found: C, 59.85; H, 3.56; N, 10.42.

4.1.3.22. *N*-[2,3-Bis(4-nitrobenzoyloxy)propyl]-*N'*-[4-(trifluoromethyl)phenyl]urea (**39**). The product was obtained as a yellow solid and purified by column chromatography using hexane–ethyl acetate (1:1) as eluent (195 mg, 68% yield), mp 186–187 °C. ¹H NMR (500 MHz, DMSO-*d*₆) δ 9.00, (s, 1H, NHAr), 8.35–8.32 (m, 4H, Ar), 8.23 (d, $J = 8.7$ Hz, 2H, Ar), 8.17 (d, $J = 8.6$ Hz, 2H, Ar), 7.56 (m, 4H, Ar), 6.65 (t, $J = 5.4$ Hz, 1H, CH₂NH), 5.54 (m, 1H, CH), 4.74 (dd, $J = 2.8$ Hz, $J = 12.1$ Hz, 1H, CH₂O), 4.61 (dd, $J = 6.4$ Hz, $J = 12.1$ Hz, 1H, CH₂O), 3.71–3.63 (m, 2H, CH₂NH). ¹³C NMR (125 MHz, DMSO-*d*₆) δ 164.0, 163.9, 155.0, 150.4, 150.3, 134.9, 134.7, 130.8, 130.6, 125.9, 123.9, 123.8, 117.3, 129.1, 129.0, 126.8, 126.6, 125.8, 125.7, 117.3, 72.4, 64.4. HRMS (m/z): calcd for C₂₅H₁₉F₃N₄O₉Na: 599.0996 [M + Na]⁺; found 599.0988. Anal. Calcd for C₂₅H₁₉F₃N₄O₉: C, 52.09; H, 3.32; N, 9.72. Found: C, 51.63; H, 3.22; N, 9.78.

4.1.3.23. *N*-[2,3-Bis[4-(trifluoromethyl)benzoyloxy]propyl]-*N'*-[4-(trifluoromethyl)phenyl]urea (**40**). The product was obtained as a white solid and purified by column chromatography using hexane–ethyl acetate (2.5:1) as eluent (236 mg, 76% yield), mp 135–136 °C. ¹H NMR (500 MHz, DMSO-*d*₆) δ 9.01 (s, 1H, NHAr), 8.17 (d, $J = 8.2$ Hz, 2H, Ar), 8.11 (d, $J = 8.2$ Hz, 2H, Ar), 7.90–7.86 (m, 4H, Ar), 7.58–7.52 (m, 4H, Ar), 6.63 (t, $J = 6.0$ Hz, 1H, CH₂NH), 5.55–5.50 (m, 1H, CH), 4.52 (dd, $J = 3.4$ Hz, $J = 12.1$ Hz, 1H, CH₂O), 4.58 (dd, $J = 6.6$ Hz, $J = 12.2$ Hz, 1H, CH₂O), 3.70–3.61 (m, 2H, CH₂NH). ¹³C NMR (125 MHz, DMSO-*d*₆) δ 164.9, 164.7, 155.5, 144.4, 133.8, 133.6, 133.3, 130.7, 130.5, 127.4, 126.4, 126.3, 126.2, 125.2, 123.9, 117.8, 72.6, 64.7. HRMS (m/z): calcd. for C₂₇H₁₉F₉N₂O₅Na 645.1042 [M + Na]⁺; found 645.1035.

4.1.3.24. *N*-[2,3-Bis(2,4-dimethoxybenzoyloxy)propyl]-*N'*-[4-(trifluoromethyl)phenyl]urea (**41**). The product was obtained as a white solid and purified by column chromatography using hexane–ethyl acetate (1:1.5) as eluent (169 mg, 56% yield), mp 101–102 °C. ¹H NMR (500 MHz, DMSO-*d*₆) δ 9.04 (s, 1H, NHAr), 7.77 (d, *J* = 8.6 Hz, 1H, Ar), 7.74 (d, *J* = 8.6 Hz, 1H, Ar) 7.61 (q, *J* = 8.0 Hz, 4H, Ar), 6.67–6.64 (m, 2H, Ar), 6.62–6.56 (m, 2H, Ar), 6.53 (t, *J* = 5.5 Hz, 1H, CH₂NH), 5.39–5.33 (m, 1H, CH), 4.50 (dd, *J* = 3.5 Hz, *J* = 12.3 Hz, 1H, CH₂O), 4.39 (dd, *J* = 6.5 Hz, *J* = 12.3 Hz, 1H, CH₂O), 3.87–3.84 (m, 6H, OCH₃), 3.83–3.78 (m, 6H, OCH₃), 3.59 (t, *J* = 8.6 Hz, 2H, CH₂NH). ¹³C NMR (125 MHz, DMSO-*d*₆) δ 164.4, 164.1, 164.0, 163.8, 160.9, 154.9, 144.0, 133.2, 125.9, 125.7, 123.5, 120.9, 117.3, 111.7, 111.4, 105.3, 105.2, 98.9, 70.4, 63.0, 55.7, 55.5, 26.7. HRMS (*m/z*): calcd for C₂₉H₂₉F₃N₂O₉Na 629.1717 [M + Na]⁺; found 629.1709. Anal. Calcd for C₂₉H₂₉F₃N₂O₉: C, 57.43; H, 4.82; N, 4.62. Found: C, 57.22; H, 4.79; N, 4.55.

4.1.3.25. *N*-[2,3-Bis(3,4,5-trimethoxybenzoyloxy)propyl]-*N'*-[4-(trifluoromethyl)phenyl]urea (**42**). The product was obtained as a white solid and purified by column chromatography using hexane–ethyl acetate (1:1) as eluent (276 mg, 82% yield), mp 185–186 °C. ¹H NMR (500 MHz, DMSO-*d*₆) δ 9.03 (s, 1H, NHAr), 7.62–7.57 (m, 4H, Ar), 7.28 (s, 2H, Ar), 7.24 (s, 2H, Ar), 6.62 (t, *J* = 5.6 Hz, 1H, CH₂NH), 5.50–5.46 (m, 1H, CH), 4.68 (dd, *J* = 3.2 Hz, *J* = 12.2 Hz, 1H, CH₂O), 4.49 (dd, *J* = 6.4 Hz, *J* = 12.2 Hz, 1H, CH₂O), 3.82–3.73 (m, 18H, OCH₃) 3.67–3.61 (m, 2H, CH₂NH). ¹³C NMR (125 MHz, DMSO-*d*₆) δ 165.0, 155.0, 152.7, 152.6, 143.9, 142.0, 141.9, 127.5, 125.9, 125.8, 124.6, 124.3, 121.0, 117.3, 106.8, 106.6, 71.6, 63.6, 60.1, 55.9, 55.8, 39.5. HRMS (*m/z*): calcd for C₃₁H₃₃F₃N₂O₁₁Na: 689.1229 [M + Na]⁺; found 689.1229. Anal. Calcd for C₃₁H₃₃F₃N₂O₁₁: C, 55.86; H, 4.99; N, 4.20. Found: C, 55.41; H, 5.05; N, 4.21.

4.1.3.26. *N*-[2,3-Bis(3,4,5-trimethoxybenzoyloxy)propyl]-*N'*-(2-methylphenyl)urea (**43**). The product was obtained as a white solid and purified by column chromatography using hexane–ethyl acetate (1:1) as eluent (254 mg, 77% yield), mp 103–104 °C. ¹H NMR (500 MHz, DMSO-*d*₆) δ 7.74–7.68 (m, 2H, NHAr, Ar), 7.27 (s, 2H, Ar), 7.23 (s, 2H, Ar), 7.13–7.05 (m, 2H, Ar), 6.90 (t, *J* = 7.4 Hz, 1H, Ar), 6.77 (t, *J* = 5.9 Hz, 1H, CH₂NH), 5.48–5.43 (m, 1H, CH), 4.67 (dd, *J* = 3.6 Hz, *J* = 11.8 Hz, 1H, CH₂O), 4.47 (dd, *J* = 7.3 Hz, *J* = 11.8 Hz, 1H, CH₂O), 3.82–3.72 (m, 18H, OCH₃), 3.64–3.58 (m, 2H, CH₂NH). ¹³C NMR (125 MHz, DMSO-*d*₆) δ 165.1, 165.0, 155.6, 152.7, 142.0, 141.9, 137.8, 130.0, 127.4, 125.9, 124.7, 124.4, 122.3, 121.2, 106.8, 71.8, 63.7, 60.1, 55.8, 17.7. HRMS (*m/z*): calcd for C₃₁H₃₆N₂O₁₁Na 635.2211 [M + Na]⁺; found 635.2207.

4.1.3.27. *N*-[2,3-Bis(3,4,5-trimethoxybenzoyloxy)propyl]-*N'*-(4-methoxyphenyl) urea (**44**). The product was obtained as a white solid and purified by column chromatography using hexane–ethyl acetate (1:1) as eluent (300 mg, 90% yield), mp 137–138 °C. ¹H NMR (500 MHz, DMSO-*d*₆) δ 8.35 (s, 1H, NHAr), 7.28 (d, *J* = 8.0 Hz, 2H, Ar), 7.23 (s, 4H, Ar), 6.81 (d, *J* = 9.0 Hz, 2H, Ar), 6.33 (t, *J* = 6.1 Hz, 1H, CH₂NH), 5.48–5.42 (m, 1H, CH), 4.66 (dd, *J* = 3.5 Hz, *J* = 11.9 Hz, 1H, CH₂O), 4.45 (dd, *J* = 7.3 Hz, *J* = 11.9 Hz, 1H, CH₂O), 3.83–3.77 (m, 12H, OCH₃), 3.76–3.69 (m, 9H, OCH₃), 3.65–3.53 (m, 2H, CH₂NH). ¹³C NMR (125 MHz, DMSO-*d*₆) δ 165.0, 164.9, 155.5, 154.0, 152.8, 152.7, 142.0, 141.9, 133.3, 124.7, 124.3, 119.6, 113.8, 106.8, 106.6, 71.8, 63.7, 60.1, 55.9, 55.8, 55.1, 36.2. HRMS (*m/z*): calcd for C₃₁H₃₆N₂O₁₂Na 651.2160 [M + Na]⁺; found 651.2154. Anal. Calcd for C₃₁H₃₆N₂O₁₂: C, 59.23; H, 5.77; N, 4.20. Found: C, 59.40; H, 5.75; N, 4.23.

4.1.4. General procedure for the synthesis of diester derivatives by reaction with carboxylic acid (**45** and **46**)

According with reported procedure [55], the carboxylic acid (2.87 mmol) was dissolved in DCM and EDCI (3.55 mmol) was added. The mixture was stirred for 1 h at rt (mixture 1). At the same time, to a suspension of urea derivative (**13** or **14**, 0.78 mmol) in DCM was added DMAP (0.78 mmol) and the mixture was stirred for 1 h at rt (mixture 2); then the mixture 2 was added dropwise into the mixture 1. The reaction was stirred for 24 h at rt. The organic layer was washed with saturated

aqueous solution of NaHCO₃ and brine, then it was dried (Na₂SO₄), filtered and evaporated *in vacuo*. The compound was further purified through flash column chromatography using the appropriate mixture hexane–ethyl acetate as eluent.

4.1.4.1. *N*-{2,3-Bis[(*E*)-(3,4,5-trimethoxyphenyl)acryloxy]prop-2-yl}-*N'*-(4-chlorophenyl)urea (**45**). The product was obtained as a white solid and purified by column chromatography using hexane–ethyl acetate (2:1) as eluent (376 mg, 69% yield), mp 120–121 °C. ¹H NMR (500 MHz, DMSO-*d*₆) δ 8.73 (s, 1H, NHAr), 7.67–7.58 (m, 2H, CH = CHCO), 7.46–7.40 (m, 2H, Ar), 7.28–7.23 (m, 2H, Ar), 7.07 (s, 4H, Ar), 6.62–6.54 (m, 2H, CH = CHCO), 6.45 (t, *J* = 5.7 Hz, 1H, CH₂NH), 5.29–5.23 (m, 1H, CH), 4.48 (dd, *J* = 3.3 Hz, *J* = 12.0 Hz, 1H, CH₂O), 4.33 (dd, *J* = 6.5 Hz, *J* = 12.2 Hz, 1H, CH₂O), 3.88–3.78 (m, 12H, OCH₃), 3.72–3.68 (m, 6H, OCH₃), 3.58–3.41 (m, 2H, CH₂NH). ¹³C NMR (125 MHz, DMSO-*d*₆) δ 166.1, 165.9, 155.1, 153.0, 145.3, 139.7, 139.6, 139.2, 129.4, 128.4, 124.6, 119.2, 117.1, 116.7, 106.1, 106.0, 70.8, 60.0, 56.0, 44.8, 30.6. HRMS (*m/z*): calcd for C₃₄H₃₇ClN₂O₁₁Na 707.1978 [M + Na]⁺; found 707.1971.

4.1.4.2. *N*-{2,3-Bis[(*E*)-(3,4,5-trimethoxyphenyl)acryloxy]prop-2-yl}-*N'*-(4-methylphenyl)urea (**46**). The product was obtained as a white solid and purified by column chromatography using hexane–ethyl acetate (2:1) as eluent (306 mg, 60% yield), mp 106–107 °C. ¹H NMR (500 MHz, DMSO-*d*₆) δ 8.44 (s, 1H, NHAr), 7.67–7.59 (m, 2H, CH = CHCO), 7.28 (d, *J* = 8.2 Hz, 2H, Ar), 7.10–7.00 (m, 6H, Ar), 6.73–6.64 (m, 2H, CH = CHCO), 6.33 (t, *J* = 5.7 Hz, 1H, CH₂NH), 5.28–5.22 (m, 1H, CH), 4.47 (dd, *J* = 3.1 Hz, *J* = 12.1 Hz, 1H, CH₂O), 4.32 (dd, *J* = 6.5 Hz, *J* = 12.1 Hz, 1H, CH₂O), 3.85–3.74 (m, 12H, OCH₃), 3.72–3.66 (m, 6H, OCH₃), 3.58–3.52 (m, 1H, CH₂NH), 3.47–3.42 (m, 1H, CH₂NH), 2.22 (s, 3H, CH₃). ¹³C NMR (125 MHz, DMSO-*d*₆) δ 166.1, 165.9, 155.2, 153.0, 145.3, 139.6, 137.7, 129.9, 129.5, 129.4, 117.8, 117.1, 116.7, 106.1, 106.0, 70.9, 63.1, 60.1, 56.0, 20.2. HRMS (*m/z*): calcd for C₃₅H₄₀N₂O₁₁Na 687.2508 [M + Na]⁺; found 687.2510.

4.1.5. General procedure for the synthesis of monoester derivatives by chemoselective *O*-acylation reaction of the primary hydroxyl (**47**–**51** and **77**)

The urea derivatives **13** or **14** (0.7 mmol) was suspended in dry DCM (15 mL), then pyridine was added until dissolution (5 mL) and the reaction was cooled to –40 °C. A solution of the appropriate acylating agent (0.6 mmol) in dry DCM (5 mL) was added dropwise and the reaction mixture was kept with stirring for 2 h. The reaction mixture was co-evaporated with toluene to remove the pyridine residue. The compound was further purified by flash column chromatography on silica gel using the appropriate eluent.

4.1.5.1. *N*-(4-Chlorophenyl)-*N'*-[2-hydroxy-3-(4-methylbenzoyloxy)propyl]urea (**47**). The product was obtained as a white solid and purified by column chromatography using hexane–ethyl acetate (1:2) as eluent (125 mg, 57% yield), mp 155–156 °C. MS (CI): *m/z* 369 (100%) [M + Na]⁺. ¹H NMR (500 MHz, DMSO-*d*₆) δ 8.74 (s, 1H, NHAr), 7.93–7.89 (m, 2H, Ar), 7.43–7.39 (m, 2H, Ar), 7.36–7.32 (m, 2H, Ar), 7.27–7.23 (m, 2H, Ar), 6.32 (t, *J* = 5.5 Hz, 1H, CH₂NH), 5.35 (d, *J* = 4.9 Hz, 1H, OH), 4.99–4.96 (m, 1H, CH), 4.23–4.20 (m, 2H, CH₂O), 3.43–3.39 (m, 1H, CH₂NH), 3.22–3.17 (m, 1H, CH₂NH), 2.40 (s, 3H, CH₃). ¹³C NMR (125 MHz, DMSO-*d*₆) δ 165.8, 155.2, 143.6, 139.5, 129.3, 129.2, 129.1, 128.5, 127.0, 124.4, 119.0, 67.6, 66.4, 42.2, 21.1. Anal. Calcd for C₁₈H₁₉ClN₂O₄: C, 59.59; H, 5.28; N, 7.72. Found: C, 59.24; H, 5.25; N, 7.69.

4.1.5.2. *N*-(4-Chlorophenyl)-*N'*-[2-hydroxy-3-(2-methylbenzoyloxy)propyl]urea (**48**). The product was obtained as a white resin and purified by column chromatography using hexane–ethyl acetate (1:2) as eluent (131 mg, 60% yield). ¹H NMR (500 MHz, DMSO-*d*₆) δ 8.73 (s, 1H, NHAr), 7.92–7.87 (m, 1H, Ar), 7.51–7.38 (m, 3H, Ar), 7.34–7.23 (m, 4H, Ar), 6.35–6.29 (m, 1H, CH₂NH), 5.33 (d, *J* = 5.2 Hz, 1H, OH), 5.08–5.03 (m, 1H, CH), 4.23–4.17 (m, 1H, CH₂O), 3.92–3.87 (m, 1H, CH₂O), 3.63–3.52 (m, 1H, CH₂NH), 3.21–3.16 (m, 1H, CH₂NH), 2.54 (s, 3H, CH₃). ¹³C NMR (125 MHz, DMSO-*d*₆) δ 166.8, 155.2, 139.4, 139.0,

132.1, 131.5, 130.2, 129.5, 128.4, 125.9, 124.4, 119.2, 74.4, 67.6, 66.4, 60.6, 42.3, 21.1. HRMS (m/z): calcd for $C_{18}H_{19}ClN_2O_4Na$ 385.0926 [$M + Na$]⁺; found 385.0921.

4.1.5.3. *N*-(4-Chlorophenyl)-*N'*-{2-hydroxy-3-[4-(trifluoromethyl)benzoyloxy]propyl}urea (**49**). The product was obtained as a white solid and purified by column chromatography using hexane–ethyl acetate (1:1.5) as eluent (120 mg, 48% yield), mp 137–138 °C. ¹H NMR (500 MHz, DMSO-*d*₆) δ 8.74 (s, 1H, NHAr), 8.23–8.18 (m, 2H, Ar), 7.93–7.88 (m, 2H, Ar), 7.43–7.36 (m, 2H, Ar), 7.28–7.23 (m, 2H, Ar), 6.32 (t, $J = 5.7$ Hz, 1H, CH₂NH), 5.44 (bs, 1H, OH), 4.33–4.24 (m, 2H, CH₂O), 3.96–3.91 (m, 1H, CH), 3.37–3.31 (m, 1H, CH₂NH), 3.26–3.19 (m, 1H, CH₂NH). ¹³C NMR (125 MHz, DMSO-*d*₆) δ 164.7, 155.2, 139.4, 133.5, 130.2, 130.1, 128.4, 128.4, 125.7, 124.5, 119.2, 119.1, 67.5, 67.2, 42.1. HRMS (m/z): calcd for $C_{18}H_{16}ClF_3N_2O_4Na$ 439.0643 [$M + Na$]⁺; found 439.0639.

4.1.5.4. *N*-[3-(2-Chloroacetoxy)-2-hydroxypropyl]-*N'*-(4-chlorophenyl)urea (**50**). The product was obtained as a white resin (380 mg, 51% yield). MS (FAB): m/z 343 (100%) [$M + Na$]⁺. ¹H NMR (500 MHz, DMSO-*d*₆) δ 8.75 (s, 1H, NHAr), 7.44 (d, $J = 8.5$ Hz, 2H, Ar), 8.16 (d, $J = 8.6$ Hz, 2H, Ar), 6.27 (t, $J = 5.8$ Hz, 1H, CH₂NH), 5.30 (d, $J = 5.1$ Hz, 1H, OH), 4.44 (s, 2H, ClCH₂), 4.12–4.09 (m, 2H, CH₂O), 3.83–3.79 (m, 1H, CH), 3.30–3.24 (m, 1H, CH₂NH), 3.16–3.10 (m, 1H, CH₂NH). ¹³C NMR (125 MHz, DMSO-*d*₆) δ 167.3, 155.1, 139.4, 128.5, 124.5, 119.0, 67.4, 67.3, 42.0, 41.1. HRMS (m/z): calcd for $C_{12}H_{14}Cl_2N_2O_4Na$ 343.0223 [$M + Na$]⁺; found 343.0220.

4.1.5.5. *N*-[3-(2-Chloroacetoxy)-2-hydroxypropyl]-*N'*-(4-methylphenyl)urea (**51**). The product was obtained as a white resin (540 mg, 49% yield). ¹H NMR (500 MHz, DMSO-*d*₆) δ 8.45 (s, 1H, NHAr), 7.27 (d, $J = 8.3$ Hz, 2H, Ar), 7.03 (d, $J = 8.62$ Hz, 2H, Ar), 6.16 (t, $J = 5.7$ Hz, 1H, CH₂NH), 5.27 (bs, 1H, OH), 4.42 (s, 2H, ClCH₂), 4.12–4.04 (m, 2H, CH₂O), 3.81–3.76 (m, 1H, CH), 3.27–3.21 (m, 1H, CH₂NH), 3.13–3.07 (m, 1H, CH₂NH). ¹³C NMR (125 MHz, DMSO-*d*₆) δ 167.3, 155.4, 137.9, 129.7, 129.0, 117.7, 67.5, 67.4, 42.0, 41.3, 20.2. HRMS (m/z): calcd for $C_{13}H_{17}ClN_2O_4Na$ 323.0769 [$M + Na$]⁺; found 323.0766.

4.1.5.6. *N*-[3-(Benzoyloxy)-2-hydroxypropyl]-*N'*-(4-chlorophenyl)urea (**77**). The product was obtained as a white solid and purified by column chromatography using hexane–ethyl acetate (1.5:1) as eluent (122 mg, 58% yield), mp 155–156 °C. ¹H NMR (500 MHz, DMSO-*d*₆) δ 8.73 (s, 1H, NHAr), 8.04–8.01 (m, 2H, Ar), 7.70–7.63 (m, 1H, Ar), 7.57–7.52 (m, 2H, Ar), 7.41 (t, $J = 8.8$ Hz, 2H, Ar), 7.28–7.24 (m, 2H, Ar), 6.33 (m, 1H, CH₂NH), 5.36 (d, $J = 4.9$ Hz, 1H, OH), 5.08–5.05 (m, 1H, CH), 4.27–4.17 (m, 2H, CH₂O), 3.45–3.39 (m, 1H, CH₂NH), 3.23–3.17 (m, 1H, CH₂NH). ¹³C NMR (125 MHz, DMSO-*d*₆) δ 165.7, 155.2, 139.4, 133.3, 129.3, 129.2, 128.7, 128.4, 124.5, 119.1, 119.0, 67.6, 66.6, 42.2. HRMS (m/z): calcd for $C_{17}H_{17}ClN_2O_4Na$ 371.0769 [$M + Na$]⁺; found 371.0763.

4.1.6. General procedure for *O*-acylation reaction of the secondary hydroxyl of *N*-[3-(2-chloroacetoxy)-2-hydroxypropyl]-*N'*-(substituted)phenylureas (**52–57**)

To a solution of chloroacetyl derivative (**50** or **51**) (0.7 mmol) in dry DCM (10 mL) and DMAP (1.4 mmol), a solution of the appropriate acylating agent (or isocyanate) (1.0 mmol) in dry DCM (2 mL) was added. The reaction mixture was stirred at rt until TLC showed that the starting material had reacted (12–24 h). The organic layer was washed with 1 N aqueous solution HCl (2 × 20 mL), saturated NaHCO₃ (2 × 20 mL), brine (20 mL); then, it was dried (MgSO₄), filtered and evaporated *in vacuo*. The product was used without further purification.

4.1.6.1. *N*-[3-(2-Chloroacetoxy)-2-(4-methylbenzoyloxy)propyl]-*N'*-(4-chlorophenyl)urea (**52**). The product was obtained as a colourless oil (230 mg, 76% yield). MS (FAB): m/z 461 (100%) [$M + Na$]⁺. ¹H NMR (500 MHz, DMSO-*d*₆) δ 8.68 (s, 1H, NHAr), 7.91–7.83 (m, 2H, Ar), 7.43–7.39 (m, 2H, Ar), 7.36–7.31 (m, 2H, Ar), 7.28–7.24 (m, 2H, Ar), 6.42 (t, $J = 6.0$ Hz, 1H, CH₂NH), 5.32–5.27 (m, 1H, CH), 4.50–4.46 (m, 1H, CH₂O), 4.40–4.32 (m, 3H, ClCH₂, CH₂O), 3.57–3.44 (m, 2H, CH₂NH), 2.41–2.37 (m, 3H, CH₃). ¹³C NMR (125 MHz, DMSO-*d*₆) δ 167.2, 165.3, 155.0, 143.8, 139.2, 129.4, 129.1, 128.4, 126.8, 124.6,

119.2, 71.1, 64.3, 40.9, 21.1.

4.1.6.2. *N*-[3-(2-Chloroacetoxy)-2-[4-(trifluoromethyl)benzoyloxy]propyl]-*N'*-(4-chlorophenyl)urea (**53**). The product was obtained as a colourless oil (235 mg, 68% yield). MS (FAB): m/z 515 (100%) [$M + Na$]⁺. ¹H NMR (500 MHz, DMSO-*d*₆) δ 8.68 (s, 1H, NHAr), 8.20–8.13 (m, 2H, Ar), 7.93–7.87 (m, 2H, Ar), 7.44–7.37 (m, 2H, Ar), 7.28–7.22 (m, 2H, Ar), 6.47 (t, $J = 5.9$ Hz, 1H, CH₂NH), 5.38–5.32 (m, 1H, CH), 4.52 (dd, $J = 3.4$ Hz, $J = 12.2$ Hz, 1H, CH₂O), 4.45–4.37 (m, 3H, ClCH₂, CH₂O), 3.60–3.48 (m, 2H, CH₂NH). ¹³C NMR (125 MHz, DMSO-*d*₆) δ 167.2, 164.2, 155.1, 139.2, 133.3, 130.2, 130.1, 128.4, 125.6, 125.5, 124.7, 119.2, 72.0, 64.2, 40.9. HRMS (m/z): calcd. for $C_{20}H_{17}Cl_2F_3N_2O_5Na$ 515.0359 [$M + Na$]⁺; found 515.0359.

4.1.6.3. *N*-[3-(2-Chloroacetoxy)-2-(4-nitrobenzoyloxy)propyl]-*N'*-(4-chlorophenyl)urea (**54**). The product was obtained as a light yellow oil (298 mg, 91% yield). ¹H NMR (500 MHz, DMSO-*d*₆) δ 8.69 (s, 1H, NHAr), 8.35 (d, $J = 8.8$ Hz, 2H, Ar), 8.23–8.19 (m, 2H, Ar), 7.46–7.38 (m, 2H, Ar), 7.30–7.23 (m, 2H, Ar), 6.47 (t, $J = 5.9$ Hz, 1H, CH₂NH), 5.40–5.33 (m, 1H, CH), 4.53 (dd, $J = 3.3$ Hz, $J = 12.2$ Hz, 1H, CH₂O), 4.47–4.36 (m, 3H, ClCH₂, CH₂O), 3.62–3.48 (m, 2H, CH₂NH). ¹³C NMR (125 MHz, DMSO-*d*₆) δ 167.2, 163.7, 155.0, 150.3, 139.1, 134.9, 130.7, 128.4, 124.6, 123.7, 119.2, 72.3, 64.2, 40.9, 26.7. HRMS (m/z): calcd for $C_{19}H_{17}Cl_2N_3O_5Na$ 492.0336 [$M + Na$]⁺; found 492.0331.

4.1.6.4. *N*-[3-(2-Chloroacetoxy)-2-(3,4,5-trimethoxybenzoyloxy)propyl]-*N'*-(4-chlorophenyl)urea (**55**). The product was obtained as a colourless oil (260 mg, 72% yield). ¹H NMR (500 MHz, DMSO-*d*₆) δ 8.74 (s, 1H, NHAr), 7.46–7.39 (m, 2H, Ar), 7.30–7.23 (m, 4H, Ar), 6.47–6.40 (m, 1H, CH₂NH), 5.36–5.40 (m, 1H, CH), 4.57–4.52 (m, 1H, CH₂O), 4.47–4.38 (m, 2H, ClCH₂), 4.34–4.28 (m, 1H, CH₂O), 3.87–3.80 (m, 6H, OCH₃), 3.78–3.72 (m, 3H, OCH₃), 3.57–3.50 (m, 1H, CH₂NH), 3.48–3.40 (m, 1H, CH₂NH). ¹³C NMR (125 MHz, DMSO-*d*₆) δ 167.0, 164.9, 155.1, 152.7, 152.6, 141.9, 139.2, 128.4, 124.7, 124.3, 119.3, 106.9, 106.7, 72.4, 63.7, 60.1, 55.9, 41.2, 40.9. HRMS (m/z): calcd for $C_{22}H_{24}ClN_2O_8Na$ 537.0802 [$M + Na$]⁺; found 537.0795.

4.1.6.5. *N*-[3-(2-Chloroacetoxy)-2-[(4-trifluoromethyl)benzoyloxy]propyl]-*N'*-(4-methylphenyl)urea (**56**). The product was obtained as a colourless oil (249 mg, 75% yield). ¹H NMR (500 MHz, DMSO-*d*₆) δ 8.43 (s, 1H, NHAr), 8.21–8.50 (m, 2H, Ar), 7.94–7.90 (m, 2H, Ar), 7.29–7.21 (m, 2H, Ar), 7.06–6.99 (m, 2H, Ar), 6.28 (t, $J = 6.0$ Hz, 1H, CH₂NH), 5.17–5.12 (m, 1H, CH), 4.52 (dd, $J = 3.5$ Hz, $J = 12.0$ Hz, 1H, CH₂O), 4.45–4.34 (m, 3H, ClCH₂, CH₂O), 3.59–3.47 (m, 2H, CH₂NH), 2.22 (s, 3H, CH₃). ¹³C NMR (125 MHz, DMSO-*d*₆) δ 167.2, 164.4, 155.3, 137.8, 130.2, 130.1, 129.1, 125.6, 118.0, 72.3, 64.1, 40.1, 40.0, 20.2. HRMS (m/z): calcd for $C_{21}H_{20}ClCF_3N_2O_5Na$ 495.0905 [$M + Na$]⁺; found 495.0898.

4.1.6.6. *N*-[3-(2-Chloroacetoxy)-2-(3,4,5-trimethoxybenzoyloxy)propyl]-*N'*-(4-methylphenyl)urea (**57**). The product was obtained as a colourless oil (274 mg, 80% yield). ¹H NMR (500 MHz, DMSO-*d*₆) δ 7.98 (s, 1H, NHAr), 7.32–7.21 (m, 4H, Ar), 7.08–6.99 (m, 2H, Ar), 6.40–6.32 (m, 1H, CH₂NH), 5.28–5.21 (m, 1H, CH), 4.53–4.48 (m, 1H, CH₂O), 4.45–4.35 (m, 2H, ClCH₂), 4.30–4.25 (m, 1H, CH₂O), 3.89–3.80 (m, 6H, OCH₃), 3.78–3.72 (m, 3H, OCH₃), 3.57–3.44 (m, 2H, CH₂NH), 2.21 (s, 3H, CH₃). ¹³C NMR (125 MHz, DMSO-*d*₆) δ 167.3, 162.3, 155.3, 152.7, 141.9, 137.7, 129.9, 129.0, 124.7, 117.9, 107.0, 106.5, 72.3, 64.1, 60.1, 56.0, 35.7, 20.3. HRMS (m/z): calcd for $C_{23}H_{27}ClN_2O_8Na$ 517.1348 [$M + Na$]⁺; found 517.1341.

4.1.7. General procedure for the deprotection reaction of *N*-[3-(2-Chloroacetoxy)-2-(acetyl)propyl]-*N'*-(substituted)ureas (**59–65**)

To a solution of chloroacetyl derivative (**52–58**, 0.4 mmol) in acetonitrile–water (3:1, 10 mL), thiourea (1.2 mmol) was added and the reaction mixture was stirred at 60 °C until TLC showed the full consumption of the starting material (12 h). After this time, a saturated solution of NaHCO₃ was added to the flask and the reaction mixture was extracted with chloroform (2 × 10 mL). The organic layer was washed with brine, dried (MgSO₄), filtered and evaporated to dryness to obtain a crude product. The compound was purified by flash column chromatography on silica gel using the appropriate eluent.

4.1.7.1. *N*-(4-Chlorophenyl)-*N'*-[3-hydroxy-2-(4-methylbenzoyloxy)propyl]urea (**59**). The product was obtained as a white solid and purified by column chromatography using hexane–ethyl acetate (2:1) as eluent (110 mg, 76% yield), mp 140–141 °C. ¹H NMR (500 MHz, DMSO-*d*₆) δ 8.67, (s, 1H, NHAr), 7.94–7.88 (m, 2H, Ar), 7.44–7.38 (m, 2H, Ar), 7.37–7.32 (m, 2H, Ar), 7.29–7.22 (m, 2H, Ar), 6.37–6.29 (m, 1H, CH₂NH), 5.07–4.98 (m, 2H, CH, OH), 3.62 (t, *J* = 5.5 Hz, 2H, CH₂NH), 3.56–3.50 (m, 1H, CH₂OH), 3.43–3.37 (m, 1H, CH₂OH), 2.39 (s, 3H, CH₃). ¹³C NMR (125 MHz, DMSO-*d*₆) δ 165.4, 155.1, 143.5, 139.3, 129.4, 129.1, 128.4, 127.2, 124.5, 119.1, 74.4, 60.5, 42.1, 21.1. HRMS (*m/z*): calcd for C₁₈H₁₉ClN₂O₄Na 385.0922 [M + Na]⁺; found 385.0920.

4.1.7.2. *N*-(4-Chlorophenyl)-*N'*-[3-hydroxy-2-[(4-trifluoromethyl)benzoyloxy]propyl]urea (**60**). The product was obtained as a white solid and purified by column chromatography using hexane–ethyl acetate (1.5:1) as eluent (120 mg, 73% yield), mp 175–176 °C. ¹H NMR (500 MHz, DMSO-*d*₆) δ 8.73, (s, 1H, NHAr), 8.23–8.18 (m, 2H, Ar), 7.94–7.89 (m, 2H, Ar), 7.43–7.36 (m, 2H, Ar), 7.28–7.22 (m, 2H, Ar), 6.32 (t, *J* = 5.7 Hz, 1H, CH₂NH), 5.38 (bs, 1H, OH), 5.13–5.07 (m, 1H, CH), 4.32–4.23 (m, 2H, CH₂NH), 3.69–3.62 (m, 1H, CH₂OH), 3.26–3.19 (m, 1H, CH₂OH). ¹³C NMR (125 MHz, DMSO-*d*₆) δ 164.6, 155.2, 139.4, 139.3, 133.5, 130.2, 130.1, 128.4, 125.7, 124.8, 119.2, 119.0, 75.5, 67.4, 42.1. HRMS (*m/z*): calcd for C₁₈H₁₆ClF₃N₂O₄Na 439.0643 [M + Na]⁺; found 439.0637. Anal. Calcd for C₁₈H₁₆ClF₃N₂O₄: C, 51.87; H, 3.87; N, 6.72. Found: C, 51.85; H, 3.88; N, 6.74.

4.1.7.3. *N*-(4-Chlorophenyl)-*N'*-[3-hydroxy-2-(4-nitrobenzoyloxy)propyl]urea (**61**). The product was obtained as a light yellow resin and purified by column chromatography using hexane–ethyl acetate (1:2) as eluent (116 mg, 73% yield). ¹H NMR (500 MHz, DMSO-*d*₆) δ 8.63, (s, 1H, NHAr), 8.38–8.33 (m, 2H, Ar), 8.27–8.22 (m, 2H, Ar), 7.43–7.37 (m, 2H, Ar), 7.28–7.23 (m, 2H, Ar), 6.38 (t, *J* = 5.9 Hz, 1H, CH₂NH), 5.14–5.08 (m, 1H, CH), 5.03 (s, *J* = 5.9 Hz, 1H, OH), 3.71–3.62 (m, 2H, CH₂NH), 3.59–3.53 (m, 1H, CH₂OH), 3.47–3.40 (m, 1H, CH₂OH). ¹³C NMR (125 MHz, DMSO-*d*₆) δ 164.0, 155.2, 150.2, 139.4, 133.5, 130.7, 128.4, 124.6, 123.7, 119.2, 75.8, 67.5, 60.4. HRMS (*m/z*): calcd for C₁₇H₁₆ClN₃O₆Na 416.0620 [M + Na]⁺; found 416.0617.

4.1.7.4. *N*-(4-Chlorophenyl)-*N'*-[3-hydroxy-2-(3,4,5-trimethoxybenzoyloxy)propyl]urea (**62**). The product was obtained as a white solid and purified by column chromatography using hexane–ethyl acetate (1.5:1) as eluent (135 mg, 77% yield), mp 155–156 °C. ¹H NMR (500 MHz, DMSO-*d*₆) δ 8.67, (s, 1H, NHAr), 7.43–7.38 (m, 2H, Ar), 7.29 (s, 2H, Ar), 7.26–7.23 (m, 2H, Ar), 6.33 (t, *J* = 5.9 Hz, 1H, CH₂NH), 5.04–4.98 (m, 2H, CH, OH), 3.83–3.79 (m, 6H, OCH₃), 3.75–3.72 (m, 3H, OCH₃), 3.65–3.61 (m, 2H, CH₂NH), 3.57–3.52 (m, 1H, CH₂OH), 3.47–3.41 (m, 1H, CH₂OH). ¹³C NMR (125 MHz, DMSO-*d*₆) δ 165.3, 155.2, 152.7, 141.9, 139.4, 128.4, 125.1, 124.8, 119.1, 106.9, 74.9, 60.4, 60.1, 56.0, 42.2. HRMS (*m/z*): calcd for C₂₀H₂₃ClN₂O₇Na 461.1086 [M + Na]⁺; found 461.1084.

4.1.7.5. *N*-[3-Hydroxy-2-(3,4,5-trimethoxybenzoyloxy)propyl]-*N'*-(4-methylphenyl)urea (**63**). The product was obtained as a white solid and purified by column chromatography using hexane–ethyl acetate (1:2) as eluent (123 mg, 73% yield), mp 170–171 °C. ¹H NMR (500 MHz, DMSO-*d*₆) δ 8.39, (s, 1H, NHAr), 7.33–7.22 (m, 4H, Ar), 7.02 (d, *J* = 8.2 Hz, 2H, Ar), 6.23 (t, *J* = 5.9 Hz, 1H, CH₂NH), 5.03–4.98 (m, 2H, CH, OH), 3.88–3.80 (m, 6H, OCH₃), 3.78–3.72 (m, 3H, OCH₃), 3.66–3.61 (m, 2H, CH₂NH), 3.57–3.51 (m, 1H, CH₂OH), 3.47–3.40 (m, 1H, CH₂OH). ¹³C NMR (125 MHz, DMSO-*d*₆) δ 165.2, 155.4, 152.6, 141.8, 137.7, 129.8, 128.9, 125.2, 117.8, 106.9, 75.0, 60.4, 60.1, 56.0, 20.2. HRMS (*m/z*): calcd for C₂₁H₂₆N₂O₇Na 441.1632 [M + Na]⁺; found 441.1629.

4.1.7.6. *N*-[3-Hydroxy-2-[(4-trifluoromethyl)benzoyloxy]propyl]-*N'*-(4-methylphenyl)urea (**64**). The product was obtained as a white resin and purified by column chromatography using hexane–ethyl acetate (1.5:1) as eluent (128 mg, 80% yield). ¹H NMR (500 MHz, DMSO-*d*₆) δ 8.48 (s, 1H, NHAr), 8.25–8.20 (m, 2H, Ar), 7.85–7.79 (m, 2H, Ar), 7.29–7.21 (m, 2H, Ar), 7.14–7.00 (m, 2H, Ar), 6.29 (m, 1H, CH₂NH), 5.12–5.06 (m, 1H, CH), 5.03 (t, *J* = 5.9 Hz, 1H, OH), 4.32–4.23 (m, 2H, CH₂NH), 3.69–3.52 (m, 2H, CH₂OH). ¹³C NMR (125 MHz, DMSO-*d*₆) δ

164.6, 155.4, 137.8, 137.7, 130.2, 129.8, 129.7, 128.9, 125.6, 125.5, 117.9, 117.7, 75.6, 60.5, 42.2, 20.2. HRMS (*m/z*): calcd for C₁₉H₁₉F₃N₂O₄Na 419.1240 [M + Na]⁺; found 419.1237.

4.1.7.7. *N*-(4-Chlorophenyl)-*N'*-[3-hydroxy-2-[(4-trifluoromethyl)phenylaminocarboxy]propyl]urea (**65**). The product was obtained as an amorphous solid and purified by column chromatography using hexane–ethyl acetate (1:2) as eluent (112 mg, 64% yield). ¹H NMR (500 MHz, DMSO-*d*₆) δ 10.11 (s, 1H, NHCOO), 8.70 (s, 1H, NHAr), 8.72–8.62 (m, 4H, Ar), 7.45–7.39 (m, 2H, Ar), 7.29–7.22 (m, 2H, Ar), 6.32 (t, *J* = 5.75 Hz, 1H, CH₂NH), 4.96 (t, *J* = 5.60 Hz, 1H, OH), 4.86–4.70 (m, 1H, CH), 3.62–3.49 (m, 4H, CH₂NH, CH₂OH). ¹³C NMR (125 MHz, DMSO-*d*₆) δ 155.1, 153.1, 142.9, 139.3, 128.4, 126.0, 125.5, 124.6, 122.5, 122.2, 119.1, 119.0, 117.9, 74.5, 67.7, 60.7. HRMS (*m/z*): calcd for C₁₈H₁₇ClF₃N₃O₄Na 454.0752 [M + Na]⁺; found 454.0748.

4.1.8. *Olefin oxidation reaction of N-Allyl-N'*-(4-chlorophenyl)urea (*N*-(4-chlorophenyl)-*N'*-(2,3-epoxypropyl)urea (**69**). According to reported procedure [56], a solution of *meta*-chloroperoxybenzoic acid (*m*-CPBA) (15 mmol), previous dried (MgSO₄) in anhydrous THF (10 mL), was added to a solution of *N*-allyl-*N'*-(4-chlorophenyl)urea (**67**, 3 mmol) in THF (30 mL) and the reaction mixture was stirred at rt until TLC showed that all the starting material had reacted (24 h). After that, ethyl acetate (30 mL) and a saturated solution of K₂CO₃ was added to the flask and the mixture was stirred for 5 min, then the phases were separated. The organic layer was washed with K₂CO₃ (3 × 20 mL) and brine, then dried (MgSO₄) and evaporated to dryness. The compound was obtained as a light yellow solid and purified by precipitation in toluene (542 mg, 80%). ¹H NMR (500 MHz, DMSO-*d*₆) δ 8.70 (s, 1H, NHAr), 7.42 (d, *J* = 8.8 Hz, 2H, Ar), 7.27 (d, *J* = 8.4 Hz, 2H, Ar), 6.32 (t, *J* = 5.0 Hz, 1H, CH₂NH), 3.22–3.17 [m, 2H, CH₂(O)CH], 3.07–3.04 [m, 1H, CH₂(O)CH], 2.73 (t, *J* = 4.7 Hz, 1H, CH₂NH), 2.57–2.55 (m, 1H, CH₂NH). ¹³C NMR (125 MHz, DMSO-*d*₆) δ 155.0, 139.3, 128.5, 124.6, 119.2, 50.6, 44.6, 40.4. HRMS (*m/z*): calcd for C₁₀H₁₂ClN₂O₂ 227.0587 [M + H]⁺; found 227.0582.

4.1.8. *Epoxide ring opening of N*-(4-chlorophenyl)-*N'*-(2,3-epoxypropyl)urea in acid condition

N-(3-Azido-2-hydroxypropyl)-*N'*-(4-chlorophenyl)urea (**70**). According to reported procedure [57], to a suspension of oxirane (**69**, 1.0 mmol) in ethanol (20 mL), were added sodium azide (1.2 mmol) and NH₄Cl (1.2 mmol) and the mixture was heated at 60 °C and stirred until TLC showed the full consumption of the starting material (15 h). The reaction was washed with water (10 mL) and brine (10 mL), then dried (MgSO₄) and evaporated under reduced pressure. The compound was obtained as a light yellow resin and purified by flash column chromatography on silica gel using hexane–ethyl acetate (1:1) as eluent (215 mg, 79% yield). ¹H NMR (500 MHz, DMSO-*d*₆) δ 8.70 (s, 1H, NHAr), 7.41 (d, *J* = 9.0 Hz, 2H, Ar), 7.27 (d, *J* = 8.5 Hz, 2H, Ar), 6.25 (t, *J* = 5.8 Hz, 1H, CH₂NH), 5.40 (d, *J* = 5.1 Hz, 1H, OH), 6.76–6.71 (m, 1H, CH), 3.30–3.26 (m, 2H, CH₂NH), 3.25–3.17 (m, 1H, N₃CH₂), 3.11–3.06 (m, 1H, N₃CH₂). ¹³C NMR (125 MHz, DMSO-*d*₆) δ 155.1, 139.4, 128.5, 124.5, 119.1, 69.1, 54.0, 42.8. HRMS (*m/z*): calcd for C₁₀H₁₂ClN₅O₂Na 292.0572 [M + Na]⁺; found 292.0574.

4.1.9. *Mesylation reaction of N*-[3-(benzoyloxy)-2-hydroxypropyl]-*N'*-(4-chlorophenyl)urea

N-[3-Benzoyloxy-2-(methylsulfonyloxy)propyl]-*N'*-(4-chlorophenyl)urea (**78**). According to reported procedure [58], to a solution of benzoyl derivative **77** (1.0 mmol) and triethylamine (2.0 mmol) in dry THF (7 mL) mesyl chloride (2.0 mmol) was added dropwise at 0 °C. The reaction mixture was heated to room temperature and stirred for 5 h, then NH₄Cl (5% water solution) and DCM were added. The phases were separated and the organic layer was washed with saturated NaHCO₃, brine and dried (MgSO₄); then filtered and evaporated *in vacuo* to give compound as colourless oil, that was used without further purification. (220 mg, 92% yield). ¹H NMR (500 MHz, DMSO-*d*₆) δ 9.01 (s, 1H, NHAr), 8.09–7.99 (m, 2H, Ar), 7.74–7.68 (m, 1H, Ar), 7.61–7.52 (m, 2H,

Ar), 7.48–7.39 (m, 2H, Ar), 7.30–7.23 (m, 2H, Ar), 6.71–6.64 (m, 1H, CH₂NH), 5.08–4.98 (m, 1H, CH), 4.64–4.39 (m, 2H, CH₂O), 3.60–3.52 (m, 2H, CH₂NH), 3.26 (s, 3H, CH₃). HRMS (*m/z*): calcd. for C₁₈H₁₉ClN₂O₆SNa 449.0545 [M + Na]⁺; found 449.0541.

4.1.10. Nucleophilic substitution reaction with sodium azide

N-[2-Azido-(3-benzoyloxy)propyl]-*N'*-(4-chlorophenyl)urea (**79**). According to reported procedure [58], to a solution of mesyl derivative (**77**, 0.5 mmol) in DMF (3 mL), was added sodium azide (2.5 mmol) at rt and the mixture was heated to 85 °C and stirred overnight. The reaction was diluted with water and extracted with ethyl acetate. The organic phase was washed with saturated solution of NaHCO₃ and brine, then was dried (MgSO₄) and filtered. The solvent was removed under reduced pressure to give compound as colourless oil, that was used without further purification (150 mg, 80% yield). ¹H NMR (500 MHz, DMSO-*d*₆) δ 8.78 (s, 1H, NHAr), 8.06–7.99 (m, 2H, Ar), 7.73–7.66 (m, 1H, Ar), 7.60–7.51 (m, 2H, Ar), 7.47–7.39 (m, 2H, Ar), 7.31–7.23 (m, 2H, Ar), 6.51 (t, *J* = 5.9 Hz, 1H, CH₂NH), 4.53 (dd, *J* = 3.5 Hz, *J* = 11.8 Hz 1H, CH₂O), 4.35 (dd, *J* = 7.5 Hz, *J* = 11.9 Hz 1H, CH₂O), 4.12–4.06 (m, 1H, CH), 3.52–3.37 (m, 2H, CH₂NH). ¹³C NMR (125 MHz, DMSO-*d*₆) δ 165.4, 155.0, 139.2, 133.5, 129.4, 129.3, 129.2, 128.7, 124.7, 119.3, 64.7, 60.2, 36.2.

4.1.11. Deprotection reaction of *N*-[2-azido-(3-benzoyloxy)propyl]-*N'*-(4-chlorophenyl)urea

N-(2-Azido-3-hydroxypropyl)-*N'*-(4-chlorophenyl)urea (**80**). According to reported procedure [59] compound **79** (0.5 mmol) was dissolved in methanol and a 0.5 M sodium hydroxide solution (0.65 mmol) was added. The reaction mixture was heated to 55 °C and stirred for 1 h (TLC revealed the full consumption of the starting material). The reaction was evaporated to dryness and the residue was crystallized in DCM, filtered and washed with fresh DCM to give compound a white solid (120, 88% yield). ¹H NMR (500 MHz, DMSO-*d*₆) δ 9.22 (s, 1H, NHAr), 7.50–7.42 (m, 2H, Ar), 7.30–7.23 (d, 2H, Ar), 6.98–6.89 (m, 1H, CH₂NH), 3.75–3.71 (m, 2H, CH₂NH), 3.63–3.45 (m, 2H, CH₂OH), 3.26–3.15 (m, 1H, CHN₃). ¹³C NMR (125 MHz, DMSO-*d*₆) δ 155.4, 139.7, 128.4, 124.4, 119.1, 63.2, 61.8, 42.8. HRMS (*m/z*): calcd for C₁₀H₁₂ClN₅O₂Na 292.0572 [M + Na]⁺; found 292.0573.

4.1.12. Synthesis of 1,2,3-triazole derivative by Cu(I)-catalyzed 1,3-dipolar cycloaddition (CuAAC) reaction (**71–76**, **81–86**)

According to reported procedure [60], the appropriate azide derivative (**70** or **80**, 0.5 mmol) was dissolved in *tert*-butanol-water (1:1, 15 mL). The appropriate acetylene (0.6 mmol), sodium ascorbate (0.020 mmol) and CuSO₄ (0.010 mmol) were added to the flask and the mixture was stirring at 25 °C. The reaction was monitored by TLC until all the starting material had reacted, then it was evaporated under *vacuum*. The product was purified by flash column chromatography on silica gel using the appropriate eluent.

4.1.13.1. *N*-(4-Chlorophenyl)-*N'*-(2-hydroxy-3-[4-(hydroxymethyl)triazolyl]propyl)urea (**71**). The product was obtained as a light yellow solid and purified by column chromatography using dichloromethane-methanol (15:1, 0.5% Et₃N) as eluent (130 mg, 79% yield), mp 131–132 °C. ¹H NMR (500 MHz, CD₃OD) δ 7.95 (s, 1H, CH triazole), 7.39 (d, *J* = 9.2 Hz, 2H, Ar), 7.26 (d, *J* = 8.5 Hz, 2H, Ar), 4.83 (s, 2H, HOCH₂), 4.71 (s, 1H, CHOH), 4.58–4.53 (m, 1H, NCH₂), 4.43–4.37 (m, 1H, NCH₂), 3.29–3.24 (m, 1H, CH₂NH), 3.21–3.16 (m, 1H, CH₂NH). ¹³C NMR (125 MHz, CD₃OD) δ 158.2, 139.8, 132.4, 129.7, 128.3, 125.3, 121.4, 70.7, 56.5, 54.9, 47.9. HRMS (*m/z*): calcd for C₁₃H₁₆ClN₅O₃Na 348.0834 [M + Na]⁺; found 348.0834.

4.1.13.2. *N*-(4-Chlorophenyl)-*N'*-(2-hydroxy-3-[4-(phthaloylaminoethyl)triazolyl]propyl)urea (**72**). The product was obtained as a white solid and purified by column chromatography using hexane–ethyl acetate (1:4, 0.5% Et₃N) as eluent (146 mg, 82% yield), mp 222–223 °C. ¹H NMR (500 MHz, DMSO-*d*₆) δ 13.20 (bs, 1H, COOH), 8.75 (s, 1H, ArCONHCH₂), 8.03 (s, 1H, NHAr), 7.94–7.84 (m, 3H, Ar), 7.79 (s, 1H, CH triazole), 7.60–7.56 (m, 1H,

Ar), 7.43–7.39 (m, 2H, Ar), 7.28–7.24 (m, 2H, Ar), 6.22 (t, *J* = 5.6 Hz, 1H, CH₂NH), 5.10 (d, *J* = 5.1 Hz, 1H, OH), 4.86 (s, 2H, ArCONHCH₂), 4.49–2.22 (m, 2H, CH₂N), 3.95–3.88 (m, 1H, CH), 3.20–3.05 (m, 2H, CH₂NH). ¹³C NMR (125 MHz, DMSO-*d*₆) δ 168.4, 167.3, 155.2, 141.9, 139.4, 134.5, 131.6, 130.6, 128.4, 124.5, 123.9, 123.2, 119.1, 68.3, 59.4, 53.3, 42.8. HRMS (*m/z*): calcd. for C₂₁H₂₁ClN₆O₅Na 495.1049 [M + Na]⁺; found 495.1044.

4.1.13.3. *N*-(4-Chlorophenyl)-*N'*-(2-hydroxy-3-[4 (diethylphosphonatemethoxymethyl)triazolyl]propyl)urea (**73**). The product was obtained as a colourless oil and purified by column chromatography using ethyl acetate–methanol (15:1, 0.5% Et₃N) as eluent (193 mg, 81% yield). ¹H NMR (500 MHz, DMSO-*d*₆) δ 8.78 (s, 1H, NHAr), 8.17 (s, 1H, CH triazole), 7.42 (d, *J* = 8.9 Hz, 2H, Ar), 7.27 (d, *J* = 8.9 Hz, 2H, Ar), 6.33 (t, *J* = 5.7 Hz, 1H, CH₂NH), 5.46 (d, *J* = 5.5 Hz, 1H, OH), 4.63 (s, 2H, OCH₂), 4.43 (dd, *J* = 13.9 Hz, *J* = 3.9 Hz, 1H, NCH₂), 4.29 (dd, *J* = 13.9 Hz, *J* = 7.5 Hz, 1H, NCH₂), 4.08–4.00 (m, 4H, OCH₂CH₃), 3.98–3.91 (m, 1H, CHOH), 3.85–3.82 (m, 2H, PCH₂O), 3.22–3.17 (m, 1H, CH₂NH), 3.13–3.07 (m, 1H, CH₂NH), 1.27–1.21 (m, 6H, OCH₂CH₃). ¹³C NMR (125 MHz, DMSO-*d*₆) δ 155.2, 142.6, 139.3, 128.4, 125.1, 124.6, 119.2, 68.6, 65.1, 63.5, 61.8, 53.2, 42.8, 16.2. HRMS (*m/z*): calcd for C₁₈H₂₇ClN₅O₆PNa 498.1280 [M + Na]⁺; found 498.1271.

4.1.13.4. *N*-(4-Chlorophenyl)-*N'*-(2-hydroxy-3-[4-(4-fluorophenyl)triazolyl]propyl)urea (**74**). The product was obtained as a white solid and purified by column chromatography hexane–ethyl acetate (1:2.5, 0.5% Et₃N) as eluent (117 mg, 60% yield), mp 230–231 °C. ¹H NMR (500 MHz, DMSO-*d*₆) δ 8.80 (s, 1H, NHAr), 8.52 (s, 1H, CH triazole), 7.92–7.89 (m, 2H, Ar), 7.43 (d, *J* = 9.2 Hz, 2H, Ar), 7.31–7.26 (m, 4H, Ar), 6.36 (t, *J* = 5.9 Hz, 1H, CH₂NH), 5.47 (d, *J* = 5.5 Hz, 1H, OH), 4.71 (dd, *J* = 13.2 Hz, *J* = 3.5 Hz, 1H, NCH₂), 4.32 (dd, *J* = 14.0 Hz, *J* = 7.5 Hz, 1H, NCH₂), 4.04–3.97 (m, 1H, CHOH), 3.29–3.24 (m, 1H, CH₂NH), 3.17–3.12 (m, 1H, CH₂NH). ¹³C NMR (125 MHz, DMSO-*d*₆) δ 162.7, 160.7, 155.2, 145.2, 139.4, 128.5, 127.5, 127.1, 124.5, 122.1, 119.1, 115.9, 115.7, 68.7, 53.6, 42.9. HRMS (*m/z*): calcd for C₁₈H₁₈ClFN₅O₂ 390.1128 [M + H]⁺; found 390.1121.

4.1.13.5. *N*-(4-Chlorophenyl)-*N'*-(2-hydroxy-3-[4-(4-methoxyphenyl)triazolyl]propyl)urea (**75**). The product was obtained as a light yellow solid and purified by column chromatography using hexane–ethyl acetate (1:2, 0.5% Et₃N) as eluent (140 mg, 71% yield), mp 218–219 °C. ¹H NMR (500 MHz, DMSO-*d*₆) δ 8.80 (s, 1H, NHAr), 8.41 (s, 1H, CH triazole), 7.79 (d, *J* = 8.8 Hz, 2H, Ar), 7.44 (d, *J* = 8.9 Hz, 2H, Ar), 7.28 (d, *J* = 8.8 Hz, 2H, Ar), 7.02 (d, *J* = 8.8 Hz, 2H, Ar), 6.37 (t, *J* = 6.7 Hz, 1H, CH₂NH), 5.47 (d, *J* = 5.5 Hz, 1H, OH), 4.48 (dd, *J* = 13.9 Hz, *J* = 3.8 Hz, 1H, CH₂N), 4.32 (dd, *J* = 14.3 Hz, *J* = 7.6 Hz, 1H, CH₂N), 4.04–3.98 (m, 1H, CHOH), 3.81 (s, 3H, OCH₃), 3.27–3.20 (m, 1H, CH₂NH), 3.17–3.11 (m, 1H, CH₂NH). ¹³C NMR (125 MHz, DMSO-*d*₆) δ 158.9, 155.2, 145.9, 139.4, 128.4, 126.4, 124.5, 123.5, 121.2, 119.1, 114.3, 68.7, 55.1, 53.5, 42.8. HRMS (*m/z*): calcd for C₁₉H₂₁ClN₅O₃Na 402.1327 [M + H]⁺; found 402.1321.

4.1.13.6. *N*-(4-Chlorophenyl)-*N'*-(2-hydroxy-3-[4-(2-formylphenyl)triazolyl]propyl)urea (**76**). The product was obtained as a white solid and purified by column chromatography using hexane–ethyl acetate (1:2, 0.5% Et₃N) as eluent (122 mg, 62% yield), mp 198–199 °C. ¹H NMR (500 MHz, DMSO-*d*₆) δ 10.51 (s, 1H, COH), 8.87 (s, 1H, NHAr), 8.66 (s, 1H, Ar), 7.94 (d, *J* = 7.5 Hz, 1H, Ar), 7.83–7.78 (m, 2H, Ar, CH triazole), 7.62–7.59 (m, 1H, Ar), 7.50–7.45 (m, 2H, Ar), 7.32–7.29 (m, 2H, Ar), 6.43 (t, *J* = 5.8 Hz, 1H, CH₂NH), 5.22 (d, *J* = 5.5 Hz, 1H, OH), 4.60 (dd, *J* = 13.9 Hz, *J* = 3.7 Hz, 1H, CH₂N), 4.42 (dd, *J* = 13.9 Hz, *J* = 7.8 Hz, 1H, CH₂N), 4.11–4.05 (m, 1H, CHN), 3.32–3.28 (m, 1H, CH₂NH), 3.22–3.18 (m, 1H, CH₂NH). ¹³C NMR (125 MHz, DMSO-*d*₆) δ 193.1, 155.7, 143.9, 139.8, 133.8, 133.7, 130.0, 128.9, 128.8, 127.9, 125.9, 125.0, 119.5, 69.1, 54.2, 43.3.

4.1.13.7. *N*-(4-Chlorophenyl)-*N'*-(3-hydroxy-2-[4-(hydroxymethyl)triazolyl]propyl)urea (**81**). The product was obtained as a light yellow solid and purified by column chromatography using dichloromethane-methanol (15:1, 0.5% Et₃N) as eluent (104 mg, 64% yield), mp

125–126 °C. ^1H NMR (500 MHz, CD_3OD) δ 8.02 (s, 1H, CH triazole), 7.36–7.32 (m, 2H, Ar), 7.28–7.23 (m, 2H, Ar), 4.83 (s, 2H, HOCH_2), 4.15–4.10 (m, 1H, CHN), 4.02–3.97 (m, 2H, CH_2NH), 4.83 (dd, $J = 5.1$ Hz, $J = 14.3$ Hz, 1H, CH_2OH), 3.74 (dd, $J = 8.4$ Hz, $J = 14.4$ Hz, 1H, CH_2OH). ^{13}C NMR (125 MHz, CD_3OD) δ 158.2, 148.9, 139.8, 129.7, 128.4, 125.3, 124.2, 121.4, 70.6, 64.7, 56.6, 44.3. HRMS (m/z): calcd. for $\text{C}_{13}\text{H}_{16}\text{ClN}_5\text{O}_3\text{Na}$ 348.0834 [$\text{M} + \text{Na}$] $^+$; found 348.0831.

4.1.13.8. *N*-(4-Chlorophenyl)-*N'*-{3-hydroxy-2-[4-(phthaloylamino-methyl)triazolyl]propyl}urea (**82**). The product was obtained as a white solid and purified by column chromatography using hexane–ethyl acetate (1:4, 0.5% Et_3N) (162 mg, 69% yield), mp 212–213 °C. ^1H NMR (500 MHz, $\text{DMSO}-d_6$) δ 8.65 (s, 1H, ArCONHCH $_2$), 8.10 (s, 1H, NHAr), 7.93–7.87 (m, 5H, Ar, CH triazole), 7.38–7.34 (m, 2H, Ar), 7.28–7.22 (m, 2H, Ar), 6.22 (t, $J = 5.8$ Hz, 1H, CH_2NH), 5.10 (t, $J = 5.4$ Hz, 1H, OH), 4.86 (s, 2H, ArCONHCH $_2$), 4.71–4.65 (m, 1H, CHN), 3.74 (t, $J = 5.5$ Hz, 2H, CH_2OH), 3.69–3.63 (m, 1H, CH_2NH), 3.57–3.49 (m, 1H, CH_2NH). ^{13}C NMR (125 MHz, $\text{DMSO}-d_6$) δ 167.3, 154.9, 141.9, 139.1, 134.5, 131.6, 128.4, 124.6, 123.2, 122.6, 119.1, 69.8, 62.8, 61.5, 33.0. HRMS (m/z): calcd. for $\text{C}_{21}\text{H}_{21}\text{ClN}_6\text{O}_5\text{Na}$ 495.9001 [$\text{M} + \text{Na}$] $^+$; found 495.8999.

4.1.13.9. *N*-(4-Chlorophenyl)-*N'*-{3-hydroxy-2-[4 (diethylphosphonatemethoxymethyl) triazolyl]propyl}urea (**83**). The product was obtained as a colourless oil and purified by column chromatography using ethyl acetate–methanol (15:1, 0.5% Et_3N) as eluent (173 mg, 72% yield). ^1H NMR (500 MHz, $\text{DMSO}-d_6$) δ 8.71 (s, 1H, NHAr), 8.18 (s, 1H, CH triazole), 7.38 (d, $J = 8.9$ Hz, 2H, Ar), 7.25 (d, $J = 8.9$ Hz, 2H, Ar), 6.27 (t, $J = 5.7$ Hz, 1H, CH_2NH), 5.16 (t, $J = 5.4$ Hz, 1H, OH), 4.77–4.68 (m, 1H, CHN), 4.63 (s, 2H, OCH_2), 4.08–3.98 (m, 4H, OCH_2CH_3), 3.87–3.82 (m, 2H, PCH_2O), 3.77 (t, $J = 5.4$ Hz, 2H, CH_2OH), 4.71–4.64 (m, 1H, CH_2NH), 4.61–4.53 (m, 1H, CH_2NH), 1.25–1.20 (m, 6H, OCH_2CH_3). ^{13}C NMR (125 MHz, $\text{DMSO}-d_6$) δ 155.5, 143.0, 139.7, 128.9, 125.1, 124.4, 119.5, 65.7, 64.0, 63.3, 62.7, 62.2, 62.0, 16.7. HRMS (m/z): calcd. for $\text{C}_{18}\text{H}_{27}\text{ClN}_5\text{O}_6\text{PNa}$ 498.1280 [$\text{M} + \text{Na}$] $^+$; found 498.1276.

4.1.13.10. *N*-(4-Chlorophenyl)-*N'*-{3-hydroxy-2-[4-(4-fluorophenyl) triazolyl]propyl} urea (**84**). The product was obtained as a white solid and purified by column chromatography using hexane–ethyl acetate (1:2, 0.5% Et_3N) as eluent (163 mg, 84% yield), mp 227–228 °C. ^1H NMR (500 MHz, $\text{DMSO}-d_6$) δ 8.70 (s, 1H, NHAr), 8.65 (s, 1H, CH triazole), 7.94–7.88 (m, 2H, Ar), 7.42–7.37 (m, 2H, Ar), 7.33–7.23 (m, 4H, Ar), 6.30 (t, $J = 5.8$ Hz, 1H, CH_2NH), 5.21 (t, $J = 5.5$ Hz, 1H, OH), 4.69–4.62 (m, 1H, CHN), 3.83 (t, $J = 5.5$ Hz, 2H, CH_2OH), 3.79–3.73 (m, 1H, CH_2NH), 3.63–3.56 (m, 1H, CH_2NH). ^{13}C NMR (125 MHz, $\text{DMSO}-d_6$) δ 160.7, 155.0, 145.2, 139.1, 128.4, 127.5, 127.4, 124.6, 120.8, 119.1, 115.8, 115.7, 63.1, 61.6, 40.0. HRMS (m/z): calcd for $\text{C}_{18}\text{H}_{18}\text{ClFN}_5\text{O}_2\text{Na}$ 390.1128 [$\text{M} + \text{H}$] $^+$; found 390.1125.

4.1.13.11. *N*-(4-Chlorophenyl)-*N'*-{3-hydroxy-2-[4-(4-methoxyphenyl) triazolyl]propyl} urea (**85**). The product was obtained as a light yellow solid and purified by column chromatography using hexane–ethyl acetate (1:1.5, 0.5% Et_3N) (104 mg, 64% yield), mp 206–207 °C. ^1H NMR (500 MHz, $\text{DMSO}-d_6$) δ 8.70 (s, 1H, NHAr), 8.51 (s, 1H, CH triazole), 7.81–7.76 (m, 2H, Ar), 7.45–7.37 (m, 2H, Ar), 7.30–7.23 (m, 2H, Ar), 7.06–6.98 (m, 2H, Ar), 6.30 (t, $J = 5.8$ Hz, 1H, CH_2NH), 5.22 (t, $J = 5.2$ Hz, 1H, OH), 4.78–4.72 (m, 1H, CHN), 4.56–4.46 (m, 1H, CH_2OH), 4.36–4.29 (m, 1H, CH_2OH), 3.28–3.21 (m, 1H, CH_2NH), 3.16–3.11 (m, 1H, CH_2NH). ^{13}C NMR (125 MHz, $\text{DMSO}-d_6$) δ 166.7, 158.8, 155.2, 155.0, 145.9, 139.1, 128.3, 127.3, 126.4, 124.7, 123.5, 121.3, 119.9, 114.2, 68.7, 62.9, 55.1, 43.5. HRMS (m/z): calcd. for $\text{C}_{19}\text{H}_{21}\text{ClN}_5\text{O}_3$ 402.8890 [$\text{M} + \text{H}$] $^+$; found 402.8889.

4.1.13.12. *N*-(4-Chlorophenyl)-*N'*-{3-hydroxy-2-[4-(2-formylphenyl) triazolyl]propyl} urea (**86**). The product was obtained as a white resin and purified by column chromatography using hexane–ethyl acetate (1:2, 0.5% Et_3N) (120 mg, 60% yield). ^1H NMR (500 MHz, $\text{DMSO}-d_6$) δ 10.37 (s, 1H, COH), 8.82 (s, 1H, NHAr), 8.73 (s, 1H, Ar), 8.62 (s, 1H, CH triazole), 7.92–7.89 (m, 1H, Ar), 7.80–7.73 (m, 1H, Ar), 7.59–7.55 (m, 1H, Ar), 7.45–7.36 (m, 2H, Ar), 7.28–7.23 (m, 2H, Ar), 6.39 (t, $J = 5.4$

Hz, 1H, CH_2NH), 5.23 (t, $J = 5.5$ Hz, 1H, OH), 4.53 (dd, $J = 13.9$ Hz, $J = 3.8$ Hz, 1H, CH_2OH), 4.38 (dd, $J = 13.9$ Hz, $J = 7.8$ Hz, 1H, CH_2OH), 4.09–4.01 (m, 1H, CHN), 3.29–3.23 (m, 1H, CH_2NH), 3.19–3.13 (m, 1H, CH_2NH). ^{13}C NMR (125 MHz, $\text{DMSO}-d_6$) δ 193.2, 155.7, 143.9, 139.8, 134.4, 133.8, 133.7, 130.0, 128.9, 128.8, 127.9, 125.9, 124.7, 119.5, 69.1, 54.2, 43.3.

4.1.13. Synthesis of terminal alkynes

4.1.14.1. *N*-propargylphthalylmonoamide (**87**) [61]. To a stirred solution of propargylamine (2.2 mmol) in THF (4 mL), phthalic anhydride (2.0 mmol) was added and the mixture was stirred at rt until TLC showed that all the starting material has reacted (18 h). The formed solid was filtered, dissolved in water and 1 N solution of HCl was added until pH 5. The reaction was extracted with ethyl acetate and the organic layer was washed with brine, dried (MgSO_4) and filtered. The solvent was removed under reduced pressure to give the compound that was used without further purification (170 mg, 83% yield). ^1H NMR (300 MHz, $\text{DMSO}-d_6$) δ 9.91 (s, 1H, NH), 7.67–7.61 (m, 1H, Ar), 7.58–7.52 (m, 1H, Ar), 7.48–7.38 (m, 2H, Ar), 3.54 (m, 2H, CH_2), 3.90 (t, $J = 2.49$ Hz, 1H, CH).

4.1.14.2. Propargyloxymethylphosphonate (**88**). A Solution of propargyl alcohol (1.5 mmol) in THF (3 mL) was added slowly to a solution of NaH (1.6 mmol, 60% dispersion in mineral oil) in THF (2 mL). The mixture was stirred for 1 h and then cooled to 0 °C. Diethyl (tosyloxy) methylphosphonate (2.0 mmol) was added to the flask and the reaction was stirred for 3 h at 0 °C and then for 24 h at rt. When TLC revealed the full consumption of the starting material, the reaction was evaporated to dryness and the residue was dissolved in ethyl acetate and washed with water (2 \times 10 mL). The organic phase was dried (MgSO_4) filtered, and the solvent was removed under vacuum to give compound as a colourless oil. The compound was used without further purification (230 mg, 74% yield). MS (FAB): m/z 229 (100%) [$\text{M} + \text{Na}$] $^+$. ^1H NMR (300 MHz, $\text{DMSO}-d_6$) δ 4.28–3.22 (m, 2H, OCH_2), 4.12–3.95 (m, 4H, OCH_2CH_3), 3.86–3.78 (m, 2H, PCH_2O), 3.33 (s, 1H, CH), 1.30–1.13 (m, 6H, OCH_2CH_3).

4.1.15. Characterization data of compound **66** (*N*-(4-Chlorophenyl)-*N'*-{2-hydroxy-3-[(*E*)-(3,4,5-trimethoxyphenyl)acryloxy]propyl}urea). Compound was isolated during the purification of compound **45** by column chromatography, using hexane–ethyl acetate (1:2) as eluent and was obtained as a white solid (55 mg, 15% yield), mp 144–145 °C. ^1H NMR (500 MHz, $\text{DMSO}-d_6$) δ 8.74, (s, 1H, NHAr), 7.67–7.59 (m, 1H, CH = CHCO), 7.42 (d, $J = 8.8$ Hz, 2H, Ar), 7.29–7.23 (m, 2H, Ar), 7.09–7.05 (m, 2H, Ar), 6.70–6.64 (m, 1H, CH = CHCO), 6.32–6.26 (m, 1H, CH_2NH), 5.27 (d, $J = 5.2$ Hz, 1H, OH), 4.97–4.92 (m, 1H, CH), 4.11 (d, $J = 5.4$ Hz, 2H, CH_2O), 3.87–3.80 (m, 6H, OCH_3), 3.73–3.69 (m, 3H, OCH_3), 3.60–3.48 (m, 1H, CH_2NH), 3.19–3.12 (m, 1H, CH_2NH). ^{13}C NMR (125 MHz, $\text{DMSO}-d_6$) δ 166.3, 155.1, 153.0, 144.8, 139.5, 139.4, 129.6, 128.4, 124.5, 119.0, 119.0, 117.6, 105.9, 105.8, 67.6, 66.0, 60.0, 56.0, 42.3. HRMS (m/z): calcd. for $\text{C}_{22}\text{H}_{25}\text{ClN}_2\text{O}_7\text{Na}$ 487.1242 [$\text{M} + \text{Na}$] $^+$; found 487.1238. Anal. Calcd for $\text{C}_{22}\text{H}_{25}\text{ClN}_2\text{O}_7$: C, 56.84; H, 5.42; N, 6.03. Found: C, 56.80; H, 5.40; N, 5.05.

4.2. Biological evaluation

4.2.1. Cell lines

Human A549 and 293 cell lines were obtained from the American Type Culture Collection (ATCC, Manassas, VA). The 293B5 stable cell line overexpressing the human $\beta 5$ integrin subunit was kindly provided by Dr. Glen Nemerow [62]. The cell lines were propagated in Dulbecco's modified Eagle medium (DMEM, Life Technologies/Thermo Fisher) supplemented with 10% fetal bovine serum (FBS) (Omega Scientific, Tarzana, CA), 10 mM HEPES, 4 mM L-glutamine, 100 units/ml penicillin, 100 mg/mL streptomycin, and 0.1 mM non-essential amino acids (complete DMEM).

Wild-type HAdV-5 were obtained from the ATCC. The HAdV-5-GFP used in this study is a replication-defective virus containing a CMV

promoter-driven enhanced green fluorescent protein (eGFP) reporter gene cassette in place of the E1/E3. HAdV were propagated in 293β5 cells and isolated from the cellular lysate by cesium chloride density centrifugation. Virus concentration, in mg/ml, was calculated with the Bio-Rad Protein Assay (Bio-Rad Laboratories) and converted to virus particles/ml (vp/ml) using 4×10^{12} vp/mg.

4.2.2. Plaque assay

Compounds were tested using low MOI infections (0.03 vp/cell) at concentrations of 10 μM. If the percentage of inhibition was upper than 60%, compounds was also tested in a dose–response assay ranging from 10 to 0.375 μM in a plaque assay. For that, 293β5 cells were seeded in 6-well plates at a density of 4×10^5 cells per well in duplicate for each condition. When cells reached 80–90% confluency, they were infected with HAdV5-GFP (0.06 vp/cell) and rocked for 2 h at 37 °C. After the incubation, the inoculum was removed and the cells were washed once with PBS. The cells were then carefully overlaid with 2 mL/well of equal parts of 1.6% (water/vol) Difco Agar Noble (Becton, Dickinson & Co., Sparks, MD), 2x EMEM (Minimum Essential Medium Eagle, Bio-Whittaker) and the compounds. EMEM was supplemented with 2x penicillin/streptomycin, 2x L-glutamine, and 10% FBS. Compounds were then added in concentrations ranging from 10 to 0.375 μM. Following incubation for 7 days at 37 °C, plates were scanned with a Typhoon FLA 9000 imager (GE Healthcare Life Sciences) and plaques were quantified with ImageJ [63].

4.2.3. Cytotoxicity assay

The cytotoxicity of the compounds was analyzed by commercial kit AlamarBlue (Invitrogen, ref DAL1025). Briefly, A549 cells at a density of 5×10^3 cells per well in 96-well plates were seeded. Decreasing concentrations of each derivative from 200 μM to 2.5 μM were diluted in 100 μL of Dulbecco's Modified Eagle Medium (DMEM), added to the cells and incubated at 37 °C for 48 h following the kit protocol. The cytotoxic concentration 50 (CC₅₀) value was obtained using the statistical package GraphPad Prism. This assay was performed in duplicate.

4.2.4. Quantification of HAdV DNA, E1A mRNA and E2B mRNA

A549 cells (1.5×10^5 cells/well in a 24-well plate) were incubated for 24 h in 500 μL of complete DMEM, and they were infected with wild-type HAdV5 (100 vp/cell) when 80–90% confluency was observed.

For DNA quantification, infected cells were incubated for 16 h at 37 °C in 500 μL of complete DMEM containing 10-fold IC₅₀ concentration obtained in the plaque assay of the compounds or the same volume of DMSO (positive control). All samples were done in duplicate.

After incubation at 37 °C and 5% CO₂, DNA was purified from the cell lysate with the E.Z.N.A. Tissue DNA Kit (Omega Biotek, Norcross, GA) following the manufacturer's instructions. TaqMan primers and probes for a common region of the HAdV5 were designed with the GenScript Real-Time PCR (TaqMan) Primer Design software (GenScript). Oligonucleotide sequences were as follows: AQ1: 5'-GCC ACG GTG GGG TTT CTA AAC TT-3'; AQ2: 5'-GCC CCA GTG GTC TTA CAT GCA CAT-3'; Probe: 6-FAM-5'-TGC ACC AGA CCC GGG CTC AGG TAC TCC GA-3'-TAMRA'. Real-time PCR mixtures consisted of 9.5 μL of the purified DNA, AQ1 and AQ2 at a concentration of 200 nM each, and probe at a concentration of 50 nM in a total volume of 12.5 μL mixed with 12.5 μL of FastGene 2x PROBE Universal (NIPPON Genetics). The PCR cycling protocol was 95 °C for 3 min followed by 40 cycles of 95 °C for 10 s and 60 °C for 30 s.

For E1A and E2B mRNA quantification, infected cells were incubated for 6 h at 37 °C in 500 μL of complete DMEM containing 10-fold IC₅₀ concentration obtained in the plaque assay of the compounds or the same volume of DMSO (positive control). All samples were done in duplicate. RNA was purified with the RNeasy Mini Kit (QIAGEN, Valencia, CA) following the manufacturer's instructions. Quantification of RNA copy numbers was performed using primers and conditions previously reported for E1A and E2B [64].

The human glyceraldehyde-3-phosphate dehydrogenase GAPDH was used as an internal control. Oligonucleotide sequences for GAPDH and the conditions were those previously reported [64]. For quantification, gene fragments from hexon and GAPDH were cloned into the pGEM-T Easy vector (Promega), and known concentrations of template were used to generate a standard curve in parallel for each experiment. All assays were performed in a thermal cycler LightCycler 96 System (Roche).

4.2.5. Quantification of Nuclear-Associated HAdV genomes

A549 cells (1×10^6 cells/well) in 6-well plates were infected with wild-type HAdV5 at MOI 2,000 in the presence of 10-fold IC₅₀ concentration obtained in the plaque assay of the compounds or the same volume of DMSO (positive control). Forty-five minutes after infection, A549 cells were trypsinized and collected and then washed twice with PBS. Then, cytoplasmic and nuclear fractions were separated using a hypotonic buffer solution and NP-40 detergent. The cell pellet was resuspended in 500 μL of 1x hypotonic buffer (20 mM Tris-HCl pH 7.4, 10 mM NaCl, 3 mM MgCl₂) and incubated for 15 min at 4 °C. Then, 25 μL of NP-40 was added, and the samples were vortexed. The homogenates were centrifuged for 10 min at 835g at 4 °C. Following supernatant contained the cytoplasmic fraction and the pellet contained the nuclear fraction. HAdV DNA was isolated from both fractions using the E.Z.N.A. Tissue DNA Kit (Omega Biotek, Norcross, GA). HAdV genomes was quantified by real-time PCR following the same protocol we described above.

4.2.6. Virus yield reduction

A549 cells (1.5×10^5 cells/well in a 24-well plate) were incubated 24 h in 500 μL of complete DMEM, and they were infected with wild-type HAdV5 (100 vp/cell) when >90% of confluency was observed. Infected cells were incubated for 48 h at 37 °C in 500 μL of complete DMEM containing 10-fold IC₅₀ concentration obtained in the plaque assay of either compounds or the same volume of DMSO (positive control). After 48 h, cells were harvested and subjected to three rounds of freeze/thaw. Serial dilutions of clarified lysates were titrated on A549 cells (3×10^4 cells/well in a 96-well plate), and TCID₅₀ values were calculated using an end-point dilution method [65].

4.2.7. Time of addition curve

The anti-HAdV effect of derivatives at different points of time was measured in a time-curve assay using 293β5 cells (3×10^5 cells/well in corning black wall, clear bottom 96-well plates) infected with HAdV5-GFP (2,000 vp/cell) in the presence of 10-fold IC₅₀ concentration obtained in the plaque assay of the compounds or the same volume of DMSO (positive control). Parallel samples of HAdV-5 were incubated with or without the selected derivatives on ice for 1 h. The virus was then added to 293β5 cells and the plate were incubated 1 h on ice. After that, the inoculum was removed and the derivatives were added at the indicated time points before or during this incubation. After a total of 2 h at 37 °C, cells were incubated for an additional 48 h at 37 °C and 5% CO₂ before being analyzed for GFP expression using the Typhoon 9410 imager (GE Healthcare Life Sciences), as above.

4.2.8. Synergy assay

For this assay, the same conditions of the plaque assay were used (293β5 cells were seeded at a density of 4×10^5 cells/well in 6 well-plate and infected at MOI 0.06 with HAdV5-GFP) but the compounds added were a combination of two compounds in a dose–response assay ranging from 2xIC₅₀ to 1/8xIC₅₀. After incubation for 7 days at 37 °C, plates were scanned with a Typhoon FLA 9000 imager (GE Healthcare Life Sciences) and plaques were quantified with ImageJ [63].

Data obtained was analysed with the CalcuSyn software (Biosoft) and the output obtained was used to define the synergistic or antagonistic effect of combinations, according to Chou-Talalay method.

4.2.9. Statistical analyses

One-way ANOVA tests (Dunnett method) were carried out using the GraphPad Prism 6. We considered a statistical significance with a $p \leq 0.05$. This statistical significance was pointed out with asterisk in graphs, and the numbers of them indicate the level of significance (* $p \leq 0.05$, ** $p \leq 0.01$, *** $p \leq 0.001$, **** $p \leq 0.0001$).

Declaration of Competing Interest

The authors declare that they have no known competing financial interests or personal relationships that could have appeared to influence the work reported in this paper.

Acknowledgements

This work has been supported by Ministerio de Ciencia, Innovación y Universidades, Plan Estatal 2017-2020 Retos - Proyectos I + D + i (PID2019-104767RB-I00); Ministerio de Economía y Competitividad, Plan Nacional I + D + i 2013-2016, Retos-Proyectos (CTQ2016-78580-C2-2-R); Instituto de Salud Carlos III, Subdirección General de Redes y Centros de Investigación Cooperativa, Ministerio de Economía, Industria y Competitividad, Spanish Network for Research in Infectious Diseases (REIPI RD16/0016/0009), cofinanced by European Development Regional Fund "A way to achieve Europe", the Instituto de Salud Carlos III, Proyectos de Investigación en Salud (PI17/01055; PI18/01191) and Proyectos de Desarrollo Tecnológico en Salud (DTS17/00130), the Spanish Adenovirus Network (AdenoNet, BIO2015/68990-REDT), and the program "Nicolás Monardes" (C-0059-2018), Servicio Andaluz de Salud, Junta de Andalucía. Authors thank CITIUS (Centro de Investigación, Tecnología e Innovación de la Universidad de Sevilla) for its contribution in recording NMR and Mass spectra and for elemental analysis determination. The authors are especially grateful to Dr. Manuel Angulo Álvarez for his assistance with heteronuclear 2D NMR and NOESY studies.

Appendix A. Supplementary material

Supplementary data to this article can be found online at <https://doi.org/10.1016/j.bioorg.2021.105095>.

References

- [1] T. Lion, Adenovirus infections in immunocompetent and immunocompromised patients, *Clin. Microbiol. Rev.* 27 (2014) 441–462, <https://doi.org/10.1128/CMR.00116-13>.
- [2] M. Echavarría, Adenoviruses in immunocompromised hosts, *Clin. Microbiol. Rev.* 21 (2008) 704–715, <https://doi.org/10.1128/CMR.00052-07>.
- [3] E. Hage, U.G. Liebert, S. Bergs, T. Ganzemueller, A. Heim, Human mastadenovirus type 70: A novel, multiple recombinant species D mastadenovirus isolated from diarrhoeal faeces of a haematopoietic stem cell transplantation recipient, *J. Gen. Virol.* 96 (2015) 2734–2742, <https://doi.org/10.1099/vir.0.000196>.
- [4] M.A. Prusinkiewicz, J.S. Mymryk, Metabolic reprogramming of the host cell by human adenovirus infection, *Viruses*. 11 (2019) 1–21, <https://doi.org/10.3390/v11020141>.
- [5] C.S. Martín, Latest insights on adenovirus structure and assembly, *Viruses*. 4 (2012) 847–877, <https://doi.org/10.3390/v4050847>.
- [6] M.K. Scott, C. Chommanard, X. Lu, D. Appelgater, L. Grenz, E. Schneider, S. I. Gerber, D.D. Erdman, A. Thomas, Human Adenovirus Associated with Severe Respiratory Infection, *Emerg. Infect. Dis.* 22 (2016) 2013–2014.
- [7] S. Abbas, J.E. Raybould, S. Sastry, O. de la Cruz, Respiratory viruses in transplant recipients: more than just a cold. Clinical syndromes and infection prevention principles, *Int. J. Infect. Dis.* 62 (2017) 86–93, <https://doi.org/10.1016/j.ijid.2017.07.011>.
- [8] D. García-Zalinskak, C. Rapuano, J.D. Sheppard, A.R. Davis, Adenovirus Ocular Infections: Prevalence, Pathology, Pitfalls, and Practical Pointers, *Eye Contact Lens*. 44 (2016) 1–7, <https://doi.org/10.1097/ICL.0000000000000226>.
- [9] K. Kosulin, E. Geiger, A. Vécsei, W.D. Huber, M. Rauch, E. Brenner, F. Wrba, K. Hammer, A. Innerhofer, U. Pötschger, A. Lawitschka, S. Matthes-Leodolter, G. Fritsch, T. Lion, Persistence and reactivation of human adenoviruses in the gastrointestinal tract, *Clin. Microbiol. Infect.* 22 (381) (2016), <https://doi.org/10.1016/j.cmi.2015.12.013>.
- [10] S.M.C. Lopez, M.G. Michaels, M. Green, Adenovirus infection in pediatric transplant recipients: Are effective antiviral agents coming our way? *Curr. Opin. Organ Transplant*. 23 (2018) 395–399, <https://doi.org/10.1097/MOT.0000000000000542>.
- [11] M.M.Y. Wayne, C.W. Sing, Anti-viral drugs for human adenoviruses, *Pharmaceuticals*. 3 (2010) 3343–3354, <https://doi.org/10.3390/ph3103343>.
- [12] L. Lenaerts, L. Naesens, Antiviral therapy for adenovirus infections, *Antiviral Res.* 71 (2006) 172–180, <https://doi.org/10.1016/j.antiviral.2006.04.007>.
- [13] K. Schaar, C. Röger, T. Pozzuto, J. Kurreck, S. Pinkert, H. Fehner, Biological antivirals for treatment of adenovirus infections, *Antivir. Ther.* 21 (2016) 559–566, <https://doi.org/10.3851/IMP3047>.
- [14] U. Yusuf, G.A. Hale, J. Carr, Z. Gu, E. Benaim, P. Woodard, K.A. Kasow, E. M. Horwitz, W. Leung, D.K. Srivastava, R. Handgretinger, R.T. Hayden, Cidofovir for the treatment of adenoviral infection in pediatric hematopoietic stem cell transplant patients, *Transplantation* 81 (2006) 1398–1404, <https://doi.org/10.1097/01.tp.0000209195.95115.8e>.
- [15] G. Lugthart, M.A. Oomen, C.M. Jol-van der Zijde, L.M. Ball, D. Bresters, W.J. W. Kollen, F.J. Smiers, C.L. Vermont, R.G.M. Bredius, M.W. Schilham, M.J.D. van Tol, A.C. Lankester, The Effect of Cidofovir on Adenovirus Plasma DNA Levels in Stem Cell Transplantation Recipients without T Cell Reconstitution, *Biol. Blood Marrow Transplant.* 21 (2015) 293–299, <https://doi.org/10.1016/j.bbmt.2014.10.012>.
- [16] A.E. Caruso Brown, M.N. Cohen, S. Tong, R.S. Braverman, J.F. Rooney, R. Giller, M.J. Levin, Pharmacokinetics and safety of intravenous cidofovir for life-threatening viral infections in pediatric hematopoietic stem cell transplant recipients, *Antimicrob. Agents Chemother.* 59 (2015) 3718–3725, <https://doi.org/10.1128/AAC.04348-14>.
- [17] J.A. Marrugal-Lorenzo, A. Serna-Gallego, J. Berastegui-Cabrera, J. Pachón, J. Sánchez-Céspedes, Repositioning salicylanilide anthelmintic drugs to treat adenovirus infections, *Sci. Rep.* 9 (2019) 1–10, <https://doi.org/10.1038/s41598-018-37290-3>.
- [18] C.C. Colpitts, L.M. Schang, A Small Molecule Inhibits Virion Attachment to Heparan Sulfate- or Sialic Acid-Containing Glycans, *J. Virol.* 88 (2014) 7806–7817, <https://doi.org/10.1128/jvi.00896-14>.
- [19] N.A. Nikitenko, E.S. Gureeva, A.A. Ozerov, A.I. Tukhvatulin, F.M. Izhaeva, V. S. Prassolov, P.G. Deryabin, M.S. Novikov, D.Y. Logunov, 1-(4-Phenoxybenzyl) 5-aminouracil derivatives and their analogues - novel inhibitors of human adenovirus replication, *Acta Naturae*. 10 (2018) 58–64, <https://doi.org/10.32607/20758251-2018-10-2-58-64>.
- [20] J. Xu, J. Berastegui-Cabrera, H. Chen, J. Pachón, J. Zhou, J. Sánchez-Céspedes, Structure-Activity Relationship Studies on Diversified Salicylamide Derivatives as Potent Inhibitors of Human Adenovirus Infection, *J. Med. Chem.* 63 (2020) 3142–3160, <https://doi.org/10.1021/acs.jmedchem.9b01950>.
- [21] D. Zhang, Qian; Xiang, Dehu; Zhang, Ling; Wang, Xia; Li, Application of aromatic ester compounds in preparing drugs for resisting Adenovirus-7 (ADV-7), *CN 2017-11446779*, 2018. <https://scifinder-cas-org.us.debiblio.com/scifinder/view/scifinder/scifinderExplore.jsf>.
- [22] S. Mazzotta, J.A. Marrugal-Lorenzo, M. Vega-Holm, A. Serna-Gallego, J. Álvarez-Vidal, J. Berastegui-Cabrera, J. Pérez del Palacio, C. Díaz, F. Aiello, J. Pachón, F. Iglesias-Guerra, J.M. Vega-Pérez, J. Sánchez-Céspedes, Optimization of piperazine-derived ureas privileged structures for effective antiadenovirus agents, *Eur. J. Med. Chem.* 185 (2020), <https://doi.org/10.1016/j.ejmech.2019.111840>.
- [23] J. Sánchez-Céspedes, P. Martínez-Aguado, M. Vega-Holm, A. Serna-Gallego, J. I. Candela, J.A. Marrugal-Lorenzo, J. Pachón, F. Iglesias-Guerra, J.M. Vega-Pérez, New 4-Acyl-1-phenylaminocarbonyl-2-phenylpiperazine Derivatives as Potential Inhibitors of Adenovirus Infection. Synthesis, Biological Evaluation, and Structure-activity Relationships, *J. Med. Chem.* 59 (2016) 5432–5448, <https://doi.org/10.1021/acs.jmedchem.6b00300>.
- [24] S. Sánchez Céspedes, Javier; Pachón Ibáñez, María Eugenia; Pachón Díaz, Jerónimo; Martínez Aguado, Pablo; Cebrero Canguero, Tania; Vega Pérez, José Manuel; Iglesias Guerra, Fernando; Vega Holm, Margarita; Candela Lena, Ignacio; Mazzotta, Piperazine Derivatives as Antiviral Agents with Increased Therapeutic Activity, US 2019 / 0308956, 2019. <https://patents.google.com/patent/US20190308956A1/en>.
- [25] S. Mazzotta, J. Berastegui-Cabrera, G. Carullo, M. Vega-Holm, M. Carretero-Ledesma, L. Mendolia, F. Aiello, F. Iglesias-Guerra, J. Pachón, J.M. Vega-Pérez, J. Sánchez-Céspedes, Serinol-based benzoic acid esters as new scaffolds for the development of adenovirus infection inhibitors: design, synthesis, and in vitro biological evaluation, *ACS Infect. Dis.* 7 (2021) 1433–1444, <https://doi.org/10.1021/acscinfecdis.0c00515>.
- [26] P. Sikka, Role of aryl urea containing compounds in medicinal chemistry, *Med. Chem.* 5 (2015) 479–483, <https://doi.org/10.4172/2161-0444.1000305>.
- [27] L. Chiummiento, M. Funicello, P. Lupatelli, F. Tramutola, F. Berti, F. Marino-Merlo, Synthesis and biological evaluation of novel small non-peptidic HIV-1 PIs: The benzothioephene ring as an effective moiety, *Bioorg. Med. Chem. Lett.* 22 (2012) 2948–2950, <https://doi.org/10.1016/j.bmcl.2012.02.046>.
- [28] F. Tramutola, M.F. Armentano, F. Berti, L. Chiummiento, P. Lupatelli, R. D'Orsi, R. Miglionico, L. Milella, F. Bisaccia, M. Funicello, New heteroaryl carbamates: Synthesis and biological screening in vitro and in mammalian cells of wild-type and mutant HIV-protease inhibitors, *Bioorg. Med. Chem.* 27 (2019) 1863–1870, <https://doi.org/10.1016/j.bmc.2019.03.041>.
- [29] D. Kang, H. Zhang, Z. Zhou, B. Huang, L. Naesens, P. Zhan, X. Liu, First discovery of novel 3-hydroxy-quinazoline-2,4(1H,3H)-diones as specific anti-vaccinia and adenovirus agents via 'privileged scaffold' refining approach, *Bioorg. Med. Chem. Lett.* 26 (2016) 5182–5186, <https://doi.org/10.1016/j.bmcl.2016.09.071>.
- [30] E. Rivero-Buceta, P. Carrero, E.G. Doyagiez, A. Madrona, E. Quesada, M. J. Camarasa, M.J. Pérez-Pérez, P. Leyssen, J. Paeshuyse, J. Balzarini, J. Neys, A. San-Félix, Linear and branched alkyl-esters and amides of gallic acid and other

- (mono-, di- and tri-) hydroxy benzoyl derivatives as promising anti-HCV inhibitors, *Eur. J. Med. Chem.* 92 (2015) 656–671, <https://doi.org/10.1016/j.ejmech.2015.01.033>.
- [31] S. Saul, S.Y. Pu, W.J. Zuercher, S. Einav, C.R.M. Asquith, Potent antiviral activity of novel multi-substituted 4-anilinoquin(az)olines, *Bioorg. Med. Chem. Lett.* 30 (2020), 127284, <https://doi.org/10.1016/j.bmcl.2020.127284>.
- [32] Z. Zhao, H. Song, J. Xie, T. Liu, X. Zhao, X. Chen, X. He, S. Wu, Y. Zhang, X. Zheng, Research progress in the biological activities of 3,4,5-trimethoxycinnamic acid (TMCA) derivatives, *Eur. J. Med. Chem.* 173 (2019) 213–227, <https://doi.org/10.1016/j.ejmech.2019.04.009>.
- [33] I.E. Glowacka, J. Balzarini, A.E. Wróblewski, The synthesis, antiviral, cytostatic and cytotoxic evaluation of a new series of acyclonucleotide analogues with a 1,2,3-triazole linker, *Eur. J. Med. Chem.* 70 (2013) 703–722, <https://doi.org/10.1016/j.ejmech.2013.10.057>.
- [34] T. Van Nguyen, A. Hospital, C. Lionne, L.P. Jordheim, C. Dumontet, C. Périgaud, L. Chaloin, S. Peyrottes, Beta-hydroxyphosphonate ribonucleoside analogues derived from 4-substituted-1,2,3-triazoles as IMP/GMP mimics: Synthesis and biological evaluation, *J. Org. Chem.* 12 (2016) 1476–1486, <https://doi.org/10.3762/bjoc.12.144>.
- [35] S.K.V. Vernekar, L. Qiu, J. Zhang, J. Kankanala, H. Li, R.J. Geraghty, Z. Wang, 5'-silylated 3'-1,2,3-triazolyl thymidine analogues as inhibitors of West Nile Virus and Dengue virus, *J. Med. Chem.* 58 (2015) 4016–4028, <https://doi.org/10.1021/acs.jmedchem.5b00327>.
- [36] E. Bonandi, M.S. Christodoulou, G. Fumagalli, D. Perdicchia, G. Rastelli, D. Passarella, The 1,2,3-triazole ring as a bioisostere in medicinal chemistry, *Drug Discov. Today* 22 (2017) 1572–1581, <https://doi.org/10.1016/j.drudis.2017.05.014>.
- [37] D.B. Goetz, M.L. Varney, D.F. Wiemer, S.A. Holstein, Amides as bioisosteres of triazole-based geranylgeranyl diphosphate synthase inhibitors, *Bioorg. Med. Chem.* 28 (2020), 115604, <https://doi.org/10.1016/j.bmc.2020.115604>.
- [38] I. Mohammed, I.R. Kummetha, G. Singh, N. Sharova, G. Lichinchi, J. Dang, M. Stevenson, T.M. Rana, 1,2,3-triazoles as amide bioisosteres: Discovery of a new class of potent HIV-1 Vif antagonists, *J. Med. Chem.* 59 (2016) 7677–7682, <https://doi.org/10.1021/acs.jmedchem.6b00247>.
- [39] Q. Qiu, J. Zhu, Q. Chen, Z. Jiang, J. Xu, X. Jiang, W. Huang, Z. Liu, J. Ye, X. Xu, Discovery of aromatic amides with triazole-core as potent reversal agents against P-glycoprotein-mediated multidrug resistance, *Bioorg. Chem.* 90 (2019), 103083, <https://doi.org/10.1016/j.bioorg.2019.103083>.
- [40] S.G. Agalave, S.R. Maujan, V.S. Pore, Click chemistry: 1,2,3-triazoles as pharmacophores, *Chem. - An Asian J.* 6 (2011) 2696–2718, <https://doi.org/10.1002/asia.201100432>.
- [41] L. Liang, D. Astruc, The copper(I)-catalyzed alkyne-azide cycloaddition (CuAAC) “click” reaction and its applications. An overview, *Coord. Chem. Rev.* 255 (2011) 2933–2945, <https://doi.org/10.1016/j.ccr.2011.06.028>.
- [42] L. Ganapathi, A. Arnold, S. Jones, A. Patterson, D. Graham, M. Harper, O. Levy, Use of cidofovir in pediatric patients with adenovirus infection, *F1000Research* 5 (2016) 758, <https://doi.org/10.12688/f1000research.8374.1>.
- [43] C.J. Burckhardt, U.F. Greber, Virus movements on the plasma membrane support infection and transmission between cells, *PLoS Pathog.* 5 (2009), <https://doi.org/10.1371/journal.ppat.1000621>.
- [44] O. Meier, U.F. Greber, Adenovirus endocytosis, *J. Gene Med.* 6 (2004) 152–163, <https://doi.org/10.1002/jgm.553>.
- [45] U.F. Greber, M. Willetts, P. Webster, A. Helenius, Stepwise dismantling of adenovirus 2 during entry into cells, *Cell* 75 (1993) 477–486, [https://doi.org/10.1016/0092-8674\(93\)90382-Z](https://doi.org/10.1016/0092-8674(93)90382-Z).
- [46] M. Charman, C. Herrmann, M.D. Weitzman, Viral and cellular interactions during adenovirus DNA replication, *FEBS Lett.* 593 (2019) 3531–3550, <https://doi.org/10.1002/1873-3468.13695>.
- [47] E.J. Kremer, G.R. Nemerow, Adenovirus tales: from the cell surface to the nuclear pore complex, *PLoS Pathog.* 11 (2015) 1–8, <https://doi.org/10.1371/journal.ppat.1004821>.
- [48] H. Matthews, J. Deakin, M. Rajab, M. Idris-Usman, N.J. Nirmalan, Investigating antimalarial drug interactions of emetine dihydrochloride hydrate using CalcuSyn-based interactivity calculations, *PLoS ONE* 12 (2017) 1–19, <https://doi.org/10.1371/journal.pone.0173303>.
- [49] N.H. Amin, M.T. El-Saadi, A.A. Ibrahim, H.M. Abdel-Rahman, Design, synthesis and mechanistic study of new 1,2,4-triazole derivatives as antimicrobial agents, *Bioorg. Chem.* 111 (2021), 104841, <https://doi.org/10.1016/j.bioorg.2021.104841>.
- [50] T.S. Ibrahim, A.J. Almalki, A.H. Moustafa, R.M. Allam, G.E.-D.A. Abu-Rahma, H. I. El Subbagh, M.F.A. Mohamed, Novel 1,2,4-oxadiazole-chalcone/oxime hybrids as potential antibacterial DNA gyrase inhibitors: Design, synthesis, ADMET prediction and molecular docking study, *Bioorg. Chem.* 111 (2021), 104885, <https://doi.org/10.1016/j.bioorg.2021.104885>.
- [51] R. Wang, Y. Fu, L. Lai, A new method for calculating partition coefficients of organic compounds, *Acta Phys. - Chim. Sin.* 13 (1997) 615–621, <https://doi.org/10.3866/pku.whxb19970101>.
- [52] W.P. Walters, A. Murcko, M.A. Murcko, Recognizing molecules with drug-like properties, *Curr. Opin. Chem. Biol.* 3 (1999) 384–387, [https://doi.org/10.1016/S1367-5931\(99\)80058-1](https://doi.org/10.1016/S1367-5931(99)80058-1).
- [53] P.F. Lamie, J.N. Philoppes, 2-Thiopyrimidine/chalcone hybrids: design, synthesis, ADMET prediction, and anticancer evaluation as STAT3/STAT5a inhibitors, *J. Enzyme Inhib. Med. Chem.* 35 (2020) 864–879, <https://doi.org/10.1080/14756366.2020.1740922>.
- [54] B.M. Minrovic, D. Jung, R.J. Melander, C. Melander, new class of adjuvants enables lower dosing of colistin against acinetobacter baumannii, *ACS Infect. Dis.* 4 (2018) 1368–1376, <https://doi.org/10.1021/acscinfed.8b00103>.
- [55] M.A. Brimble, C. Brocke, Efficient synthesis of the azabicyclo[3.3.1]nonane ring system in the alkaloid methyllycaconitine using bis(alkoxymethyl)alkylamines as aminoalkylating agents in a double Mannich reaction, *Eur. J. Org. Chem.* (2005) 2385–2396, <https://doi.org/10.1002/ejoc.200500003>.
- [56] C. Fehr, Diastereoface-selective epoxidations: dependency on the reagent electrophilicity, *Angew. Chemie - Int. Ed.* 37 (1998) 2407–2409, [https://doi.org/10.1002/\(SICI\)1521-3773\(19980918\)37:17<2407::AID-ANGE2407>3.0.CO;2-W](https://doi.org/10.1002/(SICI)1521-3773(19980918)37:17<2407::AID-ANGE2407>3.0.CO;2-W).
- [57] B. Zhao, Z. Gao, Y. Zheng, C. Gao, Scalable synthesis of positively charged sequence-defined functional polymers, *J. Am. Chem. Soc.* (2019) 1–52, <https://doi.org/10.1021/jacs.9b00172>.
- [58] E.W. Sugandhi, J.O. Falkinham, R.D. Gandour, Synthesis and antimicrobial activity of symmetrical two-tailed dendritic tricarboxylate amphiphiles, *Bioorg. Med. Chem.* 15 (2007) 3842–3853, <https://doi.org/10.1016/j.bmc.2007.03.017>.
- [59] J. Nieschalk, S. Laboratories, S. Road, A short synthesis of (1S,2R)- and (1R,2R)-[1-ZH]-glycerols, *Tetrahedron Asymmetry* 8 (1997) 2325–2330.
- [60] M. Martínez-Bailén, A.T. Carmona, E. Moreno-Clavijo, I. Robina, D. Ide, A. Kato, A. J. Moreno-Vargas, Tuning of β -glucosidase and α -galactosidase inhibition by generation and in situ screening of a library of pyrrolidine-triazole hybrid molecules, *Eur. J. Med. Chem.* 138 (2017) 532–542, <https://doi.org/10.1016/j.ejmech.2017.06.055>.
- [61] L. Liu, C. Li, S. Cochran, S. Jimmink, V. Ferro, Synthesis of a heparan sulfate mimetic library targeting FGF and VEGF via click chemistry on a monosaccharide template, *ChemMedChem* 7 (2012) 1267–1275, <https://doi.org/10.1002/cmdc.201200151>.
- [62] R.R. Nepomuceno, L. Pache, G.R. Nemerow, Enhancement of gene transfer to human myeloid cells by adenovirus-fiber complexes, *Mol. Ther.* 15 (2007) 571–578, <https://doi.org/10.1038/sj.mt.6300048>.
- [63] C.A. Schneider, W.S. Rasband, K.W. Eliceiri, NIH Image to ImageJ: 25 years of image analysis, *Nat. Methods.* 9 (2012) 671–675, <https://doi.org/10.1038/nmeth.2089>.
- [64] A.A. Rivera, M. Wang, K. Suzuki, T.G. Uil, V. Krasnykh, D.T. Curiel, D. M. Nettelbeck, Mode of transgene expression after fusion to early or late viral genes of a conditionally replicating adenovirus via an optimized internal ribosome entry site in vitro and in vivo, *Virology* 320 (2004) 121–134, <https://doi.org/10.1016/j.virol.2003.11.028>.
- [65] H.M.L.J. Reed, A Simple Method Of Estimating Fifty Per Cent Endpoints, *Am. J. Hyg.* 27 (1938) 546–558, <https://doi.org/10.7723/antiochreview.72.3.0546>.